

Aus dem Zentrum für Medizinische Forschung

der Medizinischen Fakultät Mannheim

Direktor: Prof. Dr. med. Norbert Gretz

Effects of photobiomodulation with blue light during and after adipocyte  
differentiation

Inauguraldissertation

zur Erlangung des akademischen Grades

Doctor scientiarum humanarum (Dr. sc. hum.)

der

Medizinischen Fakultät Mannheim

der Ruprecht-Karls-Universität

zu

Heidelberg

vorgelegt von

Stefania Palumbo

aus

Neapel, Italien

2020

Dekan: Prof. Dr. med.Sergij Goerd  
Referent: Prof. Dr. med. Norbert Gretz

## Table of contents

Abbreviations .....	0
1. Introduction .....	1
1.1 Photobiomodulation: definition and history .....	1
1.1.1 Irradiation parameters .....	2
1.1.2 Mechanisms of action.....	3
1.1.3 Medical applications: PBM for fat reduction and body contouring.....	4
1.2 Blue light .....	5
1.3 Obesity and Adipocytes.....	6
1.3.1 Optical properties of adipose tissue .....	9
1.4 Adipocyte differentiation by pre-adipocyte cell line: 3T3-L1.....	9
1.4.1 Factors affecting adipocyte differentiation .....	10
1.5 Aim of the study .....	11
2 Material and methods .....	13
2.1 Cell culture .....	13
2.1.1 Differentiation of 3T3 L1 Cell .....	14
2.2 Blue Light treatment.....	15
2.2.1 LED Characteristics .....	15
2.2.2 Light stimulation .....	16
2.2.3 Experimental setup.....	16
2.3 Staining and quantification.....	17
2.3.1 Oil Red O staining and quantification.....	18
2.3.2 Hoechst and AdipoRed staining and quantification.....	18
2.4 Cell metabolism and proliferation assays.....	18
2.4.1 XTT assay .....	19
2.4.2 ATP assay.....	19
2.4.3 BrdU ELISA.....	20
2.5 Mitochondrial function – ROS generation .....	20
2.5.1 Quantification of intracellular ROS .....	20
2.6 RNA-Isolation .....	21
2.7 Gene expression.....	21
2.7.1 RNA sequencing .....	21
2.7.2 Bioinformatic evaluation.....	21
3 Results .....	23
3.1 Adipogenic differentiation.....	23
3.2 Oil Red O quantification.....	26
3.3 Assessment of blue light effects on cell metabolism assays .....	30

3.4	Assessment of blue light effects on cell proliferation .....	34
3.5	Evaluation of ROS levels .....	37
3.6	Gene expression.....	39
4	Discussion .....	63
4.3	Conclusions .....	72
5	Summary .....	74
6	References .....	76
7	Appendix .....	83
8	Curriculum vitae.....	99
9	Acknowledgments.....	101

## Abbreviations

AMD	Age-related macular degeneration
AMPK	AMP-activated protein kinase
ATP	Adenosine triphosphate
BAT	Brown adipose tissue
BMI	Body mass index
BrdU	5-Bromo-2'-deoxyuridine
cAMP	cyclic-adenosine monophosphate
CDK	Cyclin-dependent kinase
CYP	Cytochrome
DCFDA	2',7' – dichlorofluorescein diacetate
DEX	Dexamethasone
DMEM	Dulbecco's modified Eagle's medium
ELISA	Enzyme-linked immunosorbent assay
FBS	Fetal bovine serum
FDR	False discovery rate
GC	Glucocorticoids
GSEA	Gene Set Enrichment Analysis
H <sub>2</sub> O <sub>2</sub>	Hydrogen peroxide
IBMX	3-isobutyl-1-methylxanthin
IQR	Interquartile range
IR	Infrared
KEGG	Kyoto Encyclopedia of Genes and Genomes
LED	Light-emitting diode
LLLT	Low-level laser (light) therapy
MCE	Mitotic clonal expansion
NAALT	North American Association for Light Therapy
NES	Normalized Enrichment Score
NF- $\kappa$ B	Nuclear factor kappa B
NIR	Near-infrared
PBM	Photobiomodulation
PBS	Phosphate buffered saline
RIN	RNA integrity number

ROS	Reactive oxygen species
scWAT	sub cutaneous white adipose tissue
SD	Standard deviation
TNF	Tumor necrosis factor
UV	Ultraviolet
VIS	Visible
WALT	World Association for Laser Therapy
WAT	White adipose tissue
WHO	World Health Organization
XTT	Sodium 3'-[1-(phenylaminocarbonyl)-3, 4-tetrazolium] bis (4-methoxy-6-nitro) benzene sulfonic acid hydrate
$\Delta\Psi_m$	Mitochondrial membrane potential

# 1. Introduction

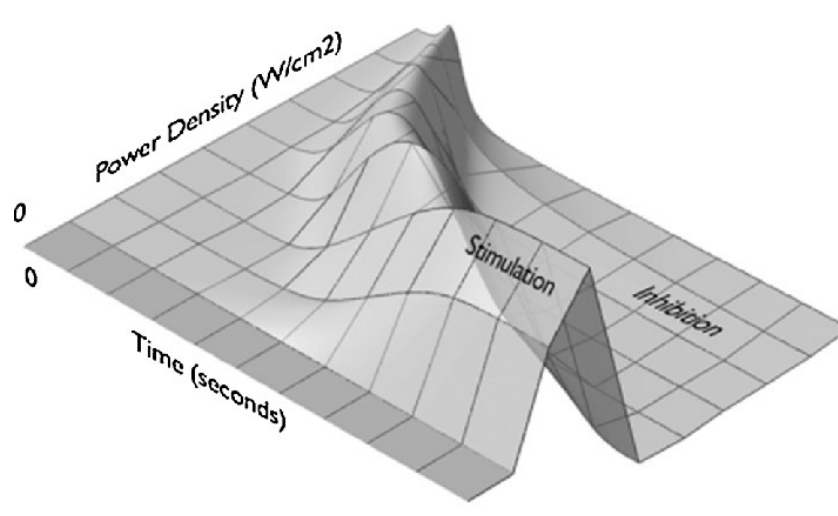
## 1.1 Photobiomodulation: definition and history

Since ancient times light has been used for therapeutic purposes first using sunlight and then electric lamps discovered around the 19th century by Davy (arc lamp) and Edison (incandescent bulb). The growing interest in laser technology led Niels Finsen to win in 1903 the Nobel Prize for physiology and medicine for his work on the treatment of skin tuberculosis with concentrated UV rays and smallpox with red light<sup>1</sup>. A new scientific branch, recognized for years under the name of low level laser therapy (LLLT), is born. However, the universally recognized father of LLLT is the Hungarian doctor Endre Mester who in the early 60's, using a ruby laser (wavelength 694.3 nm), began testing in animal models, mainly on the skin of rats, with the aim of assessing the presence of a carcinogenic effect of low energy density laser (1 J/cm<sup>2</sup>). After the first observations, no detecting differences in the carcinogenic sense between treated and untreated animals, he began to carry out studies on the effect of laser therapy in healing processes, investigating in vivo tissue repair in burns and traumas, and in vitro phagocytosis of bacteria by leukocytes, hemoglobin synthesis and healing of ulcerative lesions not responding to conventional therapies<sup>2, 3</sup>. The difficulty in defining such a vast field of application can be seen in the large number of definitions in the international scientific literature, where the term LLLT is accompanied by numerous synonyms such as "photobiomodulation", "phototherapy", "photomedicine", "photoirradiation", "biomodulation" and "biostimulation"<sup>4</sup>. Only in 2014 The North American Association of Laser Therapy (NAALT) and the World Association of Laser Therapy (WALT) reached a consensus on the nomenclature introducing the term "photobiomodulation" (PBM) which defines a form of light therapy that utilizes non-ionizing light sources, including lasers, light emitting diodes (LEDs), and/or broadband light, in the visible (400 – 700 nm) and near-infrared (700 – 1100 nm) electromagnetic spectrum. It is a non-thermal process involving endogenous chromophores eliciting photophysical (i.e., linear and nonlinear) and photochemical events at various biological scales. This process results in beneficial therapeutic outcomes including, but not limited, to the alleviation of pain or inflammation, immunomodulation, and promotion of wound healing and tissue regeneration<sup>4-5</sup>.

### 1.1.1 Irradiation parameters

The lack of knowledge of the molecular effects of PBM and a poor understanding of the radiometric parameters which influence the repeatability and reliability of the practical application of PBM is still the subject of controversy<sup>6</sup>. The studies that provided indications for the reporting of radiometric parameters indicated a maximum of ten key radiometric parameters such as: wavelength, power density, irradiation time, beam area, energy density, radiant exposure, pulse parameters, number of treatments, interval between treatments and anatomical location<sup>7</sup>.

Especially the power density or irradiance [ $\text{W}/\text{cm}^2$ ] and the energy density or fluence [ $\text{J}/\text{cm}^2$ ], are fundamental to make different studies comparable<sup>6</sup>. In fact, it is the combination of these two parameters that determines the characteristics of biomodulation. Too low dosages may not have any effect, too high ones may have an inhibitory effect. This biphasic response follows the Arndt Schultz<sup>8, 9</sup> law according to which weak stimuli slightly accelerate vital activity, stronger stimuli increase it until the maximum peak beyond which such activity is suppressed with inhibitory effects<sup>10,11</sup> (Figure 1).



**Figure 1: Biphasic dose response in LLLT.** Three dimensional surface plot illustrating the effects of an increasing irradiance [ $\text{W}/\text{cm}^2$ ] or irradiation time [s] on dose-dependent PBM resulting in stimulation or inhibition.<sup>12</sup>

Biostimulation therefore seems to require fluences between  $0.05 \text{ J}/\text{cm}^2$  and  $10 \text{ J}/\text{cm}^2$  for a positive response while above  $10 \text{ J}/\text{cm}^2$  are related to bioinhibition<sup>13</sup>.



### 1.1.2 Mechanisms of action

By convention, the PBM action mechanisms can be divided into primary and secondary mechanisms. According to the first "law of photochemistry", the primary mechanisms are dependent on the absorption of light by photo-acceptor systems (chromophores). Cytochrome C oxidase, opsins, flavins and flavoproteins and porphyrins are proposed as the main photoacceptors able to mediate a biological response in PBM<sup>14, 15</sup>.

Karu et al.<sup>16</sup> have postulated four primary mechanisms of action that can modulate biological activity: 1) alteration of the redox state and acceleration of electron transport 2) changes in biological activity due to increase in local temperature of absorbent chromophores 3) one-electron autooxidation and  $O_2^{\cdot -}$  production (and subsequent production of  $H_2O_2$ ) 4) photodynamic action and  $O_2$  production. (Figure 2). These primary light-induced mechanisms of action are followed by biochemical cascade reactions in the cells that do not require further stimulation and occur in the dark (secondary mechanisms). This signal transduction is related to changes in the parameters of cellular homeostasis. However, the crucial step seems to be an alteration of the redox state: a shift towards oxidation is associated with stimulation of cell viability while a shift towards reduction is linked to inhibition.

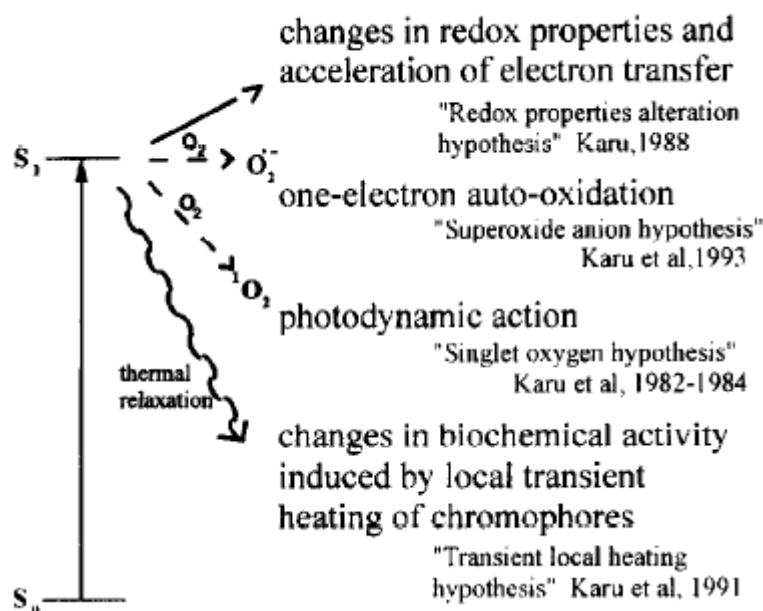
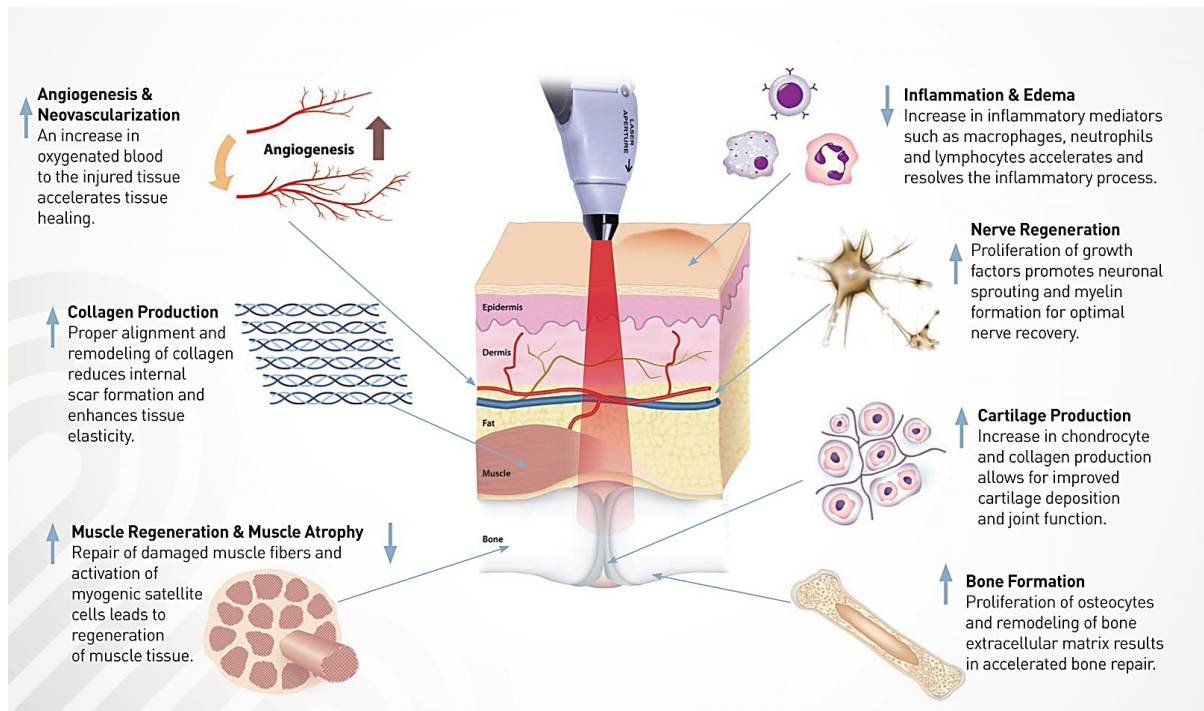


Figure 2: Possible primary reactions with a photo-acceptor molecules after promotion to excited electronic states<sup>16</sup>.

### 1.1.3 Medical applications: PBM for fat reduction and body contouring

The photochemical reactions underlying PBM can define several clinical effects: the promotion of wound healing, the anti-inflammatory action, the analgesic effect and a treatment for other neurological problems (Figure 3)<sup>12,17,18</sup>.



**Figure 3: Illustration of physiological effects of LLLT<sup>19</sup>.**

In addition to the already common clinical applications in the last decade LLLT/PBM has also been investigated as an adjuvant in liposuction<sup>20-23</sup>, cellulite reduction, non-invasive body contouring<sup>24-26</sup> and improvement of blood lipid levels<sup>27</sup>. However, further studies are necessary to clarify the mechanisms of action underlying this new fat reduction procedure. For first was proven as effect of LLLT on adipocytes the formation of transient micropores on the cell membrane and consequent the release of intracellular lipids<sup>22</sup>. Another mechanism of action proposed seems to be the activation of the complement cascade that can cause adipocyte apoptosis and subsequent release of lipids<sup>28</sup>. It is also possible that LLLT/PBM can stimulate the mitochondria in the adipocytes with an increase in ATP levels followed by an up regulation of cAMP and activation of protein kinases. The final effect is the stimulation of cytoplasmic lipase for the conversion of triglycerides into fatty acids and glycerol<sup>29,30</sup>. To date, all proposed LLLT studies use wavelengths in the red and infrared spectrum. No studies

## Introduction

concerning fat reduction and body contouring have been carried out with shorter wavelengths such as blue light.

### 1.2 Blue light

Most of the studies underpin the application of PBM using wavelengths between 600–1100 nm. Wavelengths <600 nm are less investigated or detailed. The utilization of blue light (400–500 nm) especially is moreover encompassed by critical discussion identifying with the reason that the edge between “safe” blue light and "harmful ultraviolet (UV) light" is not well characterized. (Figure 4). The fact of high photon energy makes blue light able to prompt photochemical damage inducing development of reactive oxygen species (ROS) and prompting degenerative eye ailments, for example, age-related macular degeneration (AMD)<sup>31</sup>. On the other hand blue light significantly exerts on the skin many positive attested effects such as antimicrobial (both bacteriostatic and bactericidal)<sup>32</sup> or anti-inflammatory (treatment of skin lesion as psoriasis and acne)<sup>33</sup>.

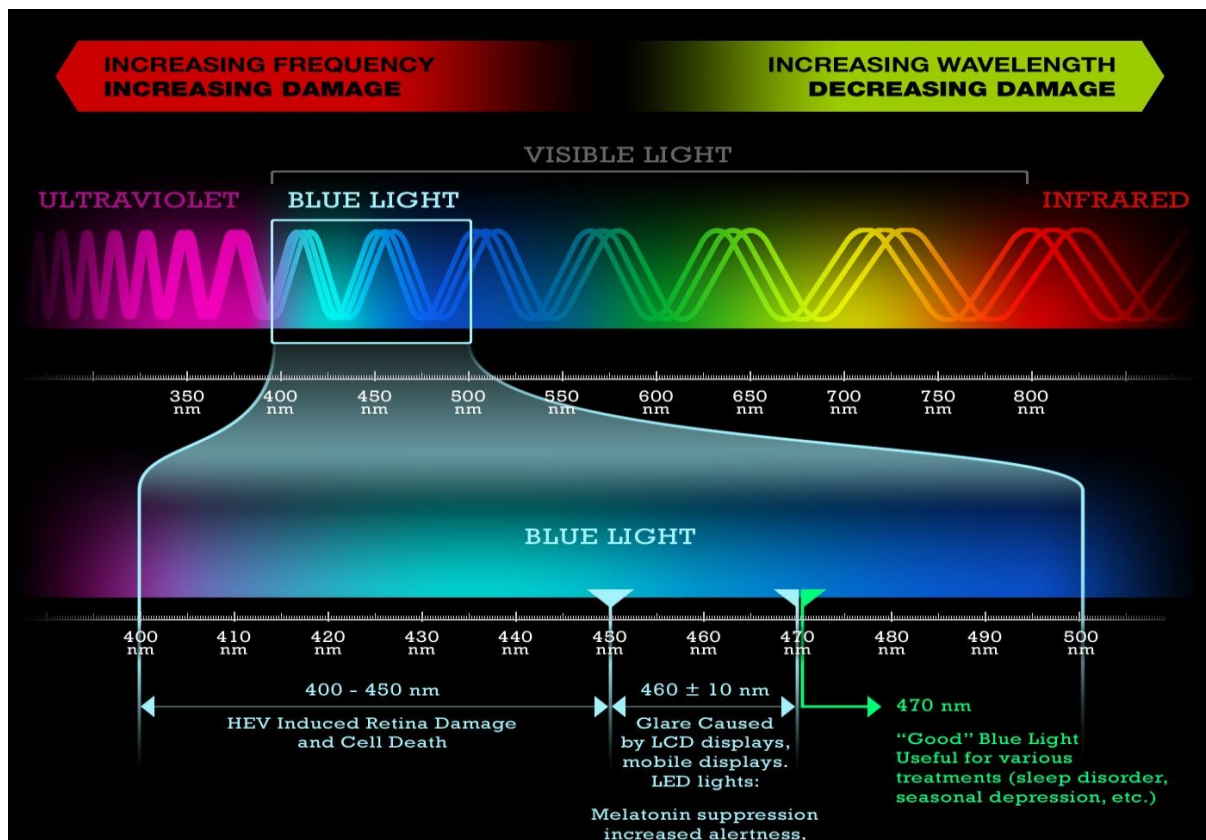


Figure 4: Electromagnetic spectrum. Distinction between the different wavelengths in the blue spectrum according to their more or less harmful effects<sup>34</sup>.

## Introduction

To date, compared to other wavelengths as red or NIR light, blue light is still limited in use. An added key caveat regarding the lower penetration depth is corresponding to an intensity decrease by  $1/e$  (approximately 63%) at 1mm through tissue compared up to 5mm of NIR light. Secondly the mechanisms through which light can trigger the activation of transcription factors are unknown, except, as mentioned above, that ROS are proposed as mediators. The increased amount of ROS in cells exposed to light is presumably the result of excitation of endogenous photosensitizers by absorption of specific wavelengths. Notwithstanding, potential biomolecular targets of blue light are generally uncommon. The best candidates include photosensitizers concentrated in the mitochondria, such as porphyrin ring structures (absorption peaks at 410 - 440 nm) and flavins (absorption peaks at 450 nm)<sup>35-37</sup>.

Since mitochondrial function is critical for cell survival, and mitochondria are a major endogenous source of ROS in cells, it has been hypothesized that blue light triggers sufficient redox-related stress to cause differential cell responses<sup>38</sup>. Limited and contrasting results on blue light induced signaling have been reported. Some investigations have shown a regulation of proliferation and differentiation or a modulation of inflammatory parameters, others growth inhibition and apoptosis in a cell-type-dependent manner<sup>39-41 42</sup>. It is clear that further studies concerning molecular and cellular mechanisms are needed to strengthen the use of blue light in clinical applications.

### 1.3 Obesity and Adipocytes

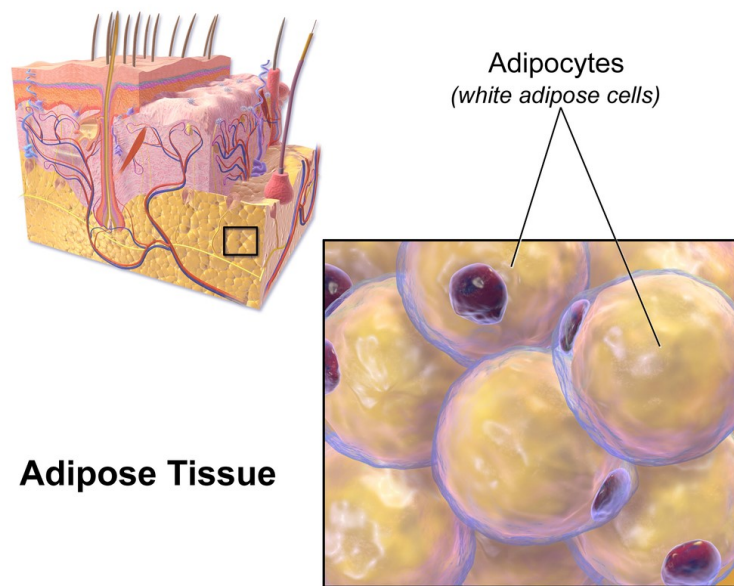
Obesity is a condition characterized by excessive accumulation of subcutaneous and visceral adipose tissue<sup>43</sup>, mainly due to a prolonged imbalance between energy intake and expenditure, with a body mass index (BMI) >30. The World Health Organization (WHO) has recently defined obesity as a "global epidemic" since over a third of the world population today is affected. If secular trends continue, by 2030 an estimated 38% of the world's adult population will be overweight and another 20% will be obese<sup>44</sup>. In parallel with the increase in the incidence of obesity and the progression of obese individuals towards higher and higher BMI values, there is an increased risk of comorbidity phenomena such as diabetes mellitus type II, glucose intolerance, insulin resistance, hyperlipidemia and hypertension with an increase in cardiovascular risk, with an exponential curve that describes the correlation between BMI and mortality from cardiovascular events<sup>45</sup>. The studies carried out so far have, in fact, led to the conclusion that the most common forms of obesity have, probably, a multifactorial etiology<sup>46</sup>,<sup>47</sup> that results from a complex interaction between the biology of energy metabolism and the

## Introduction

environment, passing through a possible genetic predisposition, but also hormonal, metabolic and behavioral aspects, such as sedentariness and high-calorie diet<sup>48, 49</sup>, are involved. Since a subversion of these lifestyles is rather unlikely, due to precise well-established socio-economic models, due to the serious metabolic dysfunctions linked to the excessive formation of adipose tissue, in recent years there has been a strong increase in scientific interest aimed at understanding the molecular pathways that regulate the energy metabolism in humans, in order to identify new strategies for prevention and treatment<sup>50, 51</sup>.

Interest in the biology of adipose tissue has increased substantially. To date this tissue is no longer considered to be an inert tissue that just stores fat<sup>52</sup> but is defined a metabolically dynamic organ that is the primary site of storage for excess energy but it serves as an endocrine organ capable of synthesizing a number of biologically active compounds that regulate metabolic homeostasis<sup>53</sup>.

In mammals adipose tissues can be of two types with distinguishing properties: white adipose tissue (WAT) and brown adipose tissue (BAT)<sup>54</sup>. The adipocyte of WAT contains a large, single lipid droplet that occupies the most of cell volume, pressing the nucleus and cytoplasm to the cell periphery (unilocular adipocyte) (Figure 5). WAT is responsible for many functions, such as synthesis of triglycerides and storage as energy reserve (1Kg = about 7000 Cal); hydrolyzation of the deposited triglycerides and release of free fatty acids into the bloodstream; synthesis of triglycerides from glucose; mechanical shock absorber, thermal insulation and producer of hormones and biologically active substances (adipokines), including leptin, adiponectin, interleukin 6 (IL-6) and tumor necrosis factor- $\alpha$ . BAT contains high mitochondrial content and multiple lipid droplets (multilocular adipocyte), and are derived from distinct highly vascular and innervated adipose tissue depots<sup>44</sup>. The main function of brown adipose tissue is to produce heat. The thermogenic activity of brown adipose tissue is also induced by excessive calories, in an attempt to dissipate unnecessary energy by avoiding excessive accumulation of fat. Essential for newborns it is scarcely present in adults.



**Adipose Tissue**

**Figure 5: Micro anatomy of subcutaneous white adipose tissue. In each adipocyte nucleus is surrounded by one (unilocular) lipid droplet<sup>55</sup>.**

The composition of adipose tissue is not homogeneous. The two-third are composed of the stroma-vascular fraction, comprising blood cells, endothelial cells, pericytes and preadipocytes cells and only one-third is represented by mature adipocytes.

The increase of the adipose tissue can occur in two ways: hyperplasia, with an increase in the number of adipocytes, or hypertrophy, with an increase in the lipid content and volume of each adipocyte<sup>56, 57</sup>. Until a few years ago, it was believed that adipocyte hyperplasia only occurred in the last semester of gestation, in the first year of life and in childhood. Today, however, we know that this phenomenon can also occur in adults, especially when we move from a condition of moderate overweight to that of severe obesity. There is in fact a limit beyond which the adipocytes cannot further increase in volume (maximum volume=1 $\mu$ g). In this situation a further increase in fat reserves can only be achieved by increasing the number of adipocytes. This phenomenon was confirmed by the discovery of preadipocytes, undifferentiated cells immersed in the adipose tissue of adult subjects. These cells retain the ability to divide and, if stimulated and activated, are able to give rise to new adipocytes<sup>58</sup>. Once formed, these new adipose cells will remain so forever in that state and may therefore increase or decrease in volume but not in number.

### 1.3.1 Optical properties of adipose tissue

Due the deeper subcutaneous position adipose tissue is not used to experience light exposure. However, a small percentage of the light can reach the hypodermis. To date a knowledge of the optical characteristics of adipose tissue is necessary for the development of various treatment methods in cosmetology and in photodynamic therapy of dermatological and oncological diseases<sup>59</sup>. The optical penetration not only depends on the wavelength of light but also on tissue structure, thickness and its vascularization. Despite numerous investigations in the field of optics of biological tissues, the optical parameters of subcutaneous adipose tissue in a wide spectrum remain poorly unknown.

Studies conducted in the range 400–2500 nm on subcutaneous adipose tissue have shown the shape of the spectra in the visible and non-visible. In the visible spectrum the major peak is determined by the absorption bands of blood hemoglobin localized in the capillary vessels of the adipose tissue while in the IR spectral range, the shape of the reflection and transmission spectra is determined by the absorption bands of water, lipids, and proteins of the tissue matrix. In both the visible and the IR spectral ranges, the role of the main scattering structures is played by spherical droplets of lipids (mainly, triglycerides), which are uniformly distributed within the adipose tissue<sup>60</sup>.

### 1.4 Adipocyte differentiation by pre-adipocyte cell line: 3T3-L1

As model of in vitro adipose tissue, 3T3-L1 cell line, derived from 3T3 cells, is widely used in biological research. 3T3-L1 cells have a fibroblast-like morphology, but, under appropriate conditions, they differentiate into an adipocyte-like phenotype. During the differentiation process, biochemical and morphological characteristics of adipocyte differentiation are shown. Indeed, 3T3-L1 cells increase the synthesis of triglycerides and acquire the behaviour of adipose cells. In particular, triglycerides accumulate in lipid droplets (LDs) embedded in the cytoplasm.

There are two important features of preadipocyte cell lines which make them eligible candidates for adipocyte differentiation study. First, it is a uniform cellular population in a similar differentiation stage allowing clonal cells to show a homogeneous response to the treatments. Secondly, the preadipocytes can be indefinitely passaged without suffering genetic mutation or functionality change, which provides a consistent source of cells for study of adipocyte differentiation<sup>58</sup>. Once preadipocyte cells reach confluence, growth arrest occurs.

## Introduction

After that cells can re-enter the cell cycle and, before differentiation, undergo mitotic clonal expansion (MCE) that consists of one or two rounds of cell division<sup>61</sup>. Whether MCE is required for differentiation is controversial<sup>62</sup>; however, it is clear that some of the checkpoint proteins for mitosis also regulate aspects of adipogenesis.

Using a defined adipogenic cocktail, confluent preadipocytes/3T3-L1 can be differentiated synchronously. Maximum differentiation can be achieved by increasing intracellular levels of cAMP (cyclic-adenosine monophosphate) by inducing cells in the initial phase (48 hours), in the presence of fetal bovine serum and a hormonal cocktail consisting of insulin, 3-isobutyl-1-methylxanthin (IBMX) and dexamethasone (DEX). 3T3-L1 can be differentiated and converted into mature adipocyte cells, with changes in morphology and expression of specific adipocyte genes. Dexamethasone is a synthetic glucocorticoid agonist (GC) that stimulates the GC receptor. After the first 48 hours, the insulin itself can continue the differentiation process. Surprisingly, DEX shows an anti-adipogenic effect at the later stage of the differentiation process (adipose maturation), while it has a powerful induction effect on adipogenesis at the early stages of differentiation, indicating the short time window of hormonal effects<sup>63</sup>.

Thus, adipogenesis, is an ordered multistep process requiring the sequential activation of several groups of transcription factors, including CCAAT/enhancer-binding protein (C/EBP) gene family and peroxisome proliferator activated receptor- $\gamma$  (PPAR- $\gamma$ ) which regulates glucose metabolism and fatty acid storage of cells<sup>64</sup>. In the first stage after induction, a signaling cascade is activated. C/EBP- $\beta$  is expressed within 2-4 hours after hormonal induction. At this time C/EBP- $\beta$  is unable to bind DNA and thus cannot play the role of a transcriptional activator. This function is acquired later in the differentiation program around 14h reaching a maximum at 24h after induction. Having acquired DNA-binding function, C/EBP- $\beta$  transcriptionally activates both PPAR- $\gamma$  and C/EBP- $\alpha$ . Because PPAR- $\gamma$  and C/EBP- $\alpha$  are both antimitotic, they seem to function as terminators of MCE. The activation of these factors leads to the expression of many adipocyte genes and an irreversible differentiation process that end with the formation of a mature adipocyte phenotype<sup>65, 66</sup>.

### 1.4.1 Factors affecting adipocyte differentiation

Adipocyte differentiation can be affected in a positive or negative way by many hormones, growth factors, cytokines, and pharmacological compounds and so on. Adipogenic factors like insulin, insulin-like growth factor-1 (IGF-1), glucocorticoids, mineralocorticoids, growth



## Introduction

hormone and PPAR- $\gamma$  agonists promote differentiation. Other growth factors like EGF or TNF and cytokines, as interleukin-11 have inhibitory effects, sometimes in a dose-dependent manner<sup>67, 68</sup>.

Epigenetic factors<sup>69</sup>, miRNAs<sup>70</sup>, some clock genes<sup>71, 72</sup>, especially Bmal1 and Rev-ErbA may play a role in adipocyte differentiation and lipogenesis. Also cell culture conditions can affect these processes. In fact, culturing 3T3-L1 cells in different culture dishes showed differences in adipocyte differentiation.<sup>73</sup>

### 1.5 Aim of the study

The rapid spread of PBM, especially for medical applications, has led to the emergence of numerous studies both in vivo and in vitro, most of them conducted with red or infrared light. This choice is due to the advantages in the application of these wavelengths, such as the deep penetration and the more elucidated mechanisms of action. On the other hand, still controversial and uncharacterized are the treatment approaches regarding blue light that, although considered a "bad light" for its dysregulating effects on the eyesight and circadian rhythm, has shown some beneficial effects for the treatment of skin diseases, such as acne and psoriasis. In addition, in defense of the beneficial potential of blue light, some recent studies have shown that exposure to sunlight can have positive effects on body weight reduction. The 38.9% of the sun's energy reaching exposed skin is in the visible wavelength range. In spite of the fact that most of sunlight in the visible spectrum does not pass through the skin, approximately 1–5% of blue/green light is able to penetrate through human skin to varying depths proportional to increasing wavelength and intensity and reach the underlying subcutaneous white adipose tissue (scWAT) modulating some functions such as lipid storage. These findings may lead to light-based treatments for obesity and other related conditions like diabetes.

In order to understand and broaden the knowledge of the mechanisms of action induced by the exposure of blue light, this study is intended to position itself in the vast panorama of scientific research with the aim to assess the potential of only VIS blue light in an in vitro model of 3T3-L1 cells, to study mechanisms governing adipose tissue development. Given the inhibitory effects of using high doses of irradiation, the 21.6 J/cm<sup>2</sup> and 43.2 J/cm<sup>2</sup> doses were chosen in this project in order to modulate the adipocyte differentiation or to induce leakage of intracellular lipids. The effects were studied during and after the differentiation process, for evaluating metabolic-functional adaptations that can be divided into:

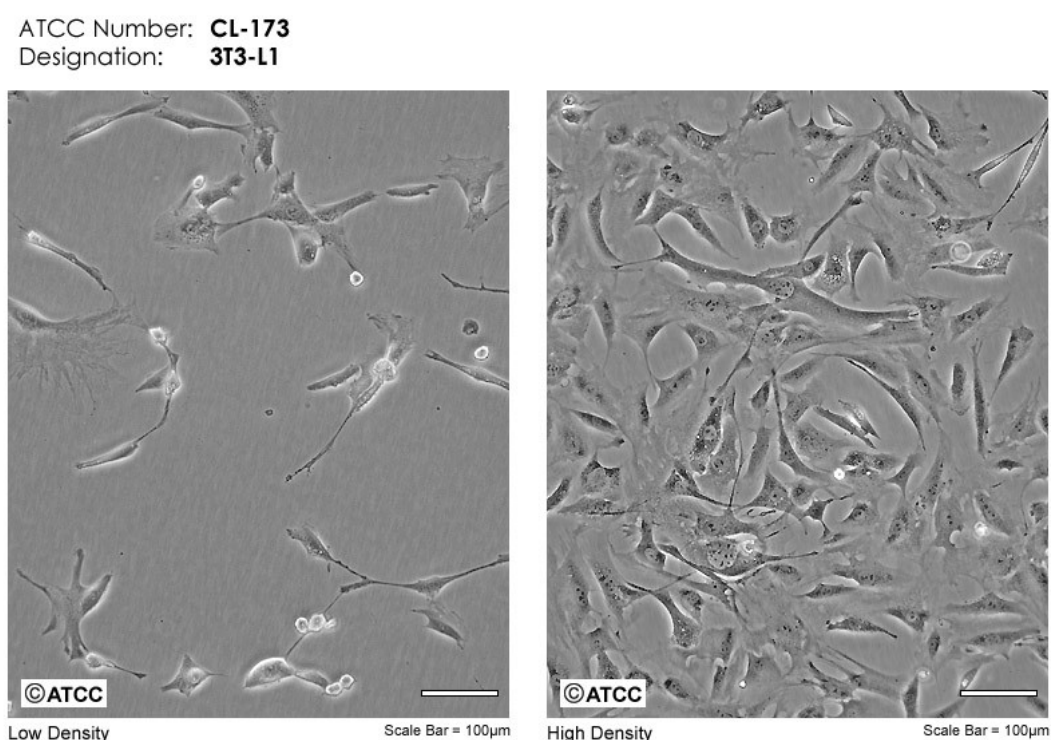
## Introduction

- Cellular response to stress damage.
- Cellular adaptations of growth and differentiation
- Increasing or decreasing of metabolism.
- Regulation of gene expression profiles

## 2 Material and methods

### 2.1 Cell culture

3T3-L1 cells (ATCC® CL-173™) (Figure 6) were cultured under standard conditions in humidified atmosphere at 37°C and 5% CO<sub>2</sub>. Cells were cultured in Dulbecco's modified Eagle's medium (DMEM) high glucose containing completed with 10% fetal bovine serum (FBS), sodium pyruvate and 1% penicillin/streptomycin (Gibco® by life technologies TM AG (Carlsbad/USA)) The cells were sub-cultivated before culture became 70 to 80% confluent and re-seeded according to the instructions of ATCC keeping a density of 2000-3000 cell/cm<sup>2</sup>. For cell detachment, 0.25% Trypsin-EDTA phenol red (Gibco®) was added in the flask for 5 minutes at 37° and 5% CO<sub>2</sub>. Viable cells, determined by Trypan Blue exclusion, were quantified with a Luna™ automatic cell counter and seeded in new flask for subculture. Irradiation treatments and all experiments described in the following sections have been performed into black 96-well plates to avoid light scattering and crosstalk between single wells.



**Figure 6: Low and high density 3T3-L1 cells (ATCC® CL-173™).**

### 2.1.1 Differentiation of 3T3 L1 Cell

3T3-L1 is a type of fibroblast cells derived from mouse that differentiates into adipocytes under appropriate condition. The differentiation of 3T3-L1 towards adipocytes involves processes such as confluent culture, growth arrest, hormonal induction, and adipocyte differentiation. Usually after the 3T3-L1 cells become confluent, growth arrest occurs and in presence of hormone like insulin, cells reenter to the cell cycle and several rounds of post confluent mitosis (Mitotic Clonal Expansion) takes place. Hormonal inducitors are provided to the cells through an adipogenic cocktail containing Insulin, 3-Isobutyl-1-methylxanthin (IBMX), Dexamethasone (DEX) in presence of FBS. Later on IBMX and DEX are removed from the cocktail because DEX shows anti adipogenic effects at the late stages of adipocyte maturation. The differentiation is performed following an established protocol (Figure 7).

To observe adipocyte differentiation under the influence of inducers, cells were seeded in 96-well black plates at an initial concentration of 1200 cells/well in standard culture medium. After 48 hours preadipocytes reached confluence and the standard culture medium was changed with a differentiation medium containing 89% DMEM, 10% FBS, 1% P/S, 0.25  $\mu$ M dexamethasone, 0.5 mM IBMX and 1.0  $\mu$ g/ml insulin.

At day 6<sup>o</sup> of the differentiation process medium was changed to adipocytes maturation medium containing 89% DMEM, 10% FBS, 1% P/S and 1.0  $\mu$ g/ml insulin. After day 12<sup>o</sup> the cells were kept in maintenance condition using basal medium without hormones. For the whole process, medium has been refreshed every two days.

Adipocyte differentiation was tested using a specific dye for lipids, Oil Red O, observable under microscope.

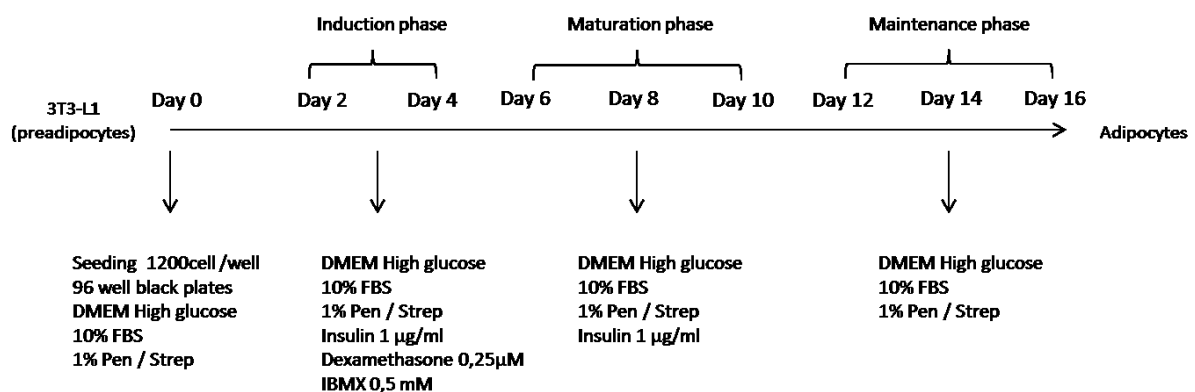
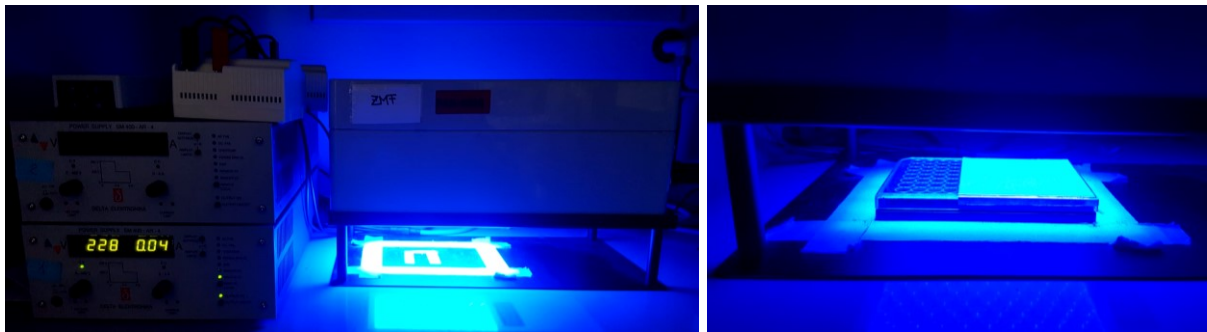


Figure 7: Experimental set-up for adipocytes differentiation with induction factors.

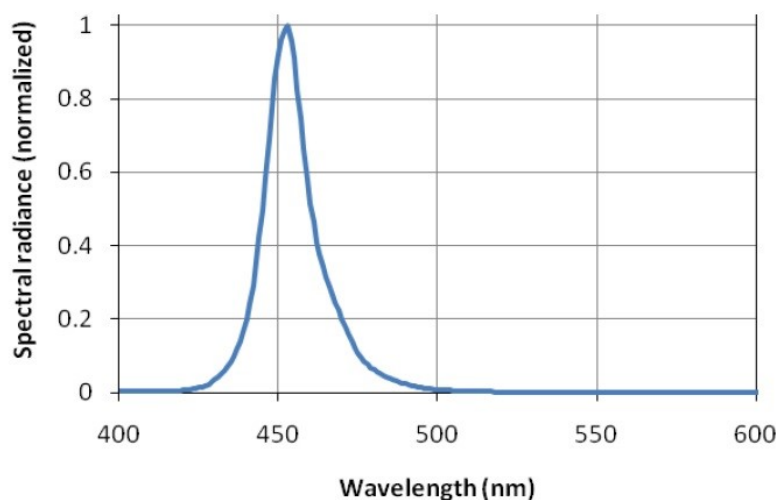
### 2.2 Blue Light treatment

#### 2.2.1 LED Characteristics

As light source a BioLight LED lamp (Figure 8) provided by Philips Research (Eindhoven/Netherlands) was used (Lumileds LUXEON Rebel LXML-PR01-0275). According to the company's specification, the LED device was distance and power adjusted to deliver a fixed irradiance of  $23 \text{ mW/cm}^2$  at the surface of irradiated cell culture plates (50mm distance from lamp casing). However, since the black plate, the lid and medium led to a power loss of about 50% due to light absorption, the irradiance was attenuated to about  $12 \text{ mW/cm}^2$ . The peak wavelength, measured in this condition was given at  $\lambda = 453 \text{ nm}$  (Figure 9). Doses resulting from different irradiation times are shown in Table 1.



**Figure 8: BioLight LED lamp equipped with one power supply delivering 1 A at 300 V (direct current) to drive the LEDs via defined presets. The fan on the top protects the lamp against overheating, especially when using higher irradiances or longer irradiation times**



**Figure 9: Emission spectrum of the Light-Emitting Diode from Koninklijke Philips N.V. (Eindhoven/Netherlands) with a peak wavelength of 453 nm.**

### 2.2.2 Light stimulation

To assess the effects of light irradiation on cell proliferation, metabolism and gene expression, 3T3L-1 cells were seeded in black 96-well plates with sterile clear flat bottom (Costar®).

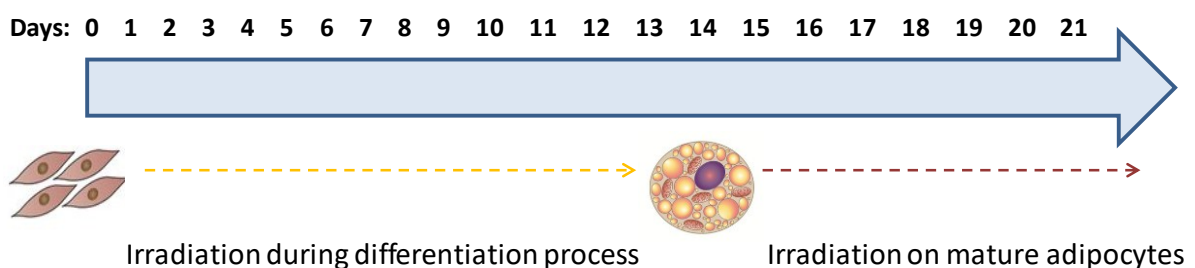
These plates prevent the light cross-talk between the wells and allow a direct microscopic cell viewing. After seeding, cells were incubated till confluence (48 h) at 37°C and 5% CO<sub>2</sub>. The medium was renewed every two days as reported by the differentiation protocol described in the section 2.1.1. According to the two different irradiation set-ups, 3T3-L1 were irradiated with a fixed irradiance of 23 mW/cm<sup>2</sup> and constant light for 30 min or 60min respectively equal to a dose of 21.6 J/cm<sup>2</sup> and 43.2 J/cm<sup>2</sup> (Table 1)

Time (min)	Irradiance (mW/cm <sup>2</sup> )	Energy density (J/ cm <sup>2</sup> )
30	12	21.6
60	12	43.2

**Table 1:** Energy densities depending on the duration of light stimulation. Energy density [J/cm<sup>2</sup>] = Irradiance [mW/cm<sup>2</sup>] x Irradiation time [sec].

### 2.2.3 Experimental setup

The effects of blue light treatments have been evaluated in two different phases of the process: during (Day0-14) and after cell differentiation (Day 15-21) (Figure 10). In both set-ups black 96-well plates were used and a number of 1200 cells/well has been seeded.



**Figure 10:** Time course of adipogenesis.

## Material and Methods

### **1° setup: Blue light treatment during differentiation process.**

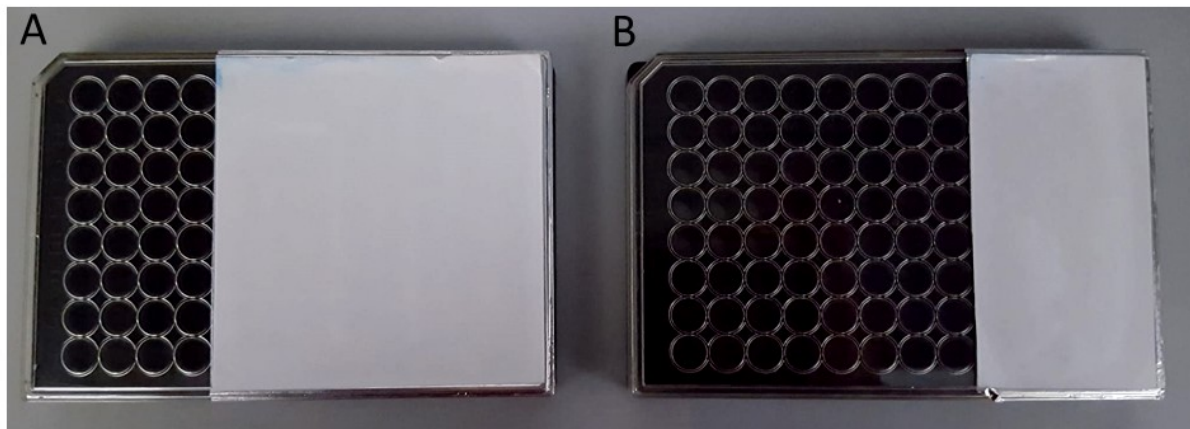
3T3-L1 cells have been irradiated 30 minutes once a day for 14 consecutive days. This period covered all the differentiation process. Each black 96-well plate has been divided in three parts: 1/3 was irradiated daily from Day0 till Day14 (Col.# 1-4); 1/3 was irradiated only the first day of differentiation (Day0) and dark taped for the following days (Col.#5-8); 1/3 was dark taped representing the untreated control (Col.#9-12).

### **2° setup: Blue light irradiation after differentiation process.**

Mature adipocytes have been irradiated 30 or 60 minutes once a day for 7 consecutive days. Each black 96-well plates has been divided in three parts: 1/3 was irradiated daily for 60 minutes (Col.#1-4); 1/3 was irradiated daily for 30 minutes (Col.#5-8); 1/3 was dark taped representing the untreated control (Col.#9-12).

Figure 11 shows plate lids used during irradiation.

Apart from blue light irradiation, for both set-ups, treated and untreated samples were always kept under the same growing and environmental conditions.



**Figure 11: Lids of a black 96-well plate** A) used for 30min daily irradiation during the 1° setup and 60min irradiation during 2° set-up. B) lid used for 30min irradiation Day0 during the 1° set-up and 30min irradiation during the 2° set-up.

### **2.3 Staining and quantification**

Several stainings and associated quantifications were performed in order to confirm differentiation, quantify lipids and to make a relative estimate of cells number.

### 2.3.1 Oil Red O staining and quantification

Independently from the different set-ups used during light stimulation, after 3h from the last irradiation the cells were washed twice with phosphate-buffered saline (PBS) and fixed in 4% paraformaldehyde for 30 minutes. After fixation, cells were washed three times and stained with Oil Red O (ORO) (Sigma Aldrich) solution (stock solution 0.5g ORO powder dissolved in 100% 2-propanol) for 1 hour at room temperature. Cells were washed again three times with water to remove unbound dye and were examined under a light microscope. The red oil droplets stained in the cells indicating lipid accumulation.

To quantify the lipid accumulation, red oil droplets stained in the cells were extracted in 100% 2-propanol. The absorbance was evaluated at 510nm using Infinite® 200 PRO microplate reader (TECAN).

### 2.3.2 Hoechst and AdipoRed staining and quantification

In order to evaluate differences in cell number between irradiated and no irradiated samples, a combined staining of Hoechst and Nile Red (AdipoRed) was performed. After treatment, cells were washed in PBS and fixed with PFA 4% for 30 minutes. After the incubation time, cell were washed again and stained with Hoechst 33342 (Sigma) for other 30 minutes. Measurements with Infinite® 200 PRO microplate reader (TECAN) were done setting the instrument with Ex/Em wavelengths 354/442 nm. Later on, AdipoRed assay (Lonza) was performed on the same samples, following the manufacturer's protocol. AdipoRed is a solution of the hydrophilic stain Nile Red that enables the quantification of intracellular lipid droplets. When partitioned in a hydrophobic environment, Nile Red becomes fluorescent. The emission maximum of the fluorescent signal is dependent on the nature of the hydrophobic environment. Nile Red Fluorescence, when bound to protein or the phospholipids of the plasmalemma of a cell, is distinct from that produced when the stain is partitioned in droplets of triglyceride. Measurements were done setting the microplate reader with Ex/Em wavelengths 485/572 nm.

## 2.4 Cell metabolism and proliferation assays

Blue light effects were studied on metabolism and proliferation using various methods.



### 2.4.1 XTT assay

Metabolic activity determined using Colorimetric Cell Viability Kit III from PromoKine (PromoCell). The assay is based on the reduction of the tetrazolium salt XTT (2, 3-bis-(2-methoxy-4-nitro-5-sulfophenyl)-2H-tetrazolium-5-carboxanilide) into a colored formazan compound by mitochondrial enzymes. Since these enzymes are inactivated shortly after cell death, this is a reliable method for the detection of viable cells. In the presence of the activation reagent, N-methyl dibenzopyrazine methyl sulfate (PMS), mitochondrial enzymes of metabolic active and viable cells reduce the yellow tetrazolium salt XTT to a water-soluble, orange-coloured formazan dye. Therefore, the resulting absorbance intensities directly correlate with the activity of mitochondrial enzymes of viable and active cells metabolizing XTT. Following irradiation, a reaction mixture of XTT and PMS (1:200) was added to the medium (50% by volume) and incubated for 45 minutes at 37°C and 5% CO<sub>2</sub>. The absorbance of the formazan product can be measured directly from a 96-well plate without additional processing. For quantification spectrophotometric absorption measurements at 450 nm with a reference reading at 690 nm were carried out with Infinite® 200 PRO microplate reader (TECAN). Non-specific signals were identified by adding XTT/PMS only to cell culture medium.

### 2.4.2 ATP assay

Metabolic activity by ATP quantification was tested using the CellTiter-Glo® Luminescent Cell Viability Assay (Promega). This test is based on a luciferase reaction to measure the amount of ATP in cells. Light and oxyluciferin are formed upon the mono-oxygenation of luciferin, which is catalyzed by Ultra-Glo™ Recombinant Luciferase in the presence of Mg<sup>2+</sup> ATP and molecular oxygen. Per well, 100 µl reagent were mixed with the same volume of culture medium. Lysing of the cells took place by 10 min incubation at RT and moderate shaking. In order to avoid luminescence loss opaque-walled 96-plates were used for measurements with Infinite® 200 PRO microplate reader (TECAN). Background signals were identified by including wells containing only medium. Read-outs correlate directly proportional to the ATP amount because cells lose the ability to synthesize this ribonucleotide triphosphate directly after loss of membrane integrity or a cytotoxic event.

### 2.4.3 BrdU ELISA

Furthermore, Colorimetric BrdU Cell Proliferation ELISA from Roche Diagnostics GmbH (Mannheim/Germany) to quantitate cell proliferation based on the measurement of BrdU incorporation during DNA synthesis in proliferating cells, was used. BrdU labeling was performed directly after the blue light irradiation adding 10  $\mu$ M BrdU for 24 hours at 37°C and 5% CO<sub>2</sub>. After 24 hours incubation time, the labeling medium was aspirated and cells were fixed for 30 minutes, while the DNA was denatured. This enabled an increased accessibility for the anti-BrdU antibody, which was incubated for 90 minutes, while free, unbound antibodies were removed by three subsequent washing steps with 1x PBS. As the antibody was conjugated to peroxidase, tetramethyl-benzidine was added for 3 minutes. Then, the reaction was stopped with 1M H<sub>2</sub>SO<sub>4</sub>. Infinite® 200 PRO microplate reader (TECAN) was used to quantify immune complexes at 450 nm with a reference reading at 690 nm. The test was performed only during the differentiation process (1° set-up) on day: 0-2-6-10-14. For each time point two replicates for two repetitions were done.

## 2.5 Mitochondrial function – ROS generation

Generation of mitochondrial ROS mainly takes place at the electron transport chain located on the inner mitochondrial membrane during the process of oxidative phosphorylation (OXPHOS).

Since mitochondria are potential targets and initiators of the blue light's photosensitization processes, the amount of intracellular ROS was quantified following irradiation.

### 2.5.1 Quantification of intracellular ROS

2',7' –dichlorofluorescein diacetate (DCFDA) (MERCK) was used to measure intracellular ROS. DCFDA is a fluorogenic dye that measures hydroxyl, peroxy and other reactive oxygen species (ROS) activity within the cell. After diffusion into the cell, DCFDA is deacetylated by cellular esterases to a non-fluorescent compound, which is later oxidized by ROS into 2',7' –dichlorofluorescein (DCF). DCF is a highly fluorescent compound which can be detected by fluorescence spectroscopy with excitation / emission at 485 nm / 535 nm. After the irradiation, cells were washed in PBS. DCFDA was added at the concentration of 20  $\mu$ M for 45 minutes in medium serum-free to avoid false results from esterases contained in it. At the end of incubation time, cells were washed in PBS and fluorescent signal measured with Infinite® 200 PRO microplate reader (TECAN).

### 2.6 RNA-Isolation

RNA was extracted using the RNeasy Lipid Tissue Mini Kit (Qiagen). The lysis step was adapted to cell culture by adding 55.5µl of Qiazol into each well. The other steps were performed following manufacturer's protocol. RNA concentration and quality were measured using a Spark™ 10M multimode microplate reader. In addition RNA purity was determined by measuring the absorbance ratio at A260/280 with acceptable values of 1.7 – 2.1. RNA integrity was assessed by capillary electrophoresis on Agilent 2100 Bioanalyzer (Agilent Technologies, CA, USA) and RNA integrity number (RIN) was calculated by a specific Agilent software tool. Only samples with RIN values higher than or equal to 7.0 were used for gene expression analysis.

### 2.7 Gene expression

Gene expression analysis is a widely used tool in biology and medicine that can provide information about the expression of genes in different tissues or under certain conditions. In this study, the effect of blue light irradiation on gene expression was investigated using RNA sequencing techniques.

#### 2.7.1 RNA sequencing

RNA sequencing was done by BGI Tech Solutions Co. (Hong Kong). For RNA sequencing, three RNA samples per condition (irradiated and no-irradiated) were analyzed by using the BGISEQ-500 method.

#### 2.7.2 Bioinformatic evaluation

To analyse the RNA sequencing data the RBioconductor software was used. Data Alignment was done by Rsubread software. For annotation the entrez-based software package TxDb.Hsapiens.UCSC.hg19.knownGene was used and differential Gene Expression Analysis was performed by a DESeq2 package. As a level of the significance  $\alpha = 0.05$  with FDR correction was chosen. The normalized enrichment score (NES) is the primary statistic for examining gene set enrichment results. By normalizing the enrichment score, GSEA accounts for differences in gene set size and in correlations between gene sets and the expression

## Material and Methods

dataset; therefore, the normalized enrichment scores (NES) can be used to compare analysis results across gene sets. GSEA was performed to determine statistically differences between blue light irradiation and no-light controls. Pathway analysis was done with the help of the public external KEGG database to transform the list of individual genes into a set of pathways.

## 3 Results

### 3.1 Adipogenic differentiation

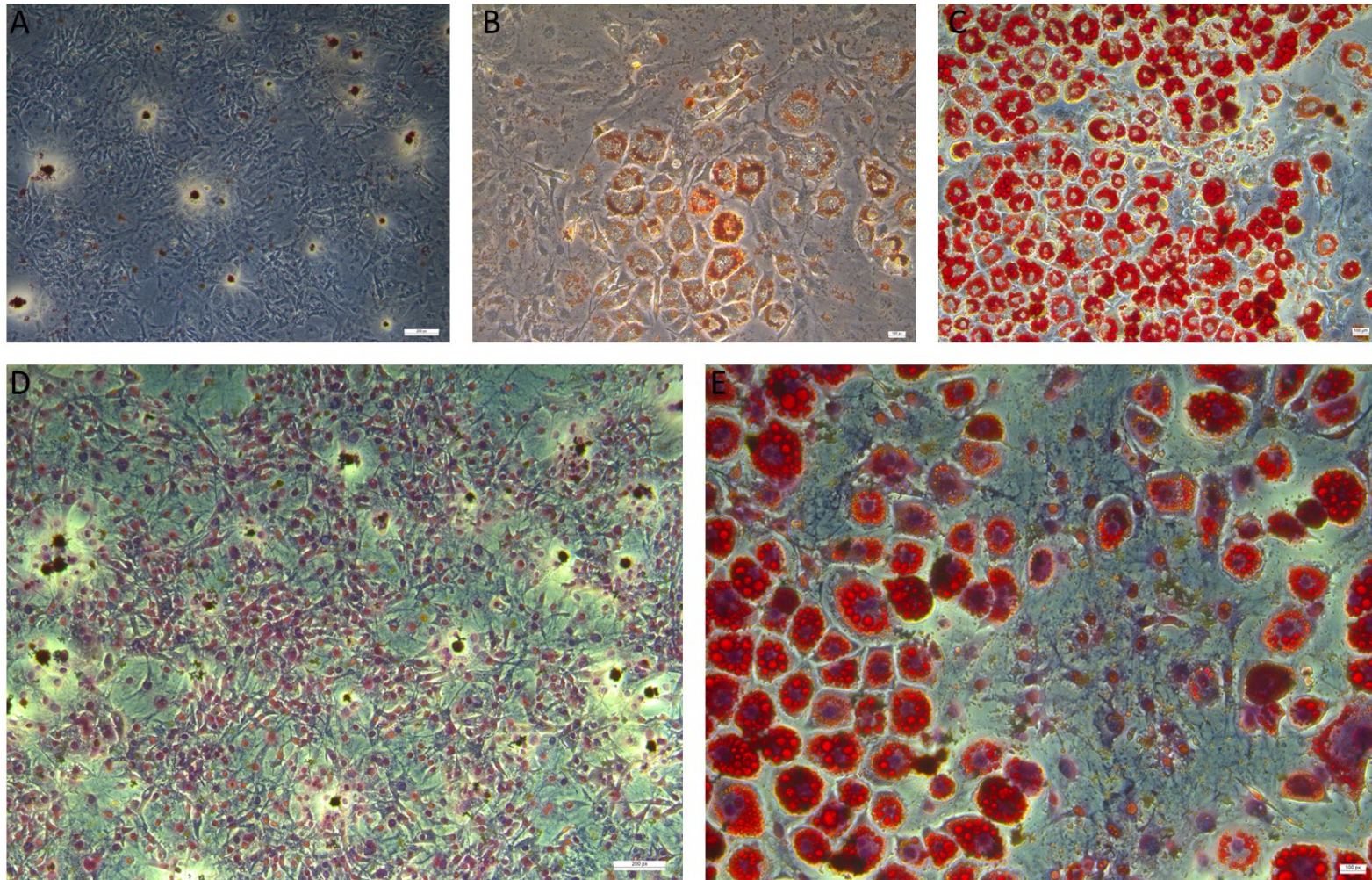
The first differentiation tests were conducted in 25cm<sup>2</sup> flasks. The 3T3-L1 were seeded at a density of 2000-3000 cells/ cm<sup>2</sup> and treated for adipogenic differentiation for 14 days. During this period the cells were observed and, at predetermined times, stained with Oil Red O and photographed under an optical microscope. (Figure 12 A-C)

The control is represented by cells maintained in complete DMEM without inductor factors. In 3T3-L1 cultures induced to adipogenic differentiation it is possible to observe that, after 6 days (Day 5) of treatment with the medium supplemented with inductor factors, the cells begin to lose the typical fibroblastic conformation that characterizes the control cultures and the appearance of small intracellular droplets, mostly located in a peripheral position along the cytoplasmic membrane. On Day 9, under stimulation, the cells continue to accumulate lipids in the form of intracellular drops. (Figure 13)

From day 10, the adipogenic induction medium is replaced with the maintenance medium that allows adipogenic differentiation to be maintained and completed. After 14 days of treatment most of the cells are positive for Oil Red O staining, the 3T3-L1 cytoplasm is entirely occupied by large intracellular staining positive deposits and the nucleus undergoes a peripheral shift. The increase in the number of intracellular drops causes most cells to show a cytoplasm rich in lipid deposits. The 3T3-L1 cell cultures used as control do not show the appearance of the drops at any of the times examined and in fact they are negative for Oil Red O staining; they maintain the fibroblast-like shape and the nucleus is clearly evident in the centre of the cells. These differences are marked by a combined staining of Haematoxylin/ Eosin and Oil Red O (Figure 12 D-E). Subsequently, in order to choose the experimental number of starting cells, various tests were conducted in which the cells were plated at different densities and treated according to the adipogenic differentiation protocol. Based on the results obtained, it was established that the initial density of 1200 cells/cm<sup>2</sup> is the one that best supports the adipogenic differentiation of 3T3-L1 according to the type of plate used as black 96-well plate.



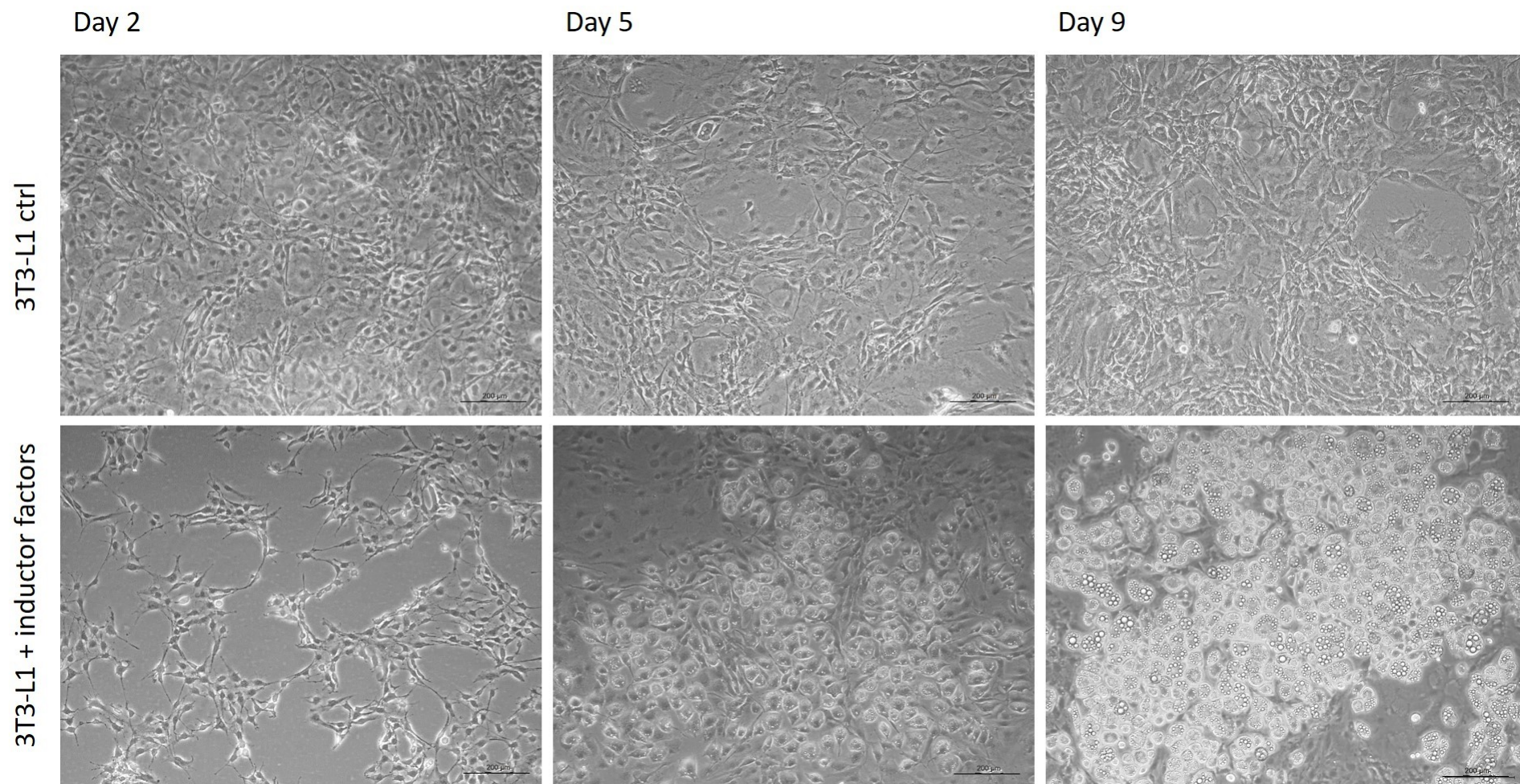
## Results



**Figure 12 :Oil Red O staining shows changes during different stages of adipogenesis A) no-induced 3T3-L1 negative to Oil Red O staining, induced 3T3-L1 positive to Oil Red O B) at day 5 and C) at day 14. Nuclei and cytoplasm are stained with Hematoxylin and Eosin in D) no-induced 3T3-L1 and E) induced and completely differentiated adipocytes.**



## Results



**Figure 13: Morphological changes during adipogenesis.** The control is represented by no stimulated 3T3-L1 cells. 3T3-L1 cells treated with inducer factors show accumulation of lipid droplets and morphology changes from spindle shape to rounded shape.

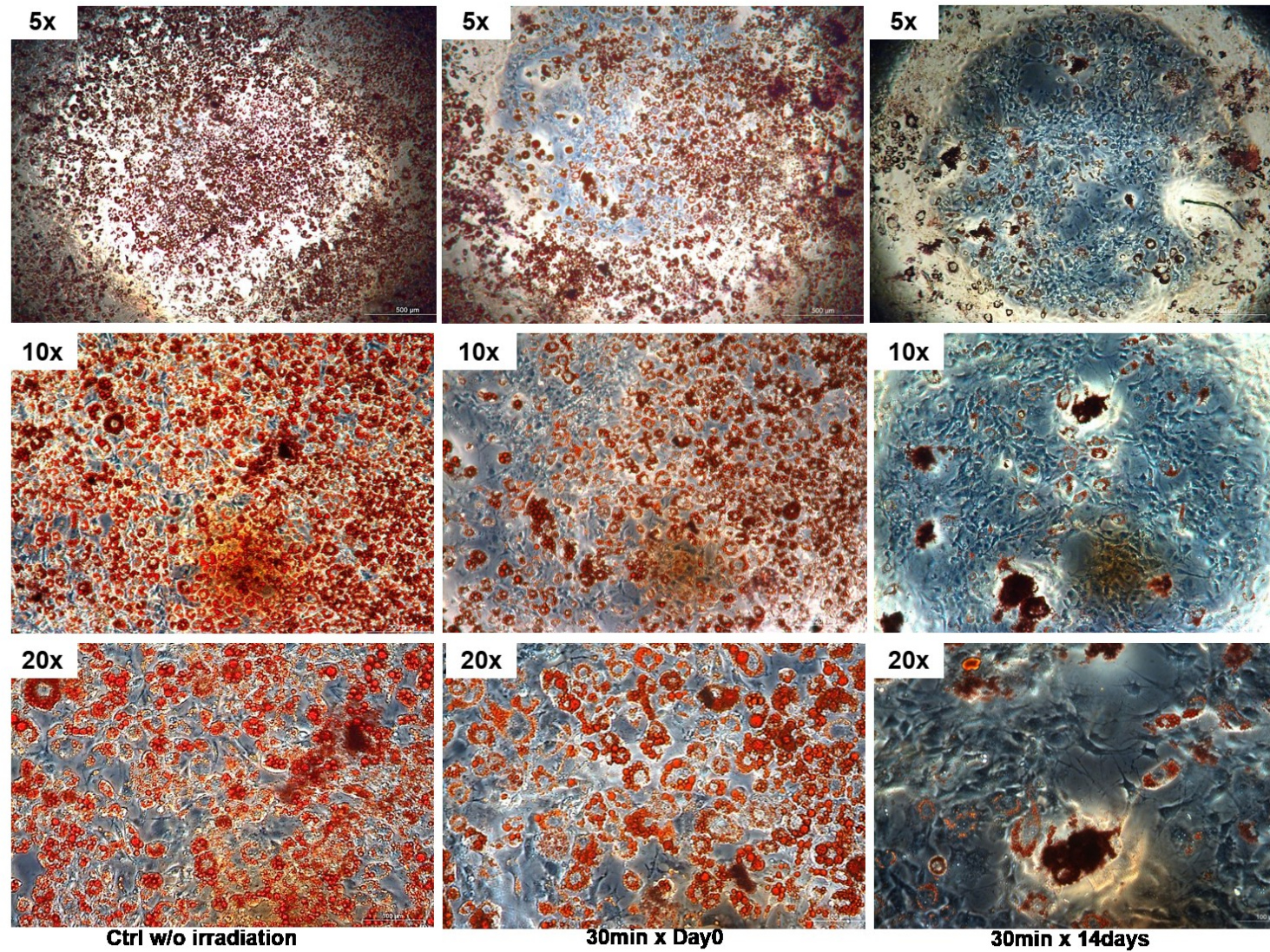
### 3.2 Oil Red O quantification

Since intracytoplasmic lipid accumulation seems to be directly proportional to the extent of differentiation, Oil Red O staining was performed at the last day of the experiment after cell fixation and examined under a light microscope. Three different microscopic fields (5x, 10x and 20x magnifications) per culture were photographed (Figure 14). A first microscopic analysis showed that a normal and complete differentiation took place in non-irradiated cultures (controls) where almost all the cells appeared as mature adipocytes. A decrease in the percentage of positive cells to the staining came up in irradiated cultures depending on the number of treatments. Cells irradiated at Day0 appeared partially differentiated compared to daily irradiated cells that looked still like fibroblasts.

Recently, Oil Red O staining is also being used for quantitative analysis of adipocyte differentiation. To enable quantitative measurements, the dye is commonly eluted from the cells using 2-propanol, and absorbance is photometrically determined at 510 nm. Figure 15 shows the negative trend related to the lipid amount after dye extraction. After a single or multiple treatments a decrease of 17% ( $p<0.0001$ ) and 38% ( $p<0.0001$ ) was respectively found at Day0 and after 14 days. These results suggest that blue light can modulate the differentiation process probably causing a stop of it; this is also reflected in reduced lipid accumulation in treated cultures.

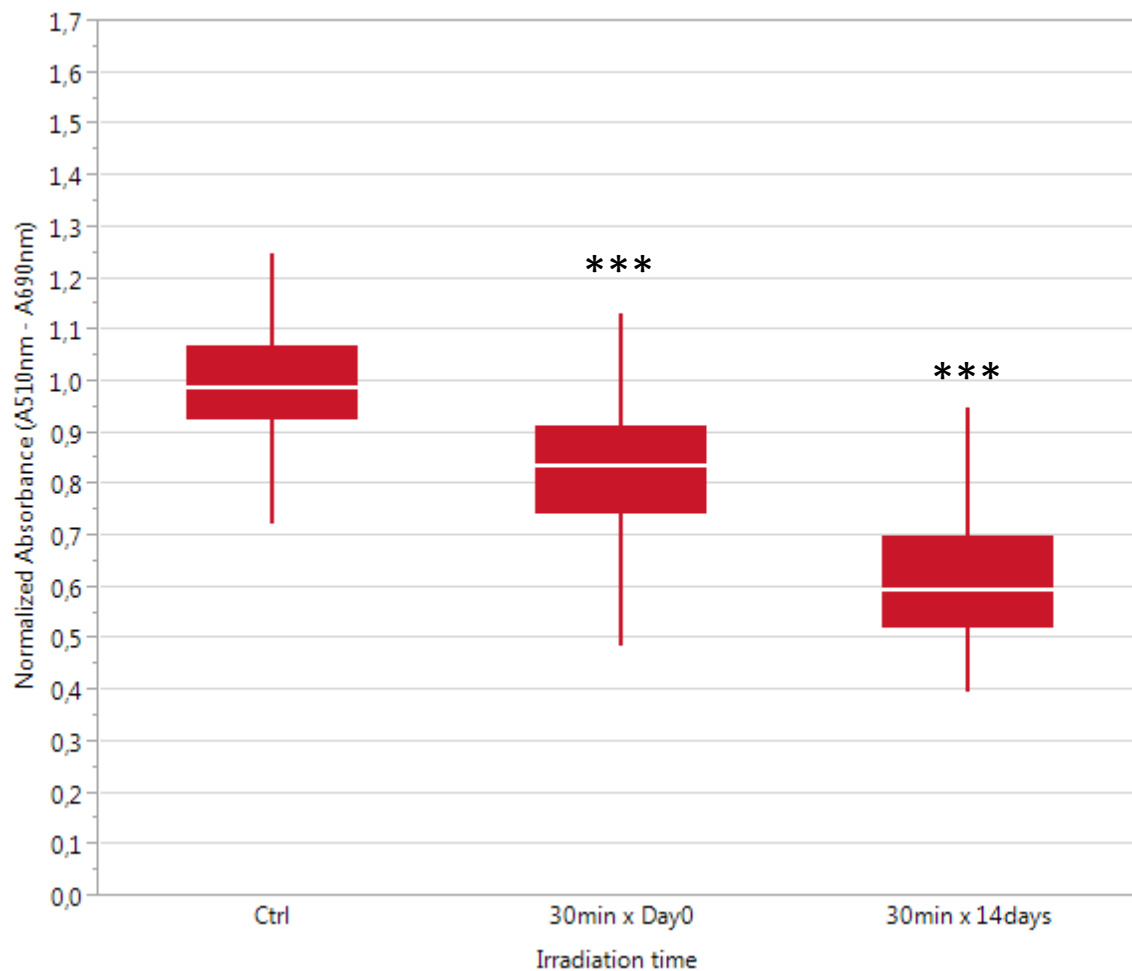


## Results



**Figure 14: Oil Red O staining.** Different microscopic fields show the effect of blue light treatment during differentiation process. Single or multiple irradiation lead to reduced cellular differentiation. Cells irradiated for 14 days still appear in their fibroblastic shape.

## Results

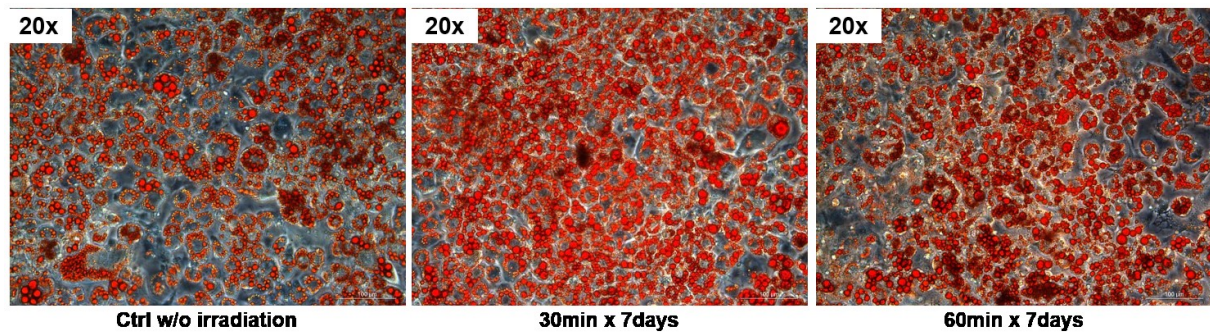


**Figure 15: Oil Red O quantification of differentiating 3T3-L1 cells. Comparison of quantitative staining of wells treated with blue light on Day0 or for 14 days.** Data are shown as box plots with the median, upper and lower quartile (interquartile range (IQR)) and whiskers (1.5 x IQR). Each box plot represents 3 repetitions x 3 replicates. Statistical significance was determined with the parametric Student t-test. Values significantly different from control are indicated as \*\*\* $p < 0.0001$

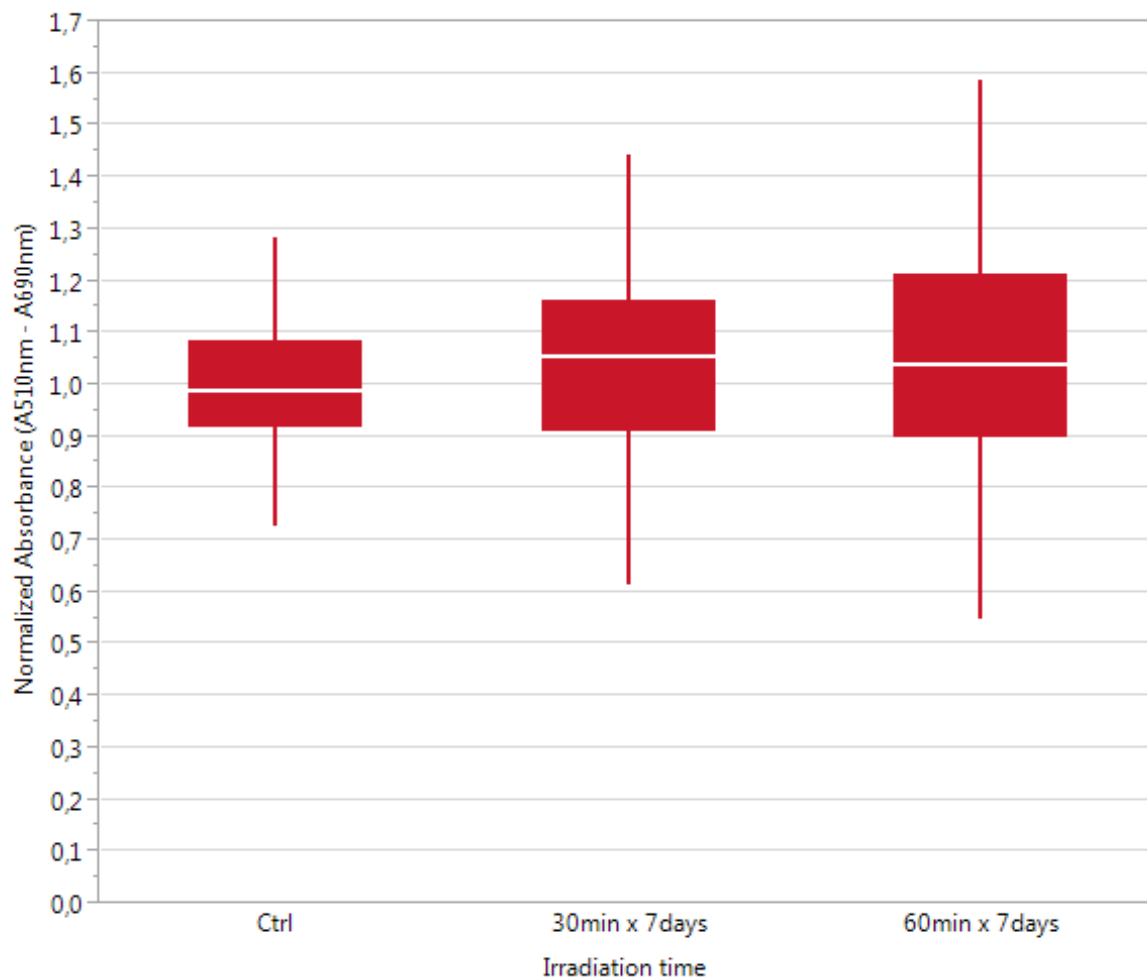
The staining was performed also on mature adipocytes irradiated for 30 or 60 minutes for 7 days. Oil Red O was eluted and quantify in the same way above. The microscope analysis did not reveal significant differences between controls and treated samples (Figure 16). Only a slight increase around 5% in lipid amount was shown in cultures irradiated for 30 minutes ( $p=0.0419$ ) or 60 minutes ( $p=0.0637$ ) after Oil Red O quantification. Light irradiation has not shown effects on lipid loss in mature adipocytes even suggesting a slight, though not significant, increase of them. (Figure 17)



## Results



**Figure 16: Oil Red O staining. No effect of blue light treatment after differentiation process.**



**Figure 17: Oil Red O quantification of mature adipocytes. Comparison of quantitative staining of wells treated with blue light for 30 or 60 minutes after complete differentiation.** Data are shown as box plots with the median, upper and lower quartile (interquartile range (IQR)) and whiskers (1.5 x IQR). Each box plot represents 3 repetitions x 3 replicates. Statistical significance was determined with the parametric Student t-test.

## Results

### **3.3 Assessment of blue light effects on cell metabolism assays**

Changes in the metabolism following blue light irradiation were assessed during and after adipogenic differentiation of 3T3-L1 cells. Metabolism was studied based on the activity of mitochondrial enzymes and ATP concentration in cell cultures.

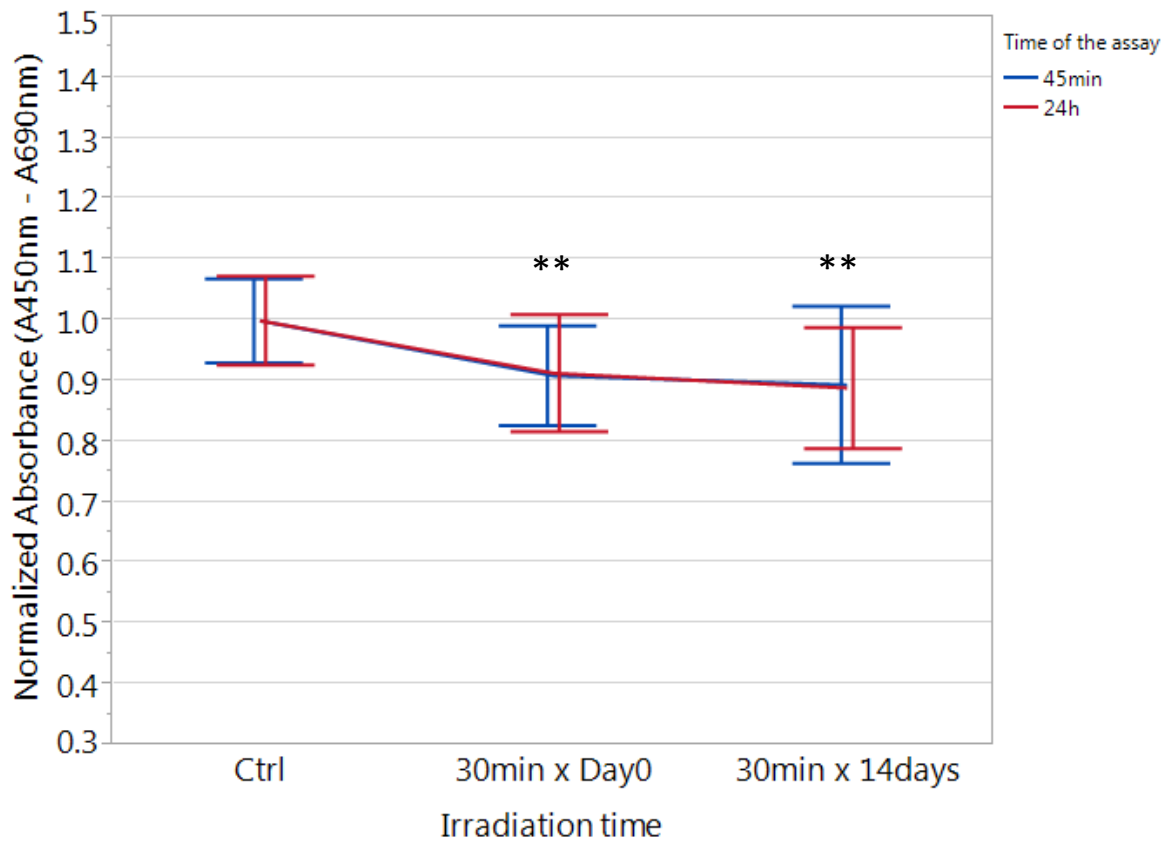
#### **3.3.1 XTT results are affected by blue light irradiation during but not after differentiation phase**

XTT assays were performed to analyse changes in cell metabolism induced by blue light irradiations. Viable cells metabolize the XTT reagent and the product is measured spectrophotometrically. To assess the duration of the effects over time, XTT tests were performed after two different time points: directly after the last irradiation (45 min, XTT incubation time) or 24 hours later.

To see the inhibitory effects of blue light, for this study the irradiation time of 30 minutes ( $21.6 \text{ J/cm}^2$ ) was tested during the differentiation process irradiating the cells only the first day (Day0) or for 14 days under adipogenic stimuli.

As shown in the figure 18, already 45 min after the last irradiation a metabolism decrease was observed by 9% ( $p < 0.001$ ) with a single irradiation on Day0 and slightly pronounced effect till 10% ( $p < 0.001$ ) for multiple irradiations. No recovery in metabolism occurred after 24 hours as evidenced by an almost perfect matching of the results.

## Results



**Figure 18: Changes in metabolic activity of 3T3-L1 cells.** Blue light treatments were performed with 21.6 J/cm<sup>2</sup> at Day0 or for 14 days. XTT tests were carried out 45min or 24h following the last irradiation. Fold changes were evaluated versus time matched, no-irradiated controls. Data are represented as mean  $\pm$  SD (N = 3 repetitions, 3 replicates). Statistical significance was determined with the parametric Student t-test. Values significantly different from control are indicated as \*\*p<0.001.

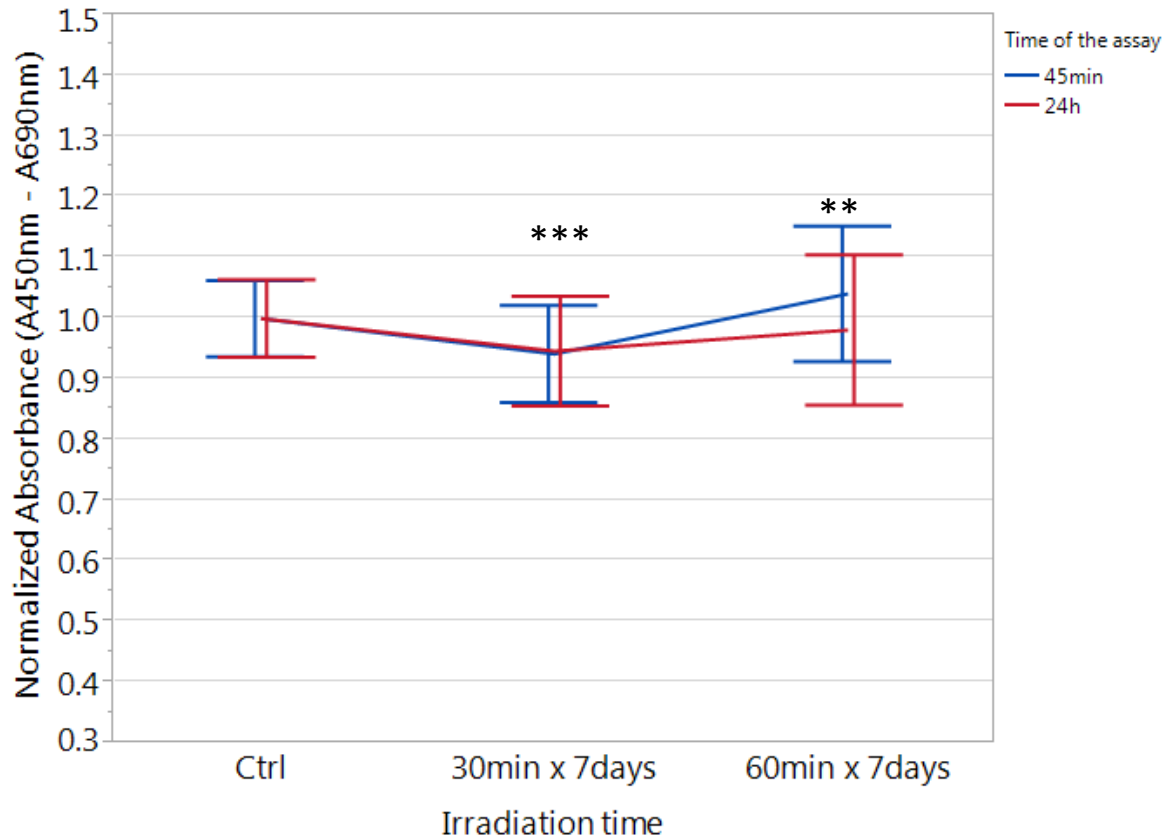
After complete differentiation, 3T3-L1/adipocytes were irradiated from Day15 for the following 7 days, for 30 (21.6 J/cm<sup>2</sup>) or 60 (43.2 J/cm<sup>2</sup>) minutes. To evaluate the effects of blue light in the short or long time, XTT tests were performed at Day21 directly after last irradiation or 24h later on.

As shown in figure 19, directly after the last irradiation (45min, XTT incubation time) cells irradiated for 30 or 60 minutes have a different behaviour. While the shortest irradiation leads to a decrease in the metabolism of around 6% (p<0.0001), the longer irradiation showed an increase in cell metabolism of 4% (p=0.0007) compared to the control with a difference of 10% (p<0.0001) compared to 30 minutes irradiation.

After 24h the situation seems to be recovered for the longer irradiation; the treated cells differ from the control by an insignificant decrease of 1.8% (p = 0.095). Instead 30 minutes irradiation showed the same trend after 24h, a decrease of 5.3% (p<0.0001), suggesting that

## Results

this irradiation time, compared to the longer irradiations, can lead to stronger and irreversible metabolic effects, at least for 24h.



**Figure 19: Changes in metabolic activity in mature adipocytes.** Blue light treatments were performed for 7 days after differentiation for 30 or 60 minutes equivalent to doses of 21.6 J/cm<sup>2</sup> and 43.2 J/cm<sup>2</sup>. XTT tests were carried out 45min or 24h following the last irradiation. Fold changes were evaluated versus time matched, non-irradiated controls. Data are represented as mean ± SD (N = 3 repetitions, 3 replicates). Statistical significance was determined with the parametric Student t-test. Values significantly different from control are indicated as \*\*p<0.001, \*\*\*p<0.0001.

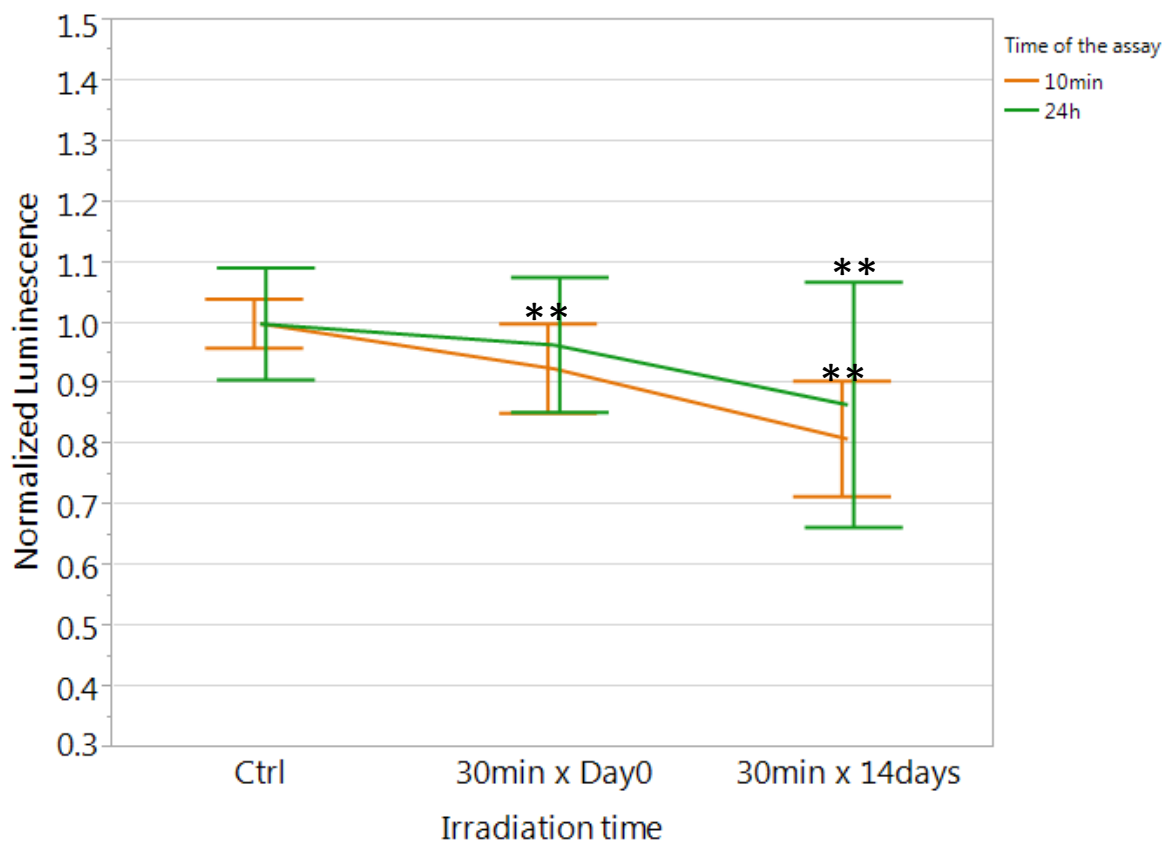
### 3.3.1.1 Single or multiple blue light exposures at 21.6 J /cm<sup>2</sup> during differentiation lead to lead to a decreased in the ATP concentration while an opposite trend is reported in mature adipocytes

A second metabolic test related to viability and cell number was performed to confirm the results obtained using the XTT tests. Since ATP plays an important role in energy exchange in biological systems such a measurement is fundamental to study living processes and mitochondria activity. A bioluminescent method for ATP quantification was chosen.

As shown in figure 20, 30min of irradiation of maturing 3T3-L1 cells led to a decrease in ATP concentration directly after the last irradiation (10min, ATP incubation time) in both

## Results

treatment conditions. A drop around 7% ( $p < 0.001$ ) was recorded in samples irradiated at the first day of induction (Day0) and a more prominent effect was reached, around 20% ( $p < 0.001$ ), for multiple and consecutive irradiations. Even though changes in ATP levels represent a fast response, the effect mediated by blue light last over time following the same trend after 24h, though signs of recovery were observed. After 24h ATP levels were reduced by 3% ( $p = 0.094$ ) and by 13% ( $p < 0.001$ ) after single or multiple irradiations.

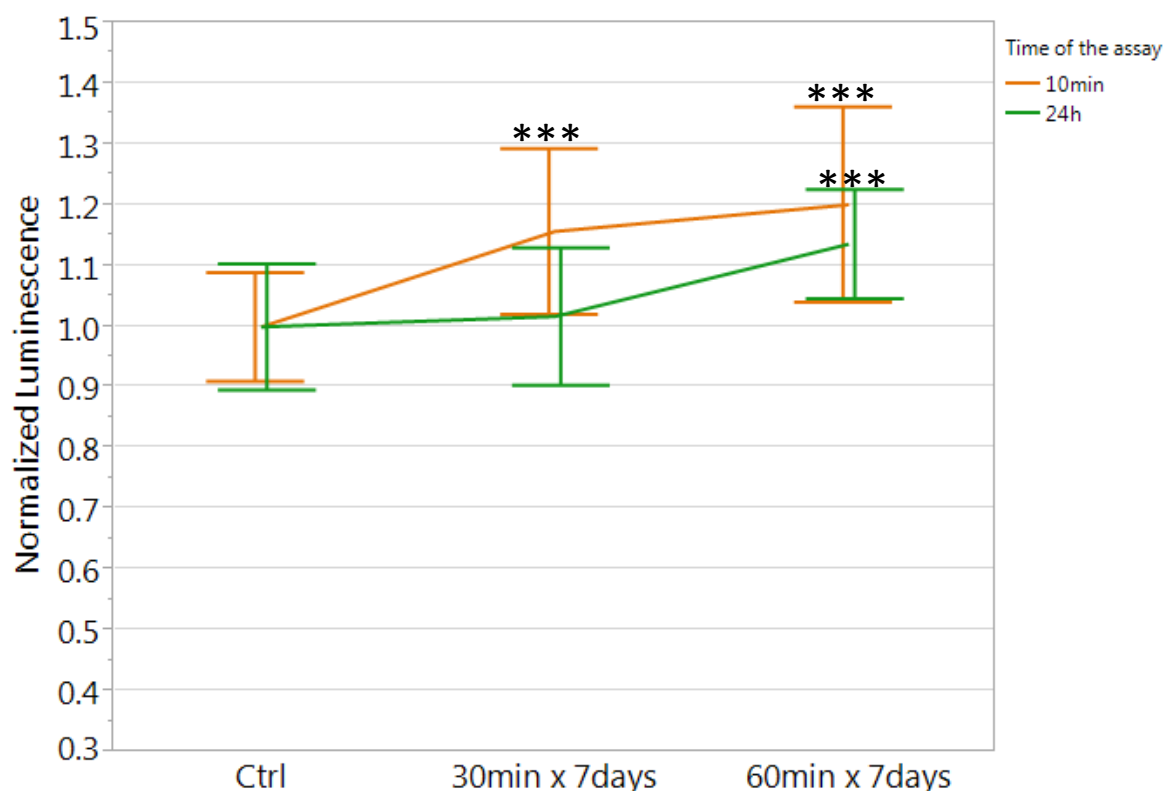


**Figure 20: Changes in ATP concentration in 3T3-L1/preadipocytes during the differentiation process.** Blue light treatments were performed with  $21.6 \text{ J/cm}^2$  at Day0 or for 14 days. ATP levels were quantified 10min or 24h following the last irradiation. Fold changes were evaluated versus time matched, non-irradiated controls. Data are represented as mean  $\pm$  SD (N = 3 repetitions, 3 replicates). Statistical significance was determined with the parametric Student t-test. Values significantly different from control are indicated as \*\* $p < 0.001$

Multiple exposures at different blue light doses on mature adipocytes showed an increase in their ATP levels (Figure 21). Following 30 or 60 minute of irradiation for 7 consecutive days, cells have risen the ATP amount in a dose dependent way with a growth of 15% and 20% ( $p < 0.0001$ ) respectively after 30 and 60 minutes of treatment when the quantification was performed directly after the last irradiation.

## Results

After 24h, cells irradiated for 30 minutes restored basal ATP levels; the same cannot be argued for longer irradiations. Although ATP amount decreased over time after 24h, the levels stayed higher than control with an increase equal to 13% ( $p<0.0001$ ) in cells daily irradiated for 60 minutes.



**Figure 21: Changes in ATP concentration in 3T3-L1/differentiated cells (mature adipocytes).** Blue light treatments were performed for 7 days after differentiation for 30 or 60 minutes equivalent to doses of  $21.6 \text{ J/cm}^2$  and  $43.2 \text{ J/cm}^2$ . ATP levels were quantified 10min or 24h following the last irradiation. Fold changes were evaluated versus time matched, non-irradiated controls. Data are represented as mean  $\pm$  SD (N = 3 repetitions, 3 replicates). Statistical significance was determined with the parametric Student t-test. Values significantly different from control are indicated as \*\*\* $p<0.0001$

### 3.4 Assessment of blue light effects on cell proliferation

#### 3.4.1 Chronic blue light exposure reduced cell proliferation rate during adipogenesis

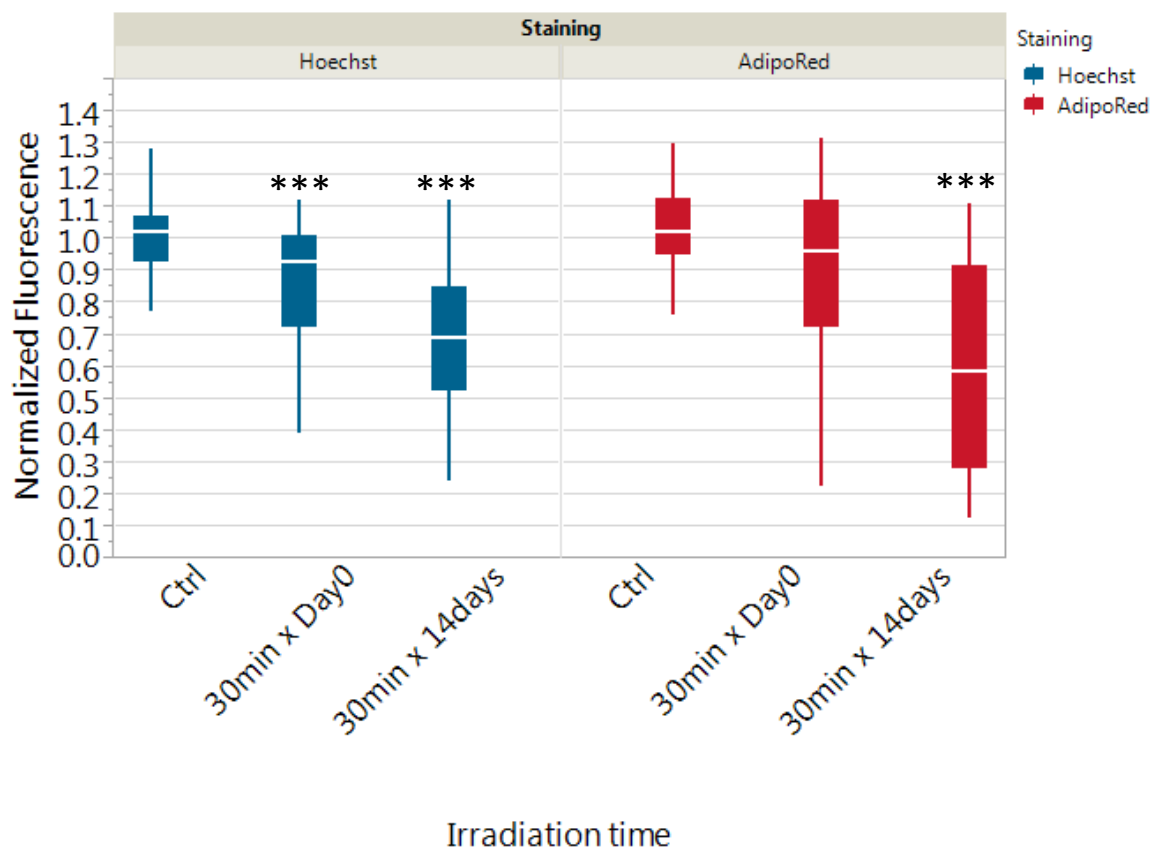
Considering the difficulty in trypsinizing and detaching cells when differentiation process is triggered, no cell count in an ordinary way was possible. To overcome this problem, a quantitative estimation of the cells number was made by staining the nuclei with Hoechst dye. After treatment with blue light, cells were fixed, stained and the fluorescence was read out spectrophotometrically. Significant results were obtained for cells treated during



## Results

adipogenesis. Treatment of 30 minutes of blue light at Day0 showed a fluorescence reduction of 13% ( $p < 0.0001$ ) and of 31% ( $p < 0.0001$ ) for daily treatments compared to control. This can be correlated to a reduced cells number.

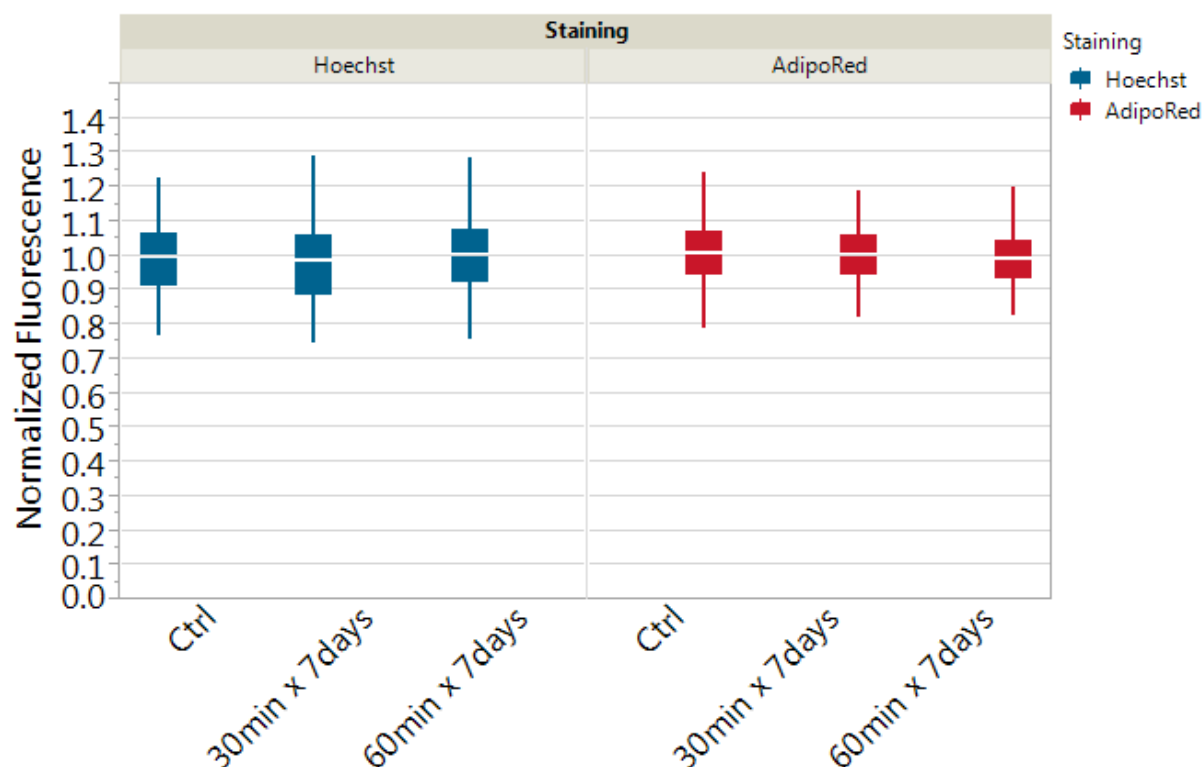
A second lipid-specific staining was used to confirm the results obtained from the Oil Red O extraction. AdipoRed assay was conducted on the same cells previously stained with Hoechst. A reduction in cellular lipids, as previously highlighted by Oil Red O staining, was noted. Compared results between cell number and lipid amount are shown in the figure 22.



**Figure 22: Comparison between nuclei quantification (Hoechst) and lipid accumulation (AdipoRed) during adipogenesis.** Data are shown as box plots with the median, upper and lower quartile (interquartile range (IQR)) and whiskers (1.5 x IQR). Each box plot represents n=3 repetitions x 3 replicates. Statistical significance was determined with the parametric Student t-test. Values significantly different from control are indicated as \*\*\* $p < 0.0001$

## Results

In contrast, treatments on mature adipocytes showed no significant changes in cell count or lipid amount (Figure 23).



**Figure 23: Comparison between nuclei quantification (Hoechst) and lipid accumulation (AdipoRed) in irradiated adipocytes.** Data are shown as box plots with the median, upper and lower quartile (interquartile range (IQR)) and whiskers (1.5 x IQR). Each box plot represents n=3 repetitions x 3 replicates. Statistical significance was determined with the parametric Student t-test.

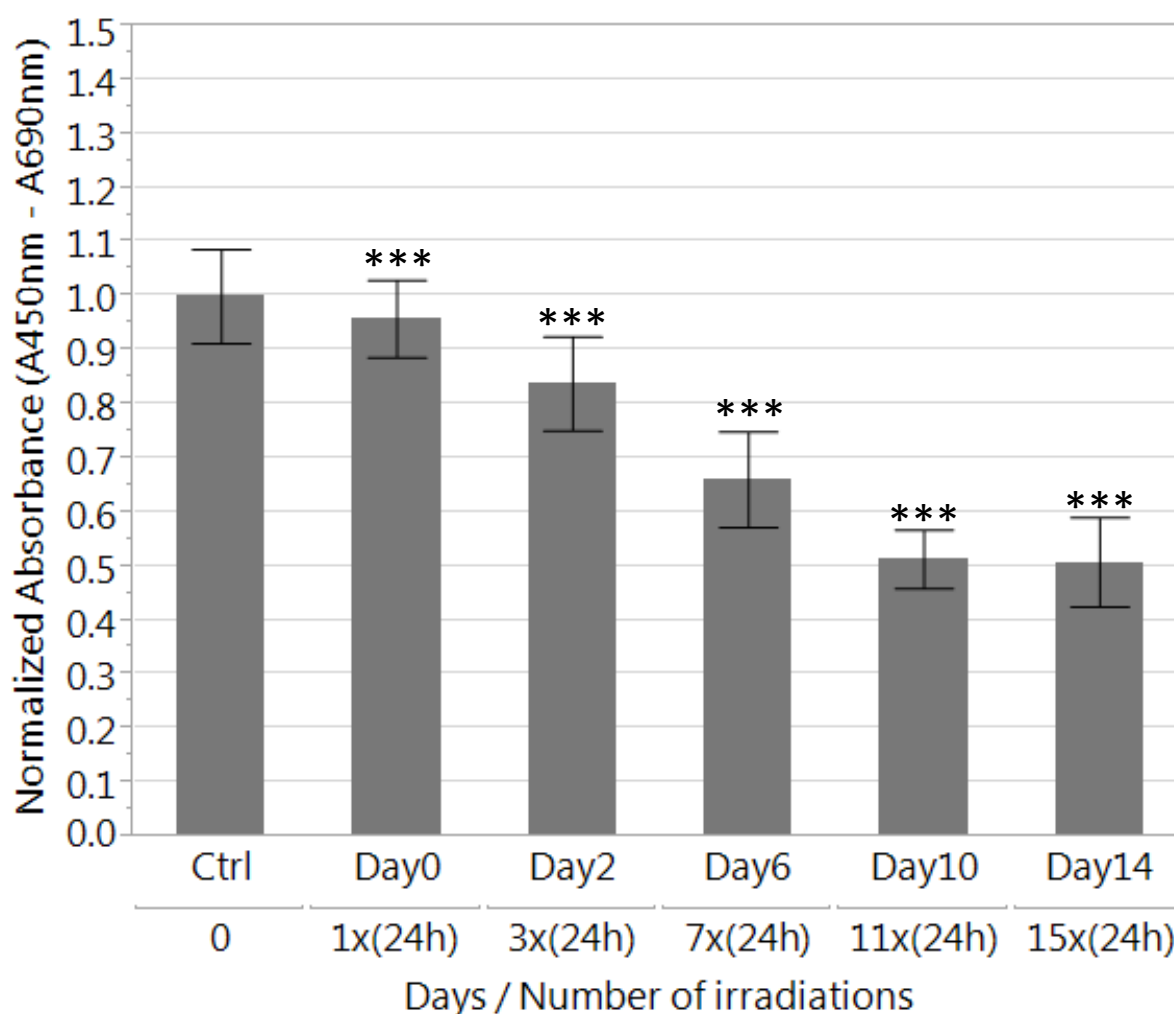
### 3.4.2 BrdU tests showed a linear decrease of DNA synthesis after consecutive irradiations

In order to confirm the anti-proliferative effects of the dose of  $21.6 \text{ J/cm}^2$ , a colorimetric Elisa test based on BrdU incorporation was performed at different harvesting times after 30min of blue light irradiation. As the doubling time of 3T3-L1 cells is 21h, an effect on BrdU incorporation was not expected in shorter times. After the irradiation BrdU was added on Day0, Day2, Day6, Day10 and Day14 to follow the trend of the proliferation rate and outcomes were read out after 24h.

Compared to the untreated control, DNA synthesis diminished in a dose dependent way over the time. Decrease was less pronounced following one irradiation on Day0 with a slight decrease of 4% ( $p < 0.0001$ ). This effect enhanced to 16% ( $p < 0.0001$ ) with three consecutive

## Results

irradiations accounting for  $64.8 \text{ J/cm}^2$  total dosage ( $3 \times (24\text{h})$ ), whereas 7 irradiations, yielding a dosage of  $151.2 \text{ J/cm}^2$  ( $7 \times (24\text{h})$ ), led to a reduction of 33% ( $p < 0.0001$ ). Maximum reduction of 48% ( $p < 0.0001$ ) is obtained after 11 consecutive irradiations, dosage of  $237.6 \text{ J/cm}^2$ , after which a plateau is reached as shown on Day14 ( $324 \text{ J/cm}^2$ ) (Figure 24).



**Figure 24: Changes in DNA synthesis in 3T3-L1 cells during the differentiation process.** Consecutive irradiation with  $21.6 \text{ J/cm}^2$  of blue light were performed every 24 hours. BrdU ELISAs were carried out at 24 hours after last irradiation. Fold changes were evaluated versus time- matched, non-irradiated controls. Data are represented as mean  $\pm$  SD (N = 2 repetitions, 2 replicates). Values significantly different from control are indicated as \*\*\* $p < 0.0001$

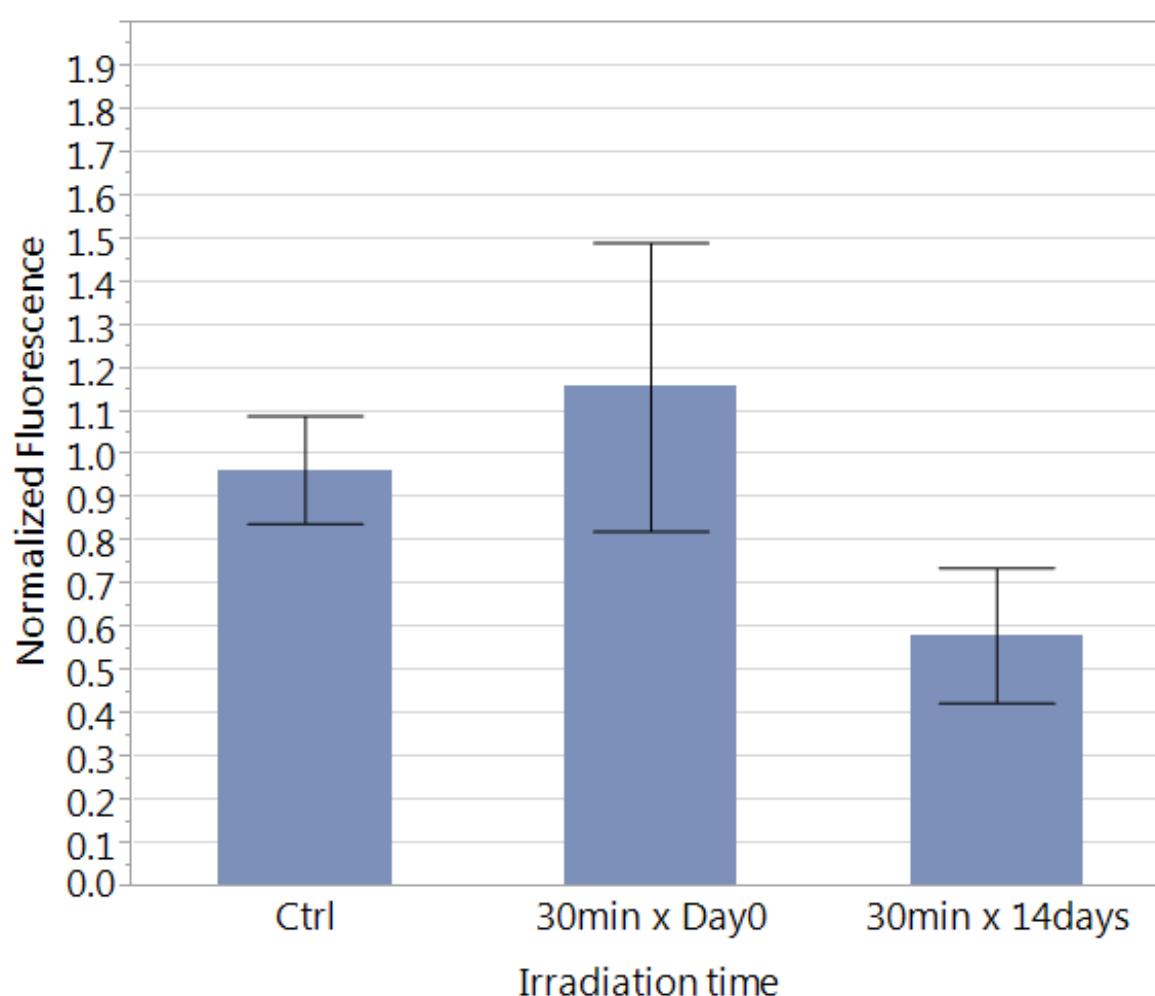
### 3.5 Evaluation of ROS levels

Since reactive oxygen species (ROS) can influence signaling and cell functions, DCFH-DA fluorescent probe was used to measure intracellular generation of  $\text{H}_2\text{O}_2$  and other oxidizers

## Results

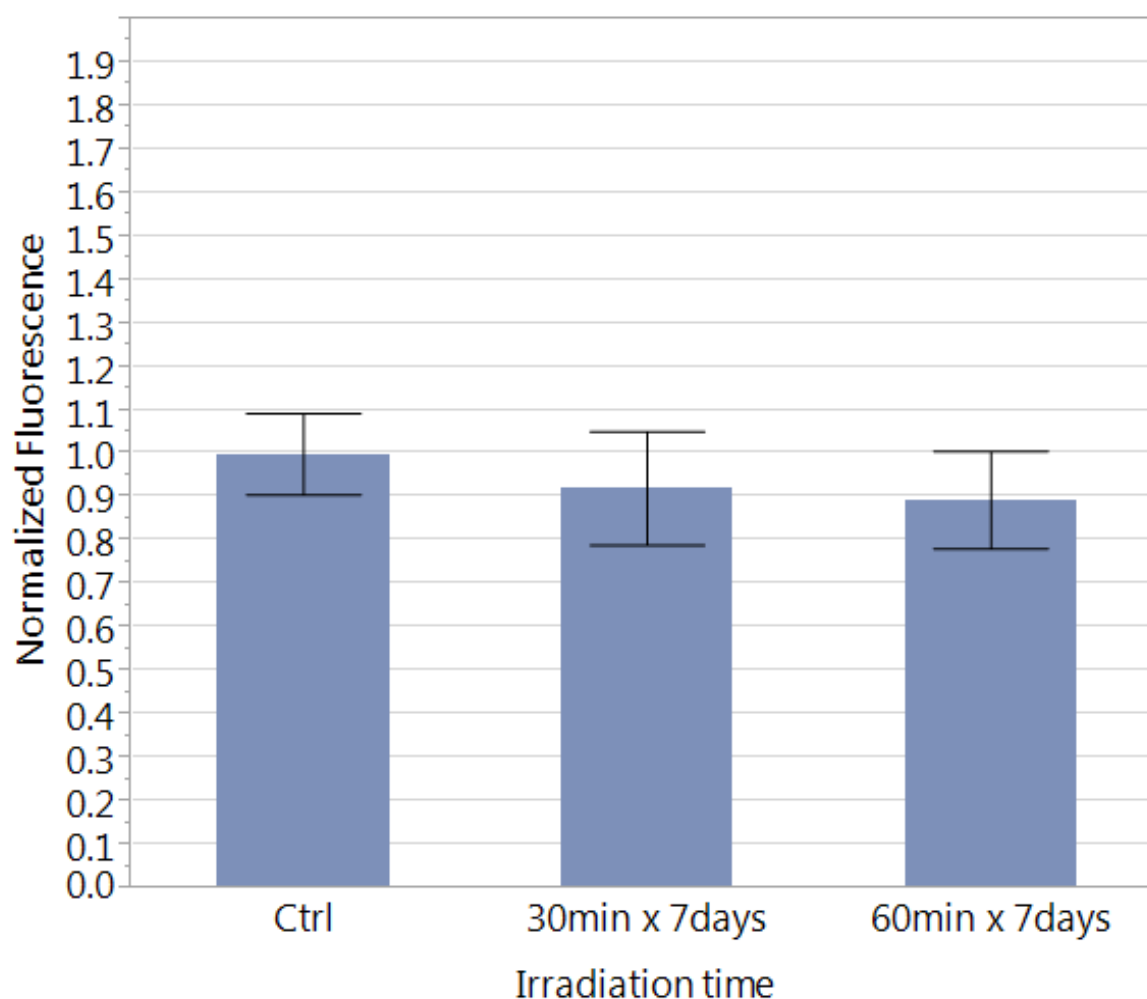
and to monitor changes in redox signalling in response to oxidative stimuli, such as blue light. DCFH-DA was added in serum free medium to the cells after the last treatment.

As evident in figure 25, ROS production increased in cells treated 30min at Day0 but decreased for daily irradiation. The high standard deviation is probably due to the instability of the probe or the capability of the intermediate radical,  $\text{DCF}^\cdot$ , formed from the one-electron oxidation of DCFH, to rapidly react with  $\text{O}_2$  to produce anion superoxide. The dismutation yields additional  $\text{H}_2\text{O}_2$ , which can establish a redox-cycling mechanism leading to artificial amplification of the fluorescence signal intensity.



**Figure 25** Changes in ROS levels of 3T3-L1 cells measured directly after the last irradiation to  $21.6 \text{ J/cm}^2$ . DCFH-DA probe was excited at  $\lambda_{\text{Ex}} = 485 \text{ nm}$ , while its fluorescence emission was measured at  $\lambda_{\text{Em}} = 535 \text{ nm}$ . Fold changes were evaluated versus time- matched, non-irradiated controls. Data are represented as mean  $\pm$  SD (N = 2 repetitions, 2 replicates).

More stable results were obtained on mature adipocytes. The irradiation with 30 or 60 minutes did not lead to an increase of ROS production as instead was expected (Figure 26).



**Figure 26: Changes in ROS levels of differentiated adipocytes measured directly after the last irradiation to 21.6 J/cm<sup>2</sup> and 43.2 J/cm<sup>2</sup>.** DCFH-DA probe was excited at  $\lambda_{\text{Ex}} = 485$  nm, while its fluorescence emission was measured at  $\lambda_{\text{Em}} = 535$  nm. Fold changes were evaluated versus time- matched, no-irradiated controls. Data are represented as mean  $\pm$  SD (N = 2 repetitions, 2 replicates).

### 3.6 Gene expression

#### 3.6.1 Gene expression analysis

Following irradiation, time-dependent changes in the gene expression were studied for both set ups. Cells were harvested and RNA extracted after the last irradiation, respectively at day 14 for the first set up and day 21 (7<sup>th</sup> experimental day) for the second set-up, with three replicates for each condition tested, light-treated and untreated control.

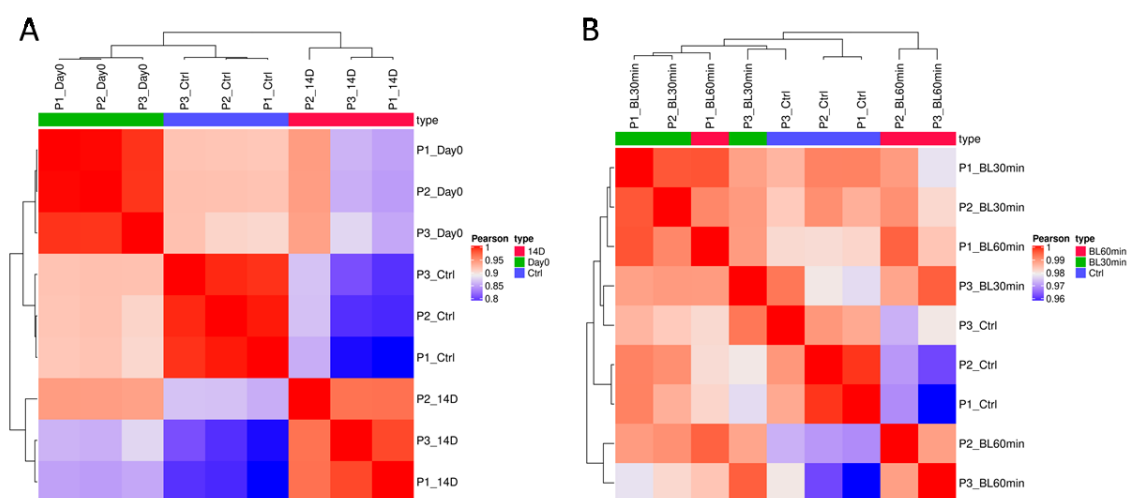
Following distribution analysis and batch normalization for separate experiments, the similarity in gene expression pattern was visualized by the tendency of points to fall near the diagonal, as measured by the Pearson's correlation coefficient. Correlation heatmaps showed

## Results

distribution of the samples in three clusters for the first set up, moreover the dendrogram presented a similar relation between control and irradiated samples at Day0.

In contrast, in the second set up the clustering was not so evident showing an ambiguous relation between the different samples probably due to some problems during the irradiation or RNA extraction (Figure 27).

From this point on, for better exposure and understanding, data from gene expression analysis will be treated separately for the two set-ups.

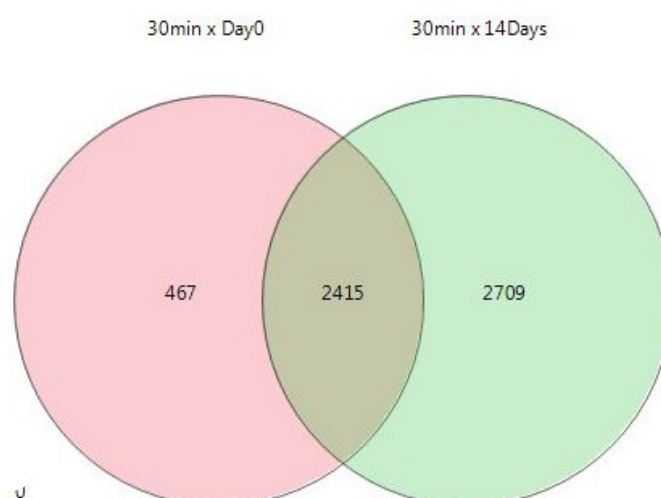


**Figure 27: Representative Pearson's correlation heatmap showing cluster analysis of untreated (control, N= 1 repetition, 3 replicates) and treated samples (N= 1 repetition, 3 replicates) following single or multiple irradiation according to the setting used in each set-up.**

### 3.6.1.1 Gene expression analysis 1° set-up: blue light irradiation on maturing preadipocytes (3T3-L1 cells)

RNA seq screened 24421 genes in total, 5591 significantly expressed (FDR <0.05) only in treated samples. Since the previous tests showed dose-dependent effects, it was investigated whether, in addition to the metabolic response, also gene expression followed the same trend. However, in relation to the number of blue light irradiations, differentially adjusted genes were increased in total number from 2882 de-regulated genes after one day of treatment (Day0), to 5124 genes after 14 days of treatment with 2415 genes triggered commonly (Figure 28). According to the results seen above, this data suggests that probably already a single irradiation on the first day of differentiation can influence the expression of important genes involved in cell differentiation and proliferation.

## Results



**Figure 28:** Venn diagram showing the number of significantly ( $FDR < 0.05$ ) commonly or differentially expressed genes in differentiating 3T3-L1 cells following single (Day0) or multiple (14 days) blue light irradiations.

In the table 2 the number of up- and down-regulated genes is listed for both treatments. Samples irradiated at Day0 have shown a majority number of down-regulated genes, which were even more in samples treated daily. Unlike a single dose of irradiation, 14 irradiations have shown a number of up- or down-regulated genes which did not differ much from each other. The data therefore have shown that treatment with blue light has tended to lower gene expression levels during adipocyte differentiation. However, differential changes emerged after irradiation were present already in the early phase of the differentiation process suggesting the high sensitivity of the cells in this phase with effects that last over the time.

Treatment group	Significantly differentially expressed genes	
	Down-regulated genes	Up-regulated genes
30min x Day0	1965	917
30min x 14Days	2935	2189

**Table 2:** Number of significantly up and down-regulated genes differentially expressed in differentiating 3T3-L1 cells following single (Day0) or multiple (14 days) blue light irradiations.

Thereafter, Gene Set Enrichment Analysis (GSEA) was performed using Kyoto Encyclopedia of Genes and Genomes (KEGG) database to transform the list of individual genes into sets of pathways. Considering a ranked differentially expressed genes a Normalized Enrichment

## Results

Scores (NES) was used to indicate the distribution of the pathway within the list. Negative or positive NES indicates a shift of gene towards the bottom or the top of the list representing respectively down- or up-regulated pathways. Table 3 accounts the number of de-regulated KEGG pathways for both treatment conditions. Starting from a total gene set number equal to 281 for both irradiation times tested, the number of down-regulated pathways for treated samples at Day0 was higher than the up-regulated pathways. Of these de-regulated pathways less than half were significant with a p-value  $< 0.05$  and, although it did not differ much, the number was even more reduced if it was considered an adjusted p-value (FDR) with the same cut-off; these pathways were therefore highly significant. A contrary trend occurred as a result of daily irradiation where up-regulated pathways prevailed over down-regulated pathways. Also in this case the number of significantly regulated pathways (p-value  $< 0.05$ ) was reduced without departing in large numbers from the highly significant ones (FDR  $< 0.05$ ).

Treatment group	30min x Day0	30min x 14Days
De-regulated pathways	281	281
Up-regulated pathways	127	178
with nominal p-value $< 0.05$	36	65
with nominal p-value $< 0.01$	25	42
with adjusted p-value (FDR) $< 0.05$	25	49
Down-regulated pathways	154	103
with nominal p-value $< 0.05$	65	55
with nominal p-value $< 0.01$	55	42
with adjusted p-value (FDR) $< 0.05$	58	45

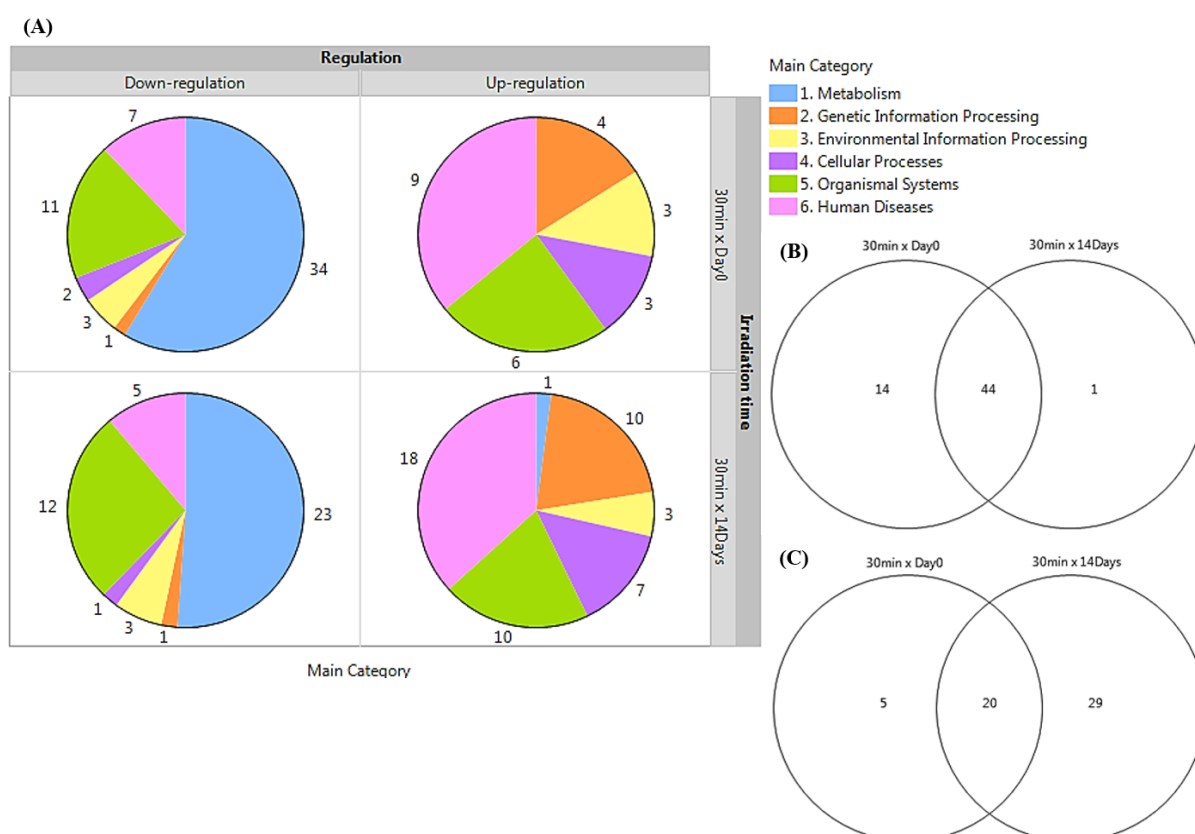
**Table 3: Number of differentially expressed KEGG pathways in differentiating 3T3-L1 cells following single (Day0) or multiple (14 days) blue light irradiations.** Starting from an overall gene set number of 281, total numbers of up- or down-regulated pathways are shown. In addition the number of significantly enriched pathways is listed for different significance levels at nominal p- value  $< 0,05$  or  $< 0,01$  and at adjusted p-value (FDR)  $< 0,05$ .

Only de-regulated pathways with an adjusted p-value (FDR)  $\leq 0.05$  have been taken into account for the subsequent analysis. The pathways were sorted into 6 main categories by KEGG for a simpler observation. This division helps to understand the effects and interactions after blue light treatment (Figure 29). For both irradiation times most down-regulated pathways belong to the Metabolism category. This result confirmed those obtained



## Results









from previous metabolic tests, in which following blue light treatment a reduced metabolic activity was found. Many metabolic pathways were involved in the production or consumption of ATP mostly related to the oxidative phosphorylation process. Oxidative phosphorylation gene set was down-regulated after blue light treatment suggesting mitochondrial damage or dysfunction already at low dose. Related to the main category of Metabolism also the subcategory of Lipid metabolism was found down-regulated reflecting a reduction in lipid production and adipocyte differentiation (Table 4).



**Figure 29: (A) Distribution of significantly enriched pathways ( $FDR < 0,05$ ) sorted by main categories of KEGG. Groups are formed by the respective doses/irradiation times. The numbers around the pie charts indicate the number of deregulated pathways contained in each category. (B) Comparison of significant pathway list with  $NES < 0$  and (C)  $NES > 0$  at different irradiation time.**

## Results

1. Metabolism				
	30min x Day0		30min x 14Days	
	NES	Adjusted p-value	NES	Adjusted p-value
<b>1.0. Global and overview maps</b>				
Metabolic pathways	-2.51	0.001302	-2.55	0.00375
Carbon metabolism	-2.81	0.001302	-2.93	0.002066
2-Oxocarboxylic acid metabolism	-2.12	0.001302	-2.11	0.002951
Fatty acid metabolism	-2.41	0.001302	-2.74	0.002066
Biosynthesis of amino acids	-2.42	0.001302	-2.13	0.002066
<b>1.1. Carbohydrate metabolism</b>				
Glycolysis Gluconeogenesis	-2.36	0.001302	-2.08	0.002066
Citrate cycle (TCA cycle)	-2.51	0.001302	-2.75	0.002066
Pentose phosphate pathway	-2.13	0.001302	-1.96	0.005409
Fructose and mannose metabolism	-2.09	0.001302	-1.61	0.057377
Starch and sucrose metabolism	-1.89	0.00341	-1.73	0.040714
Pyruvate metabolism	-2.44	0.001302	-2.68	0.002066
Glyoxylate and dicarboxylate metabolism	-2.32	0.001302	-2.5	0.002066
Propanoate metabolism	-2.48	0.001302	-2.82	0.002066
<b>1.2. Energy metabolism</b>				
Oxidative phosphorylation	-2.74	0.001302	-2.97	0.002066
<b>1.3. Lipid metabolism</b>				
Fatty acid elongation	-1.67	0.040983	-1.79	0.015703
Fatty acid degradation	-2.22	0.001302	-2.4	0.002066
Steroid biosynthesis	-2.14	0.001302	-2.2	0.002066
Glycerolipid metabolism	-2.16	0.001302	-2.22	0.002066
Glycerophospholipid metabolism	-2.08	0.001302	-2.09	0.002066
Arachidonic acid metabolism	-1.71	0.032653	-1.43	0.156942
Biosynthesis of unsaturated fatty acids	-1.94	0.001302	-2.15	0.002066
<b>1.4. Nucleotide metabolism</b>				
Pyrimidine metabolism	0.95	0.752552	1.79	0.00286
<b>1.5. Amino acid metabolism</b>				
Alanine, aspartate and glutamate metabolism	-1.88	0.001302	-1.62	0.058565
Glycine, serine and threonine metabolism	-1.76	0.017223	-1.3	0.245916
Cysteine and methionine metabolism	-1.8	0.013293	-1.46	0.11524
Valine, leucine and isoleucine degradation	-2.61	0.001302	-2.96	0.002066
Lysine degradation	-1.83	0.005277	-1.57	0.050487
Tyrosine metabolism	-1.74	0.019665	-1.66	0.059321
Tryptophan metabolism	-1.91	0.001302	-1.8	0.024021
<b>1.6. Metabolism of other amino acids</b>				
beta-Alanine metabolism	-2.01	0.001302	-1.96	0.006481
Glutathione metabolism	-1.76	0.013293	0.93	0.683004

<b>1.8. Metabolism of cofactors and vitamins</b>				
Porphyrin and chlorophyll metabolism	 -1.75	0.021895	 -1.06	0.491311
Terpenoid backbone biosynthesis	 -2	0.001302	 -2.24	0.002066
<b>1.11. Xenobiotics biodegradation and metabolism</b>				
Metabolism of xenobiotics by cytochrome P450	 -1.86	0.007397	 -1.5	0.098247
Drug metabolism	 -1.7	0.030891	 -1.31	0.230529















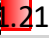

**Table 4: Significantly deregulated pathways belonging to KEGG's main category 'Metabolism'.** The main category is divided into 13 subcategories in total (only pathways related to 9 subcategories are significant and shown in the table). Significantly deregulated pathways are shown in the table with their respective NES and adjusted p-values. Down-regulated (Up-regulated) pathways are indicated by the negative (positive) NES coloured in green (red).

The table 5 shows most significant pathways of the second main category “Genetic information processing”. Except for protein export pathway, all the other considered pathways were up-regulated with effects increased according to the number of the treatments. The same trend in all subcategories was not surprising since mechanisms such as transcription, translation and downstream folding or protein degradation processes were all closely related. It is known that gene expression is regulated at both the transcriptional and post-transcriptional levels in eukaryotic transcriptomes. Moreover, several mechanisms involved in transcriptional regulation can directly affect subsequent post-transcriptional gene regulation. Blue light treatment could affect both levels during 3T3-L1 differentiation process. In addition, many of the listed pathways as mRNA surveillance, ubiquitin mediated proteolysis, base excision repair, nucleotide excision repair, mismatch repair, are related to systems of DNA repair or degradation of damaged molecules. The up-regulation of these pathways suggested that blue light irradiation, especially if prolonged, can modulate damage at different biological levels. The up-regulation of DNA replication pathway is not directly related to the proliferation or the amount of cells DNA; it reflects the expression of proteins and enzymes required for DNA replication such as DNA polymerase, DNA helicase and others. Deregulation of this path was therefore not in contrast to the results obtained from the previous cell proliferation tests.

<b>2. Genetic Information Processing</b>				
	<b>30min x Day0</b>		<b>30min x 14Days</b>	
	<b>NES</b>	<b>Adjusted p-value</b>	<b>NES</b>	<b>Adjusted p-value</b>
<b>2.1. Transcription</b>				
Spliceosome	2.1	0.0042064	2.26	0.002066
<b>2.2. Translation</b>				
Ribosome biogenesis in eukaryotes	0.72	0.9997707	1.96	0.002066
Ribosome	1.77	0.0042064	1.78	0.002066
RNA transport	1.08	0.4584289	2.07	0.002066
mRNA surveillance pathway	0.68	0.9997707	1.54	0.030225
<b>2.3. Folding, sorting and degradation</b>				
Protein export	-1.68	0.0409834	-1.7	0.035718
Ubiquitin mediated proteolysis	0.84	0.9616463	1.58	0.010012
<b>2.4. Replication and repair</b>				
DNA replication	2.04	0.0022365	2.39	0.002066
Base excision repair	0.87	0.8373597	1.58	0.047274
Nucleotide excision repair	1.61	0.0310459	1.84	0.00286
Mismatch repair	1.35	0.2352356	1.87	0.004327

**Table 5: Significantly deregulated pathways belonging to KEGG's main category 'Genetic Information Processing'.** The main category is divided into 4 subcategories. Significantly deregulated pathways are shown in the table with their respective NES and adjusted p-values. Up-regulated (Down-regulated) pathways are indicated by the positive (negative) NES coloured in red (green).

The third main category "environmental information processing" includes several signal transduction pathways such as AMPK, TNF, NF-kappa B (NF-kB) which are known to be involved in the regulation of cell metabolism, proliferation, growth and apoptosis. Three of them TNF, NF-kB and cytokine, were strongly up-regulated in both single and multiple treatments suggesting an activation of signal cascade typical of inflammatory process. In addition, also AMP-activated protein kinase (AMPK) signalling was de-regulated in opposite direction. AMPK is an essential "fuel gauge," implicated in the regulation of energy balance and metabolism including glucose transport, gluconeogenesis, lipogenesis, and lipolysis and sterol synthesis. His involvement has been demonstrated in the development and function of adipose tissue.

<b>3. Environmental Information Processing</b>				
	<b>30min x Day0</b>		<b>30min x 14Days</b>	
	<b>NES</b>	<b>Adjusted p-value</b>	<b>NES</b>	<b>Adjusted p-value</b>
<b>3.1. Membrane transport</b>				
ABC transporters	 -1.71	0.031046	 -1.69	0.035718
<b>3.2. Signal transduction</b>				
NF-kappa B signaling pathway	 1.35	0.140425	 1.56	0.039508
HIF-1 signaling pathway	 -2.14	0.001302	 -1.75	0.007735
AMPK signaling pathway	 -2.13	0.001302	 -2.34	0.002066
Hippo signaling pathway	 1.47	0.034044	 1.1	0.405693
Hippo signaling pathway - multiple species	 1.79	0.014704	 1.24	0.304142
TNF signaling pathway	 1.55	0.026383	 1.65	0.010012
<b>3.3. Signaling molecules and interaction</b>				
Cytokine-cytokine receptor interaction	 1.21	0.235236	 1.49	0.037398

**Table 6: Significantly deregulated pathways belonging to KEGG's main category 'Environmental Information Processing'.** The main category is divided into 3 subcategories. Significantly deregulated pathways are shown in the table with their respective NES and adjusted p-values. Up-regulated (Down-regulated) pathways are indicated by the positive (negative) NES coloured in red (green).

Fourth main category includes “cellular processes”. Gene expression results shown up-regulation in transport processes as lysosome and endocytosis systems. Peroxisome pathway, that contributes at many crucial metabolic processes such as fatty acid oxidation, biosynthesis of either lipids or free radical detoxification, is strongly down-regulated in both treatments. Concerning the subcategory “4.2. Cell growth and death” the cell cycle, p53 signalling and cellular senescence pathway are up-regulated for both conditions with higher significance for daily treatments (Table 7).

## Results

4. Cellular Processes				
	30min x Day0		30min x 14Days	
	NES	Adjusted p-value	NES	Adjusted p-value
<b>4.1. Transport and catabolism</b>				
Lysosome	1.53	0.026383	0.89	0.7704134
Endocytosis	1.22	0.125731	1.41	0.0253222
Peroxisome	-2.51	0.001302	-2.87	0.0020656
<b>4.2. Cell growth and death</b>				
Cell cycle	1.66	0.008966	2.08	0.0020656
Oocyte meiosis	1.3	0.133408	1.65	0.0100118
p53 signaling pathway	1.37	0.121768	1.63	0.0208405
Apoptosis	0.93	0.818856	1.47	0.0384984
Ferroptosis	-1.72	0.020172	-1.27	0.2463162
Cellular senescence	1.02	0.629387	1.67	0.0031876
<b>4.5. Cell motility</b>				
Regulation of actin cytoskeleton	1.41	0.024449	1.54	0.0099711

**Table 7: Significantly deregulated pathways belonging to KEGG's main category 'Cellular Processes'.** The main category is divided into 5 subcategories (only pathways related to 3 subcategories are significant and shown in the table). Significantly deregulated pathways are shown in the table with their respective NES and adjusted p-values. Up-regulated (Down-regulated) pathways are indicated by the positive (negative) NES coloured in red (green).

Fifth main KEGG category is "Organismal Systems" (Table 8). Most of the subcategories were down-regulated. Since all the pathways related to endocrine systems, except oocyte maturation, are connected to adipocytes, according to the hypothesis of adipocyte differentiation block induced by blue light, they were down-regulated as expected. It is important to keep in mind that the analysis was carried out by comparing the gene expression between the irradiated cells which were poorly differentiated after the treatment, and the controls which, by completing their differentiation process, result in mature adipocytes. Massive was de-regulation in the opposite direction for the pathways included in the subcategory of the immune system.

5. Organismal Systems				
	30min x Day0		30min x 14Days	
	NES	Adjusted p-value	NES	Adjusted p-value
<b>5.1. Immune system</b>				
Chemokine signaling pathway	1.26	0.155311	1.58	0.013824
Antigen processing and presentation	1.69	0.011978	1.9	0.002066
Toll-like receptor signaling pathway	1.69	0.009981	1.69	0.01011
NOD-like receptor signaling pathway	1.77	0.006418	1.97	0.002066
RIG-I-like receptor signaling pathway	1.81	0.004342	1.49	0.067395
Cytosolic DNA-sensing pathway	1.8	0.008367	2.1	0.002066
C-type lectin receptor signaling pathway	1.23	0.235236	1.52	0.038498
Natural killer cell mediated cytotoxicity	1.04	0.604921	1.54	0.046477
IL-17 signaling pathway	1.32	0.161803	1.69	0.011083
Leukocyte transendothelial migration	1.62	0.024565	1.76	0.006713
<b>5.2. Endocrine system</b>				
PPAR signaling pathway	-2.48	0.001302	-2.98	0.002066
Insulin signaling pathway	-2.08	0.001302	-2.11	0.002066
Progesterone-mediated oocyte maturation	1.25	0.214947	1.6	0.02146
Adipocytokine signaling pathway	-1.81	0.005277	-1.94	0.003141
Glucagon signaling pathway	-1.97	0.001302	-2.04	0.002066
Regulation of lipolysis in adipocytes	-1.93	0.003847	-2.11	0.002066
<b>5.3. Circulatory system</b>				
Cardiac muscle contraction	-1.99	0.002024	-2.06	0.002066
<b>5.4. Digestive system</b>				
Protein digestion and absorption	-0.99	0.700604	-1.84	0.007324
Fat digestion and absorption	-2.02	0.001302	-2.07	0.007054
Cholesterol metabolism	-1.85	0.005638	-2.14	0.002066
<b>5.6. Nervous system</b>				
Retrograde endocannabinoid signaling	-2.14	0.001302	-1.88	0.003188
<b>5.9. Aging</b>				
Longevity regulating pathway	-1.64	0.02383	-1.69	0.010281
<b>5.10. Environmental adaptation</b>				
Thermogenesis	-2.55	0.001302	-2.69	0.00211

**Table 8: Significantly deregulated pathways belonging to KEGG's main category 'Organismal Systems'.** The main category is divided into 10 subcategories (only pathways related to 7 subcategories are significant and shown in the table). Significantly deregulated pathways are shown in the table with their respective NES and adjusted p-values. Up-regulated (Down-regulated) pathways are indicated by the positive (negative) NES coloured in red (green).

## Results

Albeit related to human diseases, pathways belonging to this main category were summarized in table 9 as they could give an overview what effects treatment with blue light are linked to. Attention was focused on neurodegenerative diseases like Alzheimer, Parkinson and Huntington disease since all of these gene sets, involving mitochondrial pathways related to change in ROS or ATP production, were down-regulated as well as oxidative phosphorylation pathway seen before.

Complete list of gene expression results is reported in table 15 of the appendix.



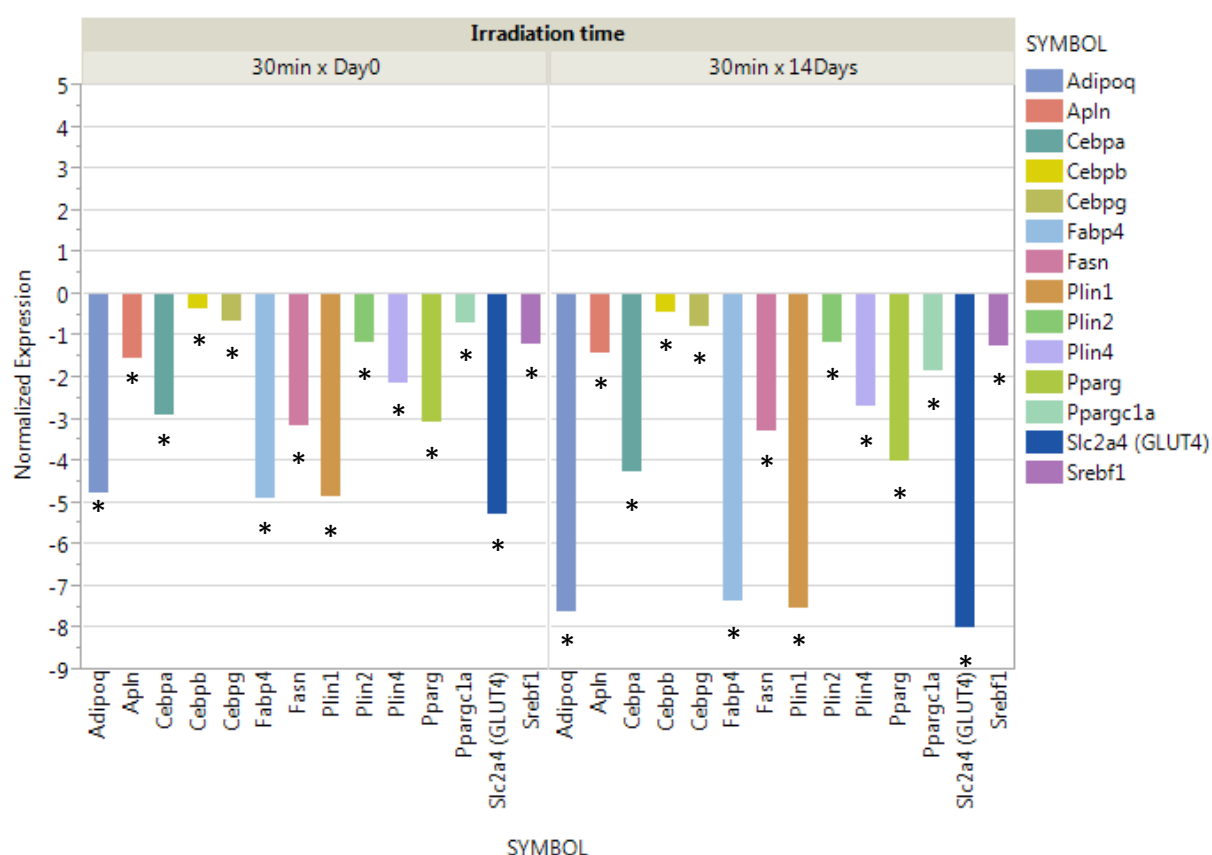
6. Human Diseases				
	30min x Day0		30min x 14Days	
	NES	Adjusted p-value	NES	Adjusted p-value
<b>6.1. Cancers: Overview</b>				
Viral carcinogenesis	1.11	0.370221	1.55	0.006713
Chemical carcinogenesis	-1.65	0.035832	-1.37	0.1759
Proteoglycans in cancer	1.4	0.022715	1.3	0.114176
MicroRNAs in cancer	1.54	0.01514	1.57	0.00964
Central carbon metabolism in cancer	-1.98	0.002024	-1.42	0.114176
<b>6.12. Drug resistance: Antineoplastic</b>				
Antifolate resistance	0.85	0.847845	1.7	0.022931
<b>6.2. Cancers: Specific types</b>				
Basal cell carcinoma	1.9	0.004206	1.62	0.033739
<b>6.3. Immune diseases</b>				
Allograft rejection	1.62	0.053509	1.67	0.026829
Graft versus host disease	1.63	0.050338	1.71	0.02146
<b>6.4. Neurodegenerative diseases</b>				
Alzheimer disease	-2.52	0.001302	-2.59	0.002084
Parkinson disease	-2.7	0.001302	-2.83	0.002066
Huntington disease	-2.56	0.001302	-2.42	0.002084
<b>6.7. Endocrine and metabolic diseases</b>				
Insulin resistance	-1.92	0.001302	-2.06	0.002066
Non-alcoholic fatty liver disease (NAFLD)	-2.67	0.001302	-2.84	0.00208
Type I diabetes mellitus	1.59	0.06617	1.76	0.011415
<b>6.8. Infectious diseases: Bacterial</b>				
Salmonella infection	1.1	0.486371	1.6	0.03011
<b>6.9. Infectious diseases: Viral</b>				
Hepatitis C	1.47	0.027166	1.78	0.002066
Hepatitis B	1.18	0.247718	1.51	0.024494
Measles	1.93	0.005277	1.99	0.002066
Human cytomegalovirus infection	1.29	0.065761	1.53	0.006713
Influenza A	1.84	0.006288	2.11	0.002066
Human T-cell leukemia virus 1 infection	0.89	0.918799	1.53	0.006713
Kaposi sarcoma-associated herpes virus infection	1.15	0.285075	1.6	0.005917
Herpes simplex infection	1.83	0.004592	1.95	0.002066
Epstein-Barr virus infection	1.91	0.00474	2.05	0.002066
Human immunodeficiency virus 1 infection	1.62	0.004952	1.99	0.002066

**Table 9: Significantly de-regulated pathways belonging to KEGG's main category 'Human Diseases'.** The main category is divided into 12 subcategories (only pathways related to 8 subcategories are significant and shown in the table). Significantly deregulated pathways are shown in the table with their respective NES and adjusted p-values. Up-regulated (Down-regulated) pathways are indicated by the positive (negative) NES coloured in red (green).

## Results

### 3.6.2 Blue light de-regulated expression of genes involved in adipogenesis and cell cycle/cell death.

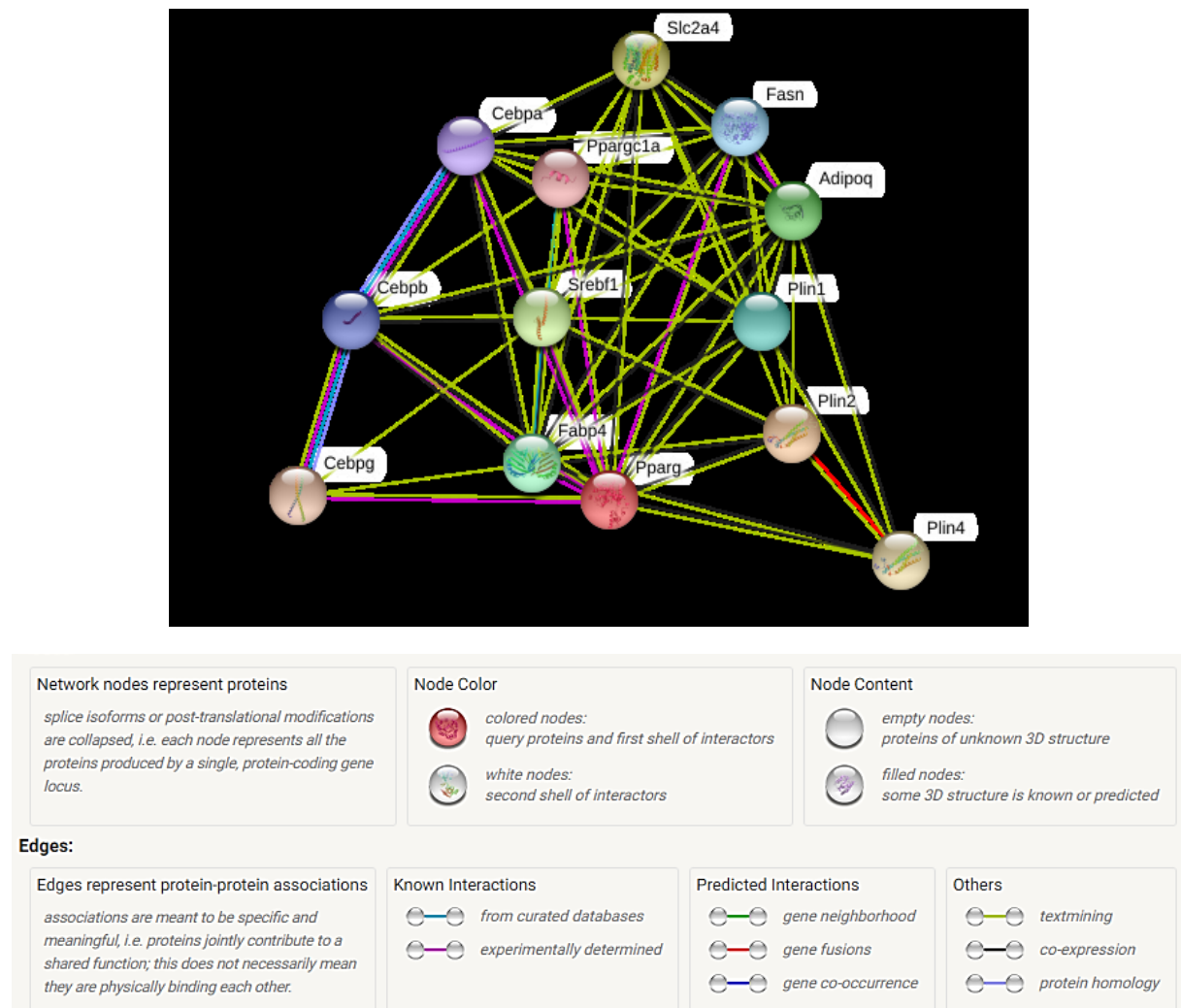
A more detailed analysis of individual genes was conducted by analysing three main biological processes: adipocyte differentiation, cell cycle / apoptosis. In order to confirm a reduced rate of differentiation in blue light treated cells, a pool of genes, known in the literature as markers of adipogenesis, has been selected. As shown in figure 30, all the genes were strongly down-regulated by blue light at both treatment conditions suggesting a different maturation state between the treated cells, partially differentiated (Day0) or undifferentiated (14Days), and the controls.



**Figure 30: Expression changes of a selected pool of genes involved in the adipogenesis.** Normalized expression is calculated as log of fold change indicating up-regulation (value >0) and down-regulation (value <0) of genes. Genes that reached significance with FDR < 0.05 are indicated with (\*).

In addition the same gene list has been entered in a database of known and predicted protein-protein interactions. The interactions, including direct (physical) and indirect (functional) associations, are shown in figure 31. The genes appeared directly correlated to different degrees as if they were at the base of the same mechanism.

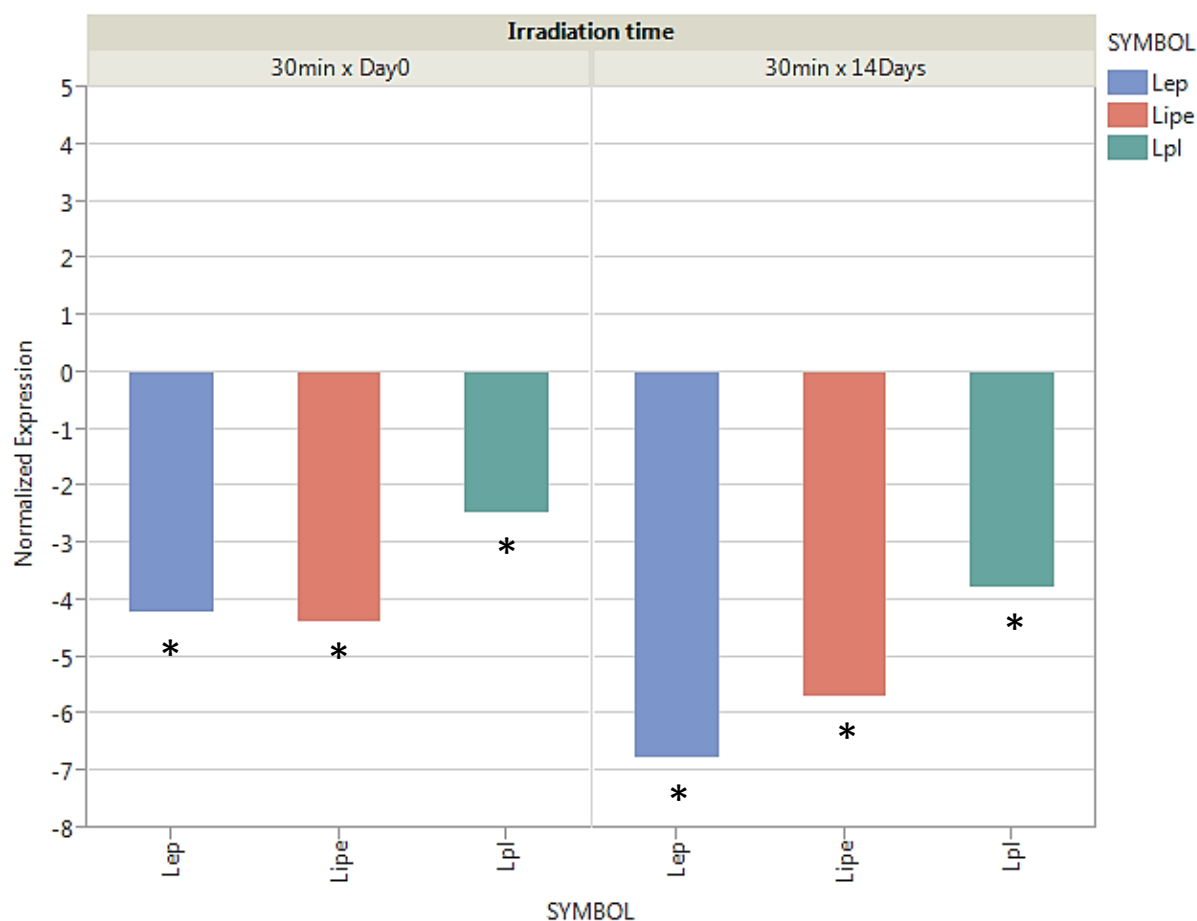
## Results



**Figure 31: Protein-protein interactions generated with STRING database.**

In order to confirm that the aforementioned decrease in lipid accumulation was mediated by decreasing adipogenesis and not by lipolysis activation, the gene expression of lipolytic enzymes hormone sensitive lipase (Lipe) and the lipogenic enzyme lipoprotein lipase (Lpl) was analysed. Also leptin expression was taken into account as marker of lipid accumulation. All three genes were down-regulated by blue light treatment as shown in figure 32.

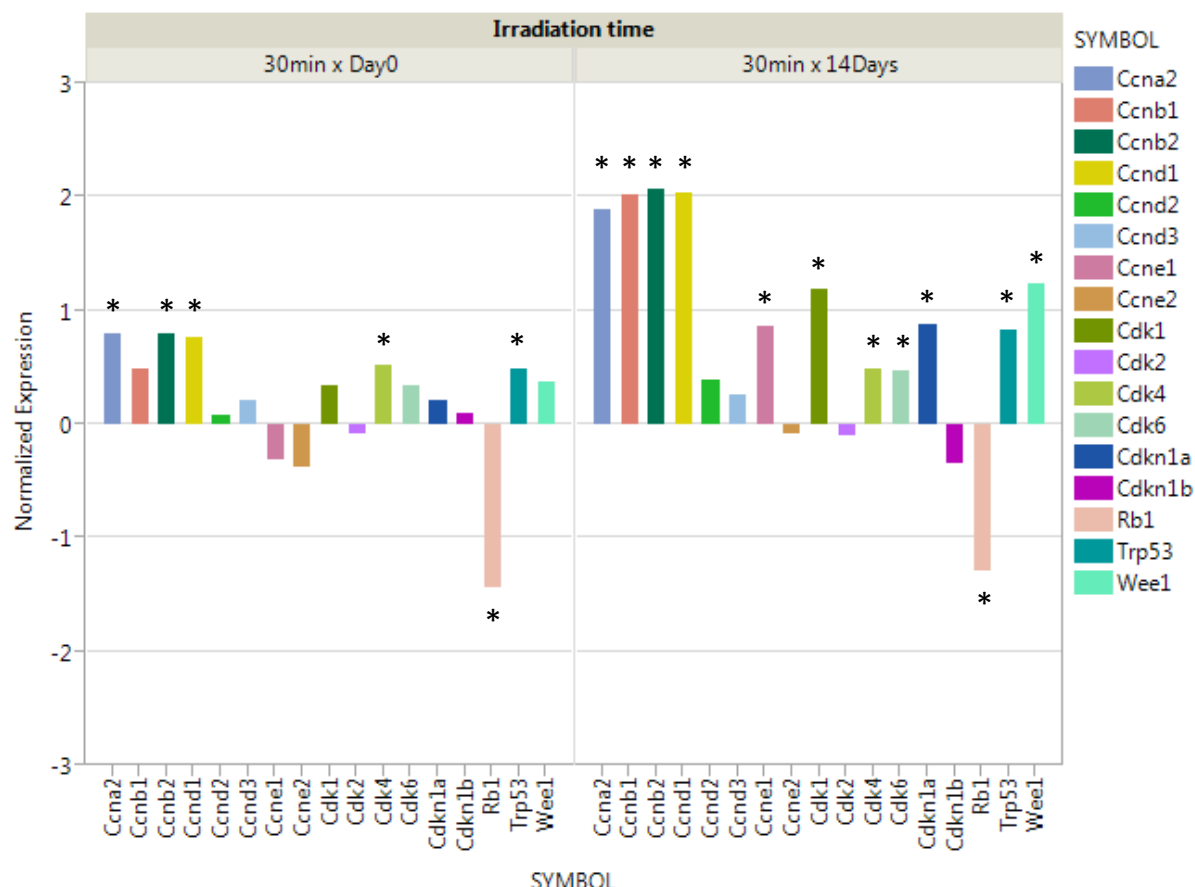
## Results



**Figure 32: Expression changes of markers of lipid accumulation** Normalized expression is calculated as log of fold change indicating up-regulation (value >0) and down-regulation (value <0) of genes. Genes that reached significance with FDR < 0.05 are indicated with (\*).

Secondly, genes involved in cell cycle have been selected. A similar trend was observed for both treatments with a pronounced de-regulation in daily treatments. According to gene expression analysis the levels of cyclins and related dependent-kinases (CDKs) revealed an increase especially in genes of S and G2 phases. Also genes involved in cell cycle inhibition (Cdkn1a), repairing systems or apoptosis (p53 and Wee1), were up-regulated following blue light chronic exposure (Figure 33).

## Results

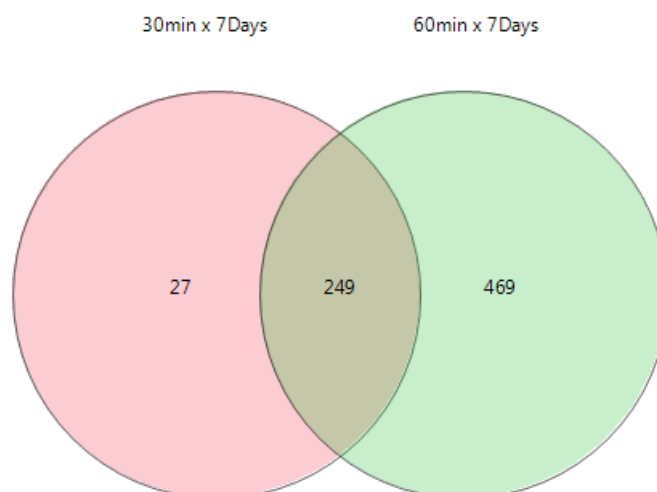


**Figure 33: Expression changes of a selected pool of genes involved in the cell cycle.** Normalized expression is calculated as log of fold change indicating up-regulation (value >0) and down-regulation (value <0) of genes. Genes that reached significance with FDR<0.05 are indicated with (\*).

### 3.6.3 Gene expression analysis 2° set-up: Blue light irradiation on mature adipocytes

Gene expression data have been analyzed as before. RNA seq screened 24421 genes in total, 745 were significantly expressed (FDR <0.05) in treated samples. The number of de-regulated genes has been really low if compared to the results obtained on maturing preadipocytes. In the previous tests were shown no evident effects on irradiated samples and also gene expression followed the same trend. However, in relation to the blue light doses, differentially adjusted genes were increased in total number from 276 de-regulated genes after 30 minutes a day (21.6 J/cm<sup>2</sup>), to 718 genes after 60 minutes a day (43.2 J/cm<sup>2</sup>). 249 genes were triggered commonly (Figure 34).

## Results



**Figure 34:** Venn diagram showing the number of significantly ( $FDR < 0.05$ ) commonly or differentially expressed genes in differentiated adipocytes following 30 min ( $21.6 \text{ J/cm}^2$ ) or 60min ( $43.2 \text{ J/cm}^2$ ) blue light doses.

In the table 10 the number of up- and down-regulated genes is given. De-regulated genes have increased by the dose used and a majority of up-regulated genes at both doses was found.

Treatment group	Significantly differentially expressed genes	
	Down-regulated genes	Up-regulated genes
30min x 7Days	81	195
60min x 7Days	301	417

**Table 10:** Number of significantly up and down-regulated genes differentially expressed in differentiated adipocytes following 30 min ( $21.6 \text{ J/cm}^2$ ) or 60min ( $43.2 \text{ J/cm}^2$ ) blue light doses.

Thereafter, Gene Set Enrichment Analysis (GSEA) was performed using Kyoto Encyclopedia of Genes and Genomes (KEGG) database to transform the list of individual genes into a set of pathways. As before a Normalized Enrichment Scores (NES) was used to indicate the distribution of the pathway within the list. Negative or positive NES indicates down- or up-regulated pathways. Table 11 lists the number of de-regulated KEGG pathways for both treatment conditions. Starting from a total gene set number equal to 281, the number of down-regulated pathways for 30min a day irradiation was lower than the up-regulated pathways. Of these de-regulated pathways one fifth was significant with a  $p\text{-value} < 0.05$  and, even less if an adjusted  $p\text{-value}$  (FDR) with the same cut-off was considered. A same trend occurred as a result of 60 minutes irradiation; up-regulated pathways prevailed over down-regulated pathways. Also in this case the number of significant pathways ( $p\text{-value} < 0.05$ ) was

## Results

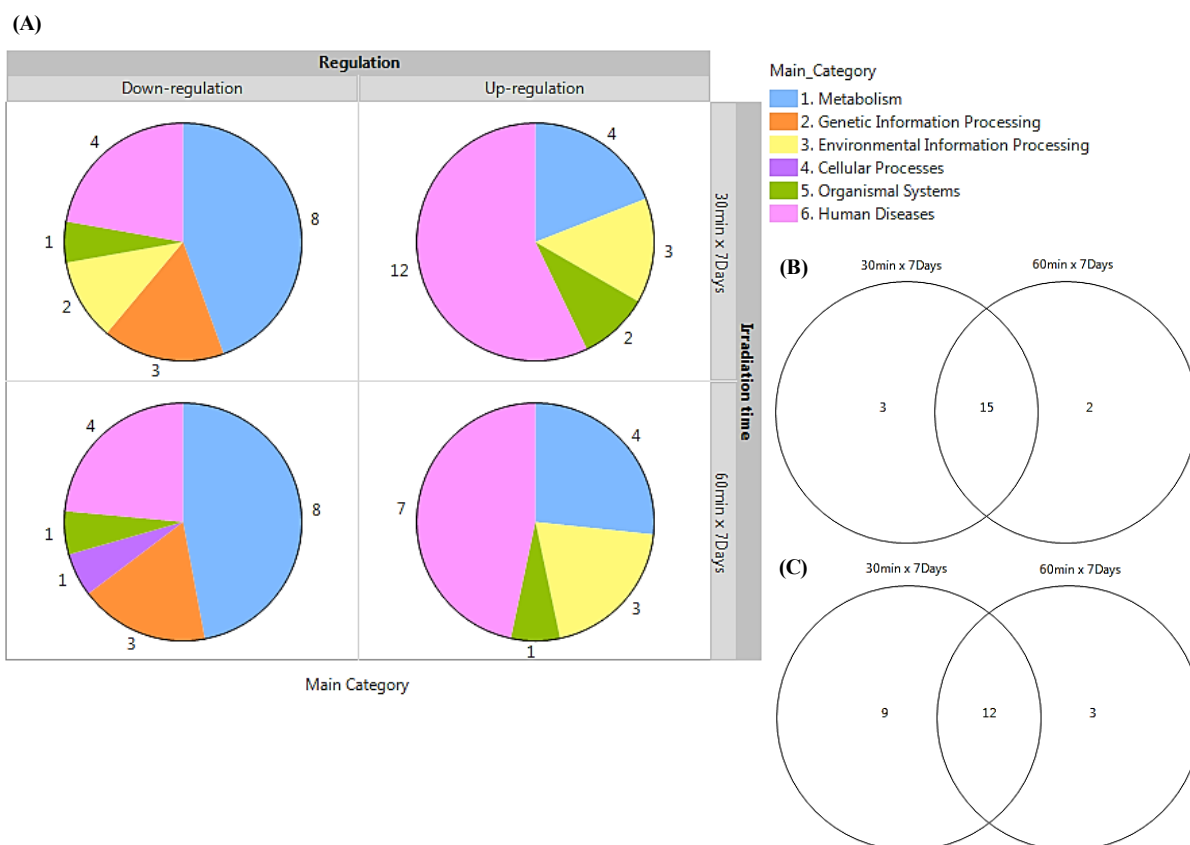
drastically reduced without departing in large numbers from the highly significant ones (FDR <0.05).

Treatment group	30min x 7Days	60min x 7Days
De-regulated pathways	307	307
<b>Up-regulated pathways</b>	<b>177</b>	<b>192</b>
with nominal p-value < 0.05	41	46
with nominal p-value < 0.01	21	25
with adjusted p-value (FDR) <0.05	21	15
<b>Down-regulated pathways</b>	<b>130</b>	<b>116</b>
with nominal p-value < 0.05	23	27
with nominal p-value < 0.01	20	17
with adjusted p-value (FDR) <0.05	18	17

**Table 11: Number of differentially expressed KEGG pathways in differentiated adipocytes following 30 min (21.6 J/cm<sup>2</sup>) or 60min (43.2 J/cm<sup>2</sup>) blue light doses.** Starting from an overall gene set number of 281, total numbers of up- or down-regulated pathways are shown. In addition the number of significantly enriched pathways is listed for different significance levels at nominal p- value < 0,05 or < 0,01 and at adjusted p-value (FDR) <0,05.

Only de-regulated pathways with an adjusted p-value (FDR)  $\leq 0.05$  have been taken into account for the subsequent analysis. As shown in figure 35 pathways were sorted into 6 main KEGG categories. For both irradiation doses most of down-regulated pathways belong to the Metabolism category with a similar behaviour also for the other categories in both treatments. In contrast, up-regulation was more pronounced in Human diseases category.










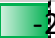







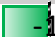








## Results



**Figure 35: (A) Distribution of significantly enriched pathways (FDR < 0.05) sorted by main categories of KEGG. Groups are formed by the respective doses/irradiation times. The numbers around the pie charts indicate the number of deregulated pathways contained in each category. (B) Comparison of significant pathway list with NES < 0 and (C) NES > 0 at different irradiation time.**

Table 12 lists de-regulated significant pathways of the first main category: Metabolism. The general metabolism seems to be down-regulated by the blue light. Two of the main cellular processes, the citrate cycle and oxidative phosphorylation, showed reduced activity in irradiated samples. Up-regulated were the pathways involved in detoxification systems such as cytochrome P450 and Glutathione metabolism.






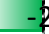






















Metabolism				
	30min x 7Days		30min x 7Days	
	NES	Adjusted p-value	NES	Adjusted p-value
<b>1.0 Global and overview maps</b>				
Metabolic pathways	 -1.27	0.006341	 -1.41	0.004806
Biosynthesis of amino acids	 -1.59	0.020963	 -1.68	0.015953
Carbon metabolism	 -1.52	0.026926	 -1.56	0.017163
2-Oxocarboxylic acid metabolism	 -1.76	0.022223	 -1.79	0.019425
<b>1.1. Carbohydrate metabolism</b>				
Citrate cycle (TCA cycle)	 -2.05	0.004753	 -2.02	0.004806
Propanoate metabolism	 -1.85	0.010783	 -1.88	0.004806
Amino sugar and nucleotide sugar metabolism	 -1.33	0.27152	 -1.67	0.026506
Inositol phosphate metabolism	 -1.77	0.009464	 -1.11	0.477763
<b>1.2. Energy metabolism</b>				
Oxidative phosphorylation	 -1.74	0.009464	 -1.91	0.004806
<b>1.6. Metabolism of other amino acids</b>				
Glutathione metabolism	 1.75	0.009869	 1.8	0.009505
<b>1.11. Xenobiotics biodegradation and metabolism</b>				
Metabolism of xenobiotics by cytochrome P450	 1.87	0.004753	 1.9	0.007585
Drug metabolism (cytochrome P450)	 1.89	0.004753	 1.91	0.007585
Drug metabolism (other enzymes)	 1.79	0.004753	 1.72	0.009505

**Table 12: Significantly de-regulated pathways belonging to KEGG's main category 'Metabolism'.** The main category is divided into 13 subcategories in total (only pathways related to 5 subcategories are significant and shown in the table). Significantly deregulated pathways are shown in the table with their respective NES and adjusted p-values. Down-regulated (Up-regulated) pathways are indicated by the negative (positive) NES coloured in green (red).

Few pathways have reached statistical significance in the other categories. Among these Jak-Stat signalling, cytokine-cytokine receptor interaction and thermogenesis pathways that could be involved in important mechanisms in the adipose tissue (Table 13).

## Results

<b>2. Genetic Information Processing</b>				
	<b>30min x 7Days</b>		<b>30min x 7Days</b>	
	<b>NES</b>	<b>Adjusted p-value</b>	<b>NES</b>	<b>Adjusted p-value</b>
<b>2.2. Translation</b>				
Aminoacyl-tRNA biosynthesis	 -1.78	0.017661	 -1.81	0.015953
<b>2.3. Folding, sorting and degradation</b>				
Protein processing in endoplasmic reticulum	 -2.07	0.004753	 -2.21	0.004806
Protein export	 -2.01	0.004753	 -2.06	0.004806
<b>3. Environmental Information Processing</b>				
<b>3.2. Signal transduction</b>				
JAK-STAT signaling pathway	 1.54	0.020015	 1.57	0.011737
Phospholipase D signaling pathway	 -1.55	0.020361	 -1.18	0.335519
Phosphatidylinositol signaling system	 -1.74	0.007398	 -1.1	0.48188
<b>3.3. Signaling molecules and interaction</b>				
Cytokine-cytokine receptor interaction	 1.54	0.009464	 1.6	0.004806
Neuroactive ligand-receptor interaction	 1.41	0.022223	 1.47	0.011737
<b>4. Cellular Processes</b>				
<b>4.1. Transport and catabolism</b>				
Endocytosis	 -1.35	0.051984	 -1.4	0.038663
<b>5. Organismal Systems</b>				
<b>5.1. Immune system</b>				
Cytosolic DNA-sensing pathway	 1.52	0.097055	 1.67	0.030948
Complement and coagulation cascades	 1.73	0.004753	 1.57	0.055223
Hematopoietic cell lineage	 1.6	0.026416	 1.36	0.156005
<b>5.10. Environmental adaptation</b>				
Thermogenesis	 -1.42	0.031242	 -1.59	0.007572

**Table 13: Significantly de-regulated pathways belonging to KEGG's main category 'Genetic information processing', "Signal transduction", "Cellular processes", "Organismal systems".** Significantly deregulated pathways are shown in the table with their respective NES and adjusted p-values. Down-regulated (Up-regulated) pathways are indicated by the negative (positive) NES coloured in green (red).

In the table 14 are shown Human diseases pathways. Also in this case neurodegenerative diseases appeared down-regulated according to the theory of reduction in oxidative phosphorylation.

Complete list of gene expression results is reported in table 16 of the appendix.

6. Human Diseases				
	30min x 7Days		30min x 7Days	
	NES	Adjusted p-value	NES	Adjusted p-value
<b>6.1. Cancers: Overview</b>				
Chemical carcinogenesis	1.97	0.004753	1.89	0.004806
MicroRNAs in cancer	1.02	0.702703	1.5	0.01406
<b>6.2. Cancers: Specific types</b>				
Acute myeloid leukemia	1.65	0.022223	1.58	0.060973
<b>6.3. Immune diseases</b>				
Autoimmune thyroid disease	1.92	0.004753	1.57	0.060894
Graft-versus-host disease	1.85	0.004753	1.57	0.071698
Allograft rejection	1.78	0.00676	1.57	0.072807
<b>6.4. Neurodegenerative diseases</b>				
Huntington disease	-1.73	0.004753	-1.83	0.004806
Alzheimer disease	-1.98	0.004753	-2.11	0.004806
Parkinson disease	-1.76	0.007398	-1.96	0.004806
<b>6.6. Cardiovascular diseases</b>				
Fluid shear stress and atherosclerosis	1.56	0.021578	1.39	0.103312
<b>6.7. Endocrine and metabolic diseases</b>				
Non-alcoholic fatty liver disease (NAFLD)	-1.6	0.014312	-1.71	0.004806
Type I diabetes mellitus	1.63	0.026926	1.39	0.186243
<b>6.8. Infectious diseases: Bacterial</b>				
Staphylococcus aureus infection	2.13	0.004753	1.78	0.004806
<b>6.9. Infectious diseases: Viral</b>				
Epstein-Barr virus infection	1.69	0.004753	1.62	0.004806
Hepatitis C	1.46	0.041657	1.62	0.009505
Herpes simplex infection	1.64	0.004753	1.56	0.009505
Influenza A	1.48	0.031242	1.44	0.060894
<b>6.12. Drug resistance: Antineoplastic</b>				
Platinum drug resistance	1.46	0.107209	1.66	0.030098

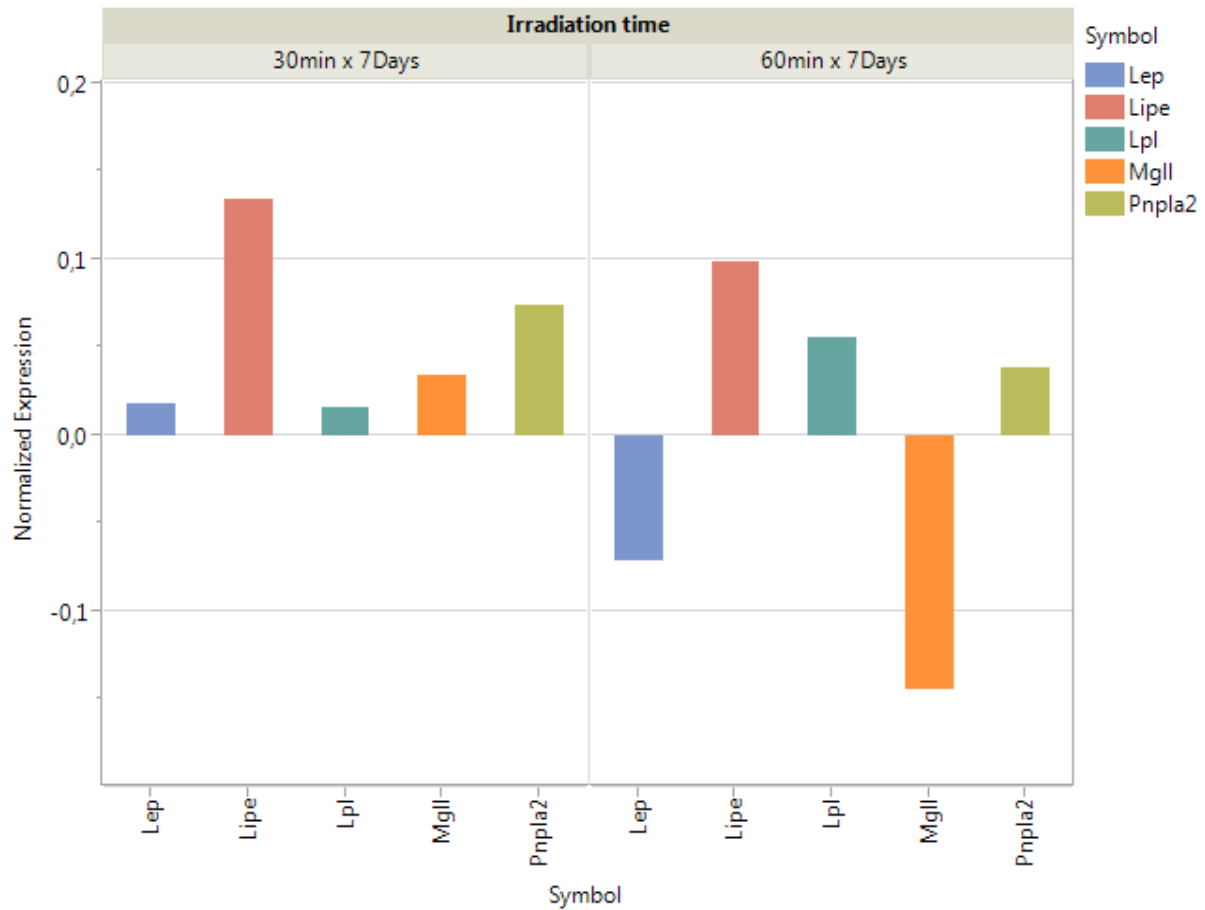
**Table 14: Significantly de-regulated pathways belonging to KEGG's main category 'Human Diseases'.** The main category is divided into 12 subcategories (only pathways related to 10 subcategories are significant and shown in the table). Significantly deregulated pathways are shown in the table with their respective NES and adjusted p-values. Up-regulated (Down-regulated) pathways are indicated by the positive (negative) NES coloured in red (green).

### 3.6.4 Blue light did not affect lipolysis in mature adipocytes.

In order to evaluate blue light effects on the lipolysis, the expression of genes involved in this process was analysed. To the expression analysis of leptin, hormone sensitive lipase (LIPE) and lipoprotein lipase (LPL) genes previous considered, also monoglyceride lipase (Mgl) and

## Results

adipose.tissue trygliceride lipase (Pnpla2) were added. Although the expression of some genes was reduced or even downgraded after 60-minute treatments, this change was not statistically significant. (Figure 36).



**Figure 36: Expression changes of markers of lipolysis and lipogenesis** Normalized expression is calculated as log of fold change indicating up-regulation (value >0) and down-regulation (value <0) of genes. Genes did not reach significance.

## 4 Discussion

### 4.1 Effects of single or multiple exposures of blue light at 21.6 J/cm<sup>2</sup> dosage during adipocyte differentiation.

The interest in PBM has rapidly grown for medical application requiring reduction of pain, inflammation and stimulation of healing and tissue regeneration. Stimulatory or inhibitory effects on biological processes depend on the wavelength, energy dose and cell type. Traditionally red (600–700 nm) and near-infrared (NIR, 780–1100 nm) wavelengths were employed in many studies and their effects have been better characterized. However evidence is mounting that shorter visible wavelengths such as blue and green light can also have photobiomodulatory effects showing distinct differences from those generally observed with red/NIR light. One of the limitation in the use of these short wavelengths is represented by the low penetrating capacity. It has been demonstrated that in spite of the fact that most of sunlight in the visible spectrum does not pass through the skin, approximately 1–5% of blue/green light is able to penetrate it to varying depths proportional to increasing wavelength and intensity and reach the underlying subcutaneous white adipose tissue (scWAT). The purpose of this study has been to improve the knowledge regarding the effects of blue light by evaluating the response of 3T3-L1 cells to 453nm blue light. On the basis of biphasic dose-response curves, Schulz's law<sup>8, 9</sup> specifies that therapeutically applied energy must be of the proper intensity per unit of time to stimulate the desired physiological response. Low energies evoke stimulation reaching their maximum following even stronger stimuli; instead, high energies result in inhibitory effects. In order to use blue light in body-shaping or disease treatments such as obesity or lipid dysfunctions, high blue light doses were applied, 21.6 J/cm<sup>2</sup> and 43.2 J/cm<sup>2</sup>, in a different number of treatments for each set-ups. Photomodulatory effects were investigated during and after differentiation process using 3T3-L1 cells as model of adipose tissue. Various stainings were performed to evaluate variations in lipid accumulation while XTT, ATP and BrdU assays were used to follow changes on metabolism and proliferation. In addition, to elucidate which genes and signalling pathways were commonly or differentially expressed after different irradiation doses, gene expression analyses were performed.

According to the protocol illustrated by Zebisch et al<sup>74</sup>, 3T3-L1 preadipocytes have been differentiated. Setting a constant irradiance value of 12 mW/cm<sup>2</sup> at plate surface, single or multiple blue light irradiations were applied on cells during the differentiation process using a

## Discussion

dose of  $21.6 \text{ J/cm}^2$  equal to an irradiation time of 30 minutes performed on the first day (Day0) or during all 14 days of differentiation. Using Oil Red O staining and related quantification, changes in lipid accumulation were investigated. Single irradiation on Day0 has shown a reduction of 17% of lipid amount while a reduction of 38% was reached with daily irradiation with the same dose (Figure 15). Cells treated for 14 days appeared poorly differentiated under the microscope when compared to one-day treatment or to the controls. The reduction in lipid accumulation could be due to reduced adipogenesis. These data seem to be supported by gene expression results which showed a strongly down-regulated lipid metabolism in relation to the number of treatments received. A more detailed analysis presented a reduced expression of a selected group of genes involved in the differentiation (Figure 30). PPAR- $\gamma$  and several members of the C/EBP family of transcription factors participate in a signalling cascade that culminates in the transcriptional activation of genes involved in the production of the adipocyte phenotype. The expression of these markers of adipogenesis was found strongly decreased after multiple treatments although the effects already occur on Day0 long-lasting up to two weeks. Although there is still no evidence in the literature on the effects of blue light on 3T3-L1 differentiation, the results of this study are partially in line with Lee et al.<sup>75</sup> who showed how ultraviolet A (UVA) irradiation inhibits adipogenic differentiation of human adipose tissue-derived mesenchymal stem cells. In their findings effects are mediated by expression of KLF2 which operates as an anti-adipogenic factor binding and repressing the PPAR- $\gamma$  promoter. Although they reported reduced mRNA levels of PPAR- $\gamma$  and C/EBP- $\alpha$  after UVA irradiation, C/EBP- $\beta$  and  $\delta$ , the upstream regulators of PPAR- $\gamma$  and C/EBP  $\alpha$ , have not undergone variations in expression.

In the present study all the aforementioned genes were down-regulated by blue light irradiation suggesting an inhibitory mechanism independent of KLF2 action. Ju Kim et al.<sup>76</sup> and Wen-Hwa Li et al.<sup>77</sup> observed increased levels of TNF- $\alpha$  and several cytokines (IL-11, IL-1 $\alpha$ , IL-6, IL-8) following chronic UV irradiation that leads to inhibition of preadipocytes differentiation into mature adipocytes by selective inhibition of expression of the adipogenic transcription factors, i.e., peroxisome proliferator-activated receptor gamma (PPAR-g) and CCAAT / enhancer binding protein alpha (CERB-a), and lipogenesis. Consistent with those data, despite TNF- $\alpha$  expression was not detected by RNA sequencing following blue light exposure of 3T3-L1, an activation of TNF- $\alpha$  signalling was found for both irradiation times while IL-6, IL-11 levels were enriched only following daily exposures. This inflammatory process could suggest a possible mechanism of inhibition

## Discussion

of differentiation. In addition, AMPK protein is demonstrated to be activated in adipose tissue under inflammatory conditions in order to inhibit this condition<sup>78</sup>. Blue light treatments tended to lower AMPK transcription, especially in the  $\alpha$ 1-catalytic subunit, suggesting an amplified inflammation. AMPK activation is also involved in numerous mechanisms such as lipolysis, lipogenesis and adipogenesis. These processes have been found deregulated in 3T3-L1 cells irradiated with blue light assuming mechanisms independent of AMPK activity, although little is known about the inhibition of this kinase and nothing is reported in relation to blue light exposure.

The promotion of an undifferentiated phenotype is due to changes in transcription and gene expression that inevitably leads to alterations in cell metabolism. Using XTT cell viability assay mitochondrial activity and cell viability were investigated at the end of the differentiation process directly after the last irradiation or 24h later. Single or multiple irradiations did not show a pronounced alteration of metabolism that in both conditions decreased about 10% compared to the untreated samples without recovering this condition after 24h (Figure 18). Following exposure to several blue light sources in normal and cancer cells, different effects were obtained in Wataha et al<sup>79</sup> studies. They estimated cell energy consumption by population doubling time and cell survival and growth by succinate dehydrogenase (SDH) activity. Cells with a short doubling time, such as aneuploid mouse lung fibroblasts (Balb/c), revealed a constant suppression of SDH activity while slower-growing cells reacted differently. Indeed blue light exposure of human gingival fibroblasts (HGF) resulted in a transient suppression of SDH activity by 30% at 24 hours, attenuated within the next 48 hours. Based on these cell type-specific responses, population doubling time and related energy consumption mediate differential effects suggesting besides that rapidly dividing cells are more sensitive to irradiation. With a population doubling time of  $25.7 \pm 1.3$  hours, 3T3-L1 cells used in this study are in midway between a fast-growing and a slow-growing cell line showing moderate effects on viability and mitochondrial activity.

In literature strong evidence exists that LLLT acts on mitochondria which, containing an high degree of cytochromes and flavins, are logical mediators of the effects of blue light in increased ATP<sup>80</sup> and ROS production and in the induction of transcription factors<sup>81</sup>. For this reason modulation of mitochondrial function was evaluated assessing the ATP levels in light-treated and untreated cells. Although most of the studies reported elevated ATP levels after laser / LED treatment, ATP was diminished directly after blue light irradiation in



## Discussion

differentiating 3T3-L1 cells in a dose dependent manner. A slight recovery was recorded after 24 hours. (Figure 20). Collected outcomes are in line with Wang et al<sup>82</sup> studies on adipose-derived stem cells (ASCs), describing lower ATP contents after blue/green light opposite to a biphasic increase for red/NIR.

A rise in the AMP/ATP ratio is typical of a metabolic stress condition. In several neurodegenerative diseases mitochondria play a crucial role<sup>83</sup>. In this context pathways like Alzheimer, Parkinson and Huntington disease were found down-regulated in both conditions. In detail, oxidative phosphorylation and the expression of genes like NDUFA1, SDBH, CYC1, and ATP5A1 encoding subunits of respiratory chain complexes I-V were significantly lower in single and multiple irradiated samples compared to the controls. The reduced activity of these complexes could lead to a compromised energy metabolism by blocking the transfer of electrons within the respiratory chain which may result in reduced susceptibility to apoptosis<sup>84</sup>. In addition, SLC25A4, which encodes for the ADP/ATP carrier subunit through the mitochondrial membrane, was found significantly down-regulated, favouring an unbalanced energy state.

The mitochondrial theory of ageing<sup>85, 86</sup> argues that reduction in ATP synthesis and increase in ROS production are the consequence of a progressive accumulation of mutations or environmental influences on mitochondria or their DNA (mtDNA) resulting in a thus driving oxidative stress, inflammation and cell loss. Based on this interplay between down regulation of ATP and up regulation of ROS in oxidatively stressed cells, also intracellular ROS levels were assessed. ROS levels were measured spectrophotometrically using an intracellular fluorescent dye, DCFDA, that measures hydroxyl, peroxy and other reactive oxygen species (ROS) activity within the cell. Unexpectedly a high standard deviation was recorded when the test was performed 14 days after last irradiation for irradiated samples at Day0, complicating data interpretation (Figure 25). ROS levels similar or equal to controls were expected. The high standard deviation probably is due to the instability of the probe or the capability of the intermediate radical, DCF•-, formed from the one-electron oxidation of DCFH, to rapidly react with O<sup>2</sup> to form superoxide. Instead dosage of 14 x 26.1 J/cm<sup>2</sup> did not show an increase in ROS levels that were even lower than untreated controls. Furthermore, since the DCFDA is a cytoplasmic dye probably it is not able to give a correct estimation of the general ROS content within the mitochondria. Some reactive oxygen species, such as superoxide, are strongly charged and do not cross the mitochondrial membrane<sup>87</sup>, thus remaining confined in

## Discussion

the organelle, and are probably unable to react with the DCFDA. The ROS content may have been therefore underestimated. Detailed analysis of genes encoding ROS metabolism enzymes confirmed the ROS increase though was not revealed by DCFDA assay. Poglio et al.<sup>88</sup> studies showed how ionizing radiations could decrease gene expression ROS metabolism enzymes improving their harmful activity. Similarly, blue light irradiation leads to a reduction in detoxifying enzymes such as SOD2. Aconitase, a mitochondrial enzyme particularly sensible to ROS activity, is also reduced while NADPH oxidase, major source of reactive species, increased its expression levels following irradiation.

Based on gene expression levels, KEGG pathways related to repair mechanisms were found up-regulated. While a single irradiation has shown significance only in “nucleotide excision repair” pathway, multiple irradiations were significant also for “base excision repair” and “mismatch repair” which are ascribed to VIS or UV irradiation. In contrast Taoufik et al.<sup>89</sup> did not observe DNA double strand breaks in primary human gingival fibroblasts even treated with higher blue light doses. Besides, Mignon et al.<sup>90</sup> have found several repair pathways down-regulated following blue light exposure of primary reticular fibroblasts. In contrast Yuan et al.<sup>41</sup> described a high percentage of damaged DNA in bone marrow-derived mesenchymal stem cells (BMSCs).

KEGG pathway related to apoptosis showed significant up-regulation after  $14 \times 21.6 \text{ j/cm}^2$  dosage. However a detailed analysis of caspases or other pro-apoptotic genes did not reveal an increase in the expression. Though some pro-apoptotic factors like Bid and Bax showed a slight and statistical significant increase, the gene expression of XIAP, AIF-1 CASP3 CASP9, and Cytochrome-C, involved in apoptotic extrinsic pathway, were down or not significantly expressed. Literature reported that, even in the absence of caspase activity, cells can succumb to a slower form of death termed caspase independent cell death (CICD). CICD ensues when a signal that normally induces apoptosis fails in caspase activation ensuring a failsafe mechanism that leads to cell death. Chautan et al.<sup>91</sup> reported that CICD is not a secondary mechanism but occurs for up to 10% of cells thus representing the major cell death modality. Moreover animal studies reported how in Bax/Bak deficient mice and Apaf-1 deficient mice CICD can substitute apoptosis during development<sup>92</sup>. Even if CICD is a caspase independent mechanism it often shares common characteristics with apoptosis, including signalling pathways that are critical for both forms of death, such as mitochondrial outer membrane permeabilization (MOMP). MOMP is often deregulated in cancer and can be initiated by a range of physical, chemical and pathophysiological stimuli including lysosomal/ER stress,

## Discussion

DNA damage, metabolic stress, cellular stress caused by ionizing radiation, heat, hypoxia, cytokine deprivation and chemotherapeutic drugs. How CICD can occur following MOMP is still unknown and varies in a cell-type dependent manner. The main models by which MOMP can bring about CICD are either through a general decline in mitochondrial function and/or through the release of mitochondrial proteins such as AIF-1 that can actively induce CICD in some settings. Mitochondria have various critical cellular functions, the most important is the generation of ATP through the process of aerobic respiration. Under apoptotic conditions, caspase-3 dependent cleavage of p75 of mitochondrial respiratory chain complex I leads to disruption of electron transport, loss of mitochondrial membrane potential ( $\Delta\psi_m$ ) and reduction of ATP levels<sup>93</sup>. However, under conditions of CICD, mitochondria gradually lose  $\Delta\psi_m$  independently of p75 cleavage<sup>94</sup>. Why this occurs is not clear but one reason may be a gradual release of respiratory chain components from the mitochondria following MOMP. Gradual loss of  $\Delta\psi_m$  consequently leads to the loss of ATP generation. According to these lines, cells that undergo CICD present a rapid reduction in mitochondrial respiratory complexes-I and IV. Furthermore, given the important role that AIF-1 has in maintaining respiratory complex I function, loss or low levels, can also promote and sustain mitochondrial dysfunction. This condition leads to metabolic catastrophe and at the end to cell death. In line with a reduction of ATP and rise in DNA repair pathways, CICD could explain the possible reduction in cell number highlighted by Hoechst staining. Besides, also p53 signaling was up-regulated as well as ATM. These proteins positively influence the Bid/Bax expression to promote the MOMP. Moreover ATM can directly phosphorylate p53 inducing the activation of DNA repair proteins and cell growth arrest.

The reduction in metabolic activity, revealed by XTT and ATP assays following blue light, cannot be directly correlated to cell proliferation rate. Using BrdU ELISA, DNA synthesis was studied during 14 days of differentiation. A continuous decline in DNA synthesis was recorded (Figure 24), accompanied by a reduction in cell count performed with Hoechst staining (Figure 22). In line with this data, Liebmann et al.<sup>39</sup> have reported a lower proliferation in keratinocytes irradiated with blue light at 453nm though attributable to differentiation induction. Shreder et al.<sup>95</sup> have tested the effects of X-rays on Simpson-Golabi-Behmel Syndrome (SGBS) preadipocytes and human primary preadipocytes ascertaining decreased proliferation rate and clonogenic capacity of both cell strains. Thus, the regenerative potential of irradiated preadipocytes was reduced. Furthermore, the authors

## Discussion

claimed that the weak apoptotic response after preadipocytes irradiation indicated that the reduction in proliferation rate was likely a result of cell cycle arrest rather than cell death. The effects of blue light during 3T3-L1 differentiation remain still unknown. In this context KEGG's cell cycle pathway was up-regulated with both irradiation times. Assuming a possible delay or arrest in cell cycle process the expression of genes involved were analysed in detail. This pathway considers both cyclin expression and DNA damage repair systems. Following multiple irradiations the oncogene c-myc was significantly up-regulated. It has been proven to be a powerful activator of the cell cycle in serum starved 3T3-L1 cells<sup>96</sup> Moreover overexpression of c-myc was shown to inhibit adipogenesis in 3T3-L1 cells possibly by precluding the entry into a distinct pre-differentiation stage in G0/G1, a fundamental condition for terminal differentiation<sup>97</sup>. Although this is an important factor, mere overexpression of c-myc is not sufficient for the progression in the cell cycle. The cell cycle process is based on a series of phosphorylation/de-phosphorylation reactions regulating the balance between promoters and inhibitors. The cyclin-cdk complexes form holoenzymes that phosphorylate the proteins of the Retinoblastoma family (pRb, p107 and p130) which act at different passages of the cell cycle. Phosphorylation levels are dependent on the cycle phase; for example in exceeding the restriction point of G1 phase, Rb is phosphorylated by the Cyclin D/cdk4-6 activated complex. The hypophosphorylated forms dominate in G0 and in the early G1 phase, while the more phosphorylated forms are present in the S phase, G2 and M. Further levels of phosphorylation may appear dependent on the type of cell considered. When Rb is phosphorylated, it loses affinity for the E2F protein which acquires the ability to activate the transcription of genes involved in the progression of the cycle from one phase to the next. In this study Rb expression was found significantly low in irradiated samples during differentiation. The reduced Rb expression probably is similar to the effects of mutant Rb, thus preventing E2F-mediated transcription. A common aspect of proteins linked to pRb and tumour suppressor genes such as p53 is their ability to inhibit cell proliferation. In addition, studies of Reichert et al.<sup>98</sup> have shown changes in cyclins levels depending on stages of adipogenesis and addition or different percentage of serum. Taking these variables into consideration, the analysis in relation to treatments with blue light becomes even more complex. Although the levels of the complex Cyclin D/Cdk4-6 showed an increase, the negative trend of the Cyclin E/Cdk2 complex, combined with the down regulation of the Rb gene, has been supposed to lead to a cellular delay in G1/S phase. A second delay or arrest may occur in phase G2. Since phase G2 provides the time for proofreading and packaging the replicated DNA prior to cell division, its prolongation may indicate an accumulation of

## Discussion

replication errors, which keeps the 3T3-L1 cells irradiated at checkpoint G2 / M preventing them from proceeding through the cell cycle. As discussed earlier, the path of mismatch repairs, activated in response to replication errors, has been greatly enhanced. In addition, several genes involved in network reporting of DNA damage response were found positively expressed. Indeed, the activation of Chk1 mediated by the ATM/ATR system that recognizes single-stranded DNA (ssDNA) can be the result of UV-induced damage, replication stress and cross-linking between strands<sup>99, 100</sup>. In addition, activated Chk1 promotes ubiquitination and degradation of Cdc25 phosphatase, activates repair factors, such as cellular nuclear antigen proliferation (PCNA) or Rad51, and interacts with many downstream effectors such as Wee1 kinase and PLK1. This complex signalling results in cell cycle stoppage and DNA repair. In addition, Chk1 plays a role in the control point of the spindle during mitosis interacting with the proteins of the Aurora A kinase and Aurora B kinase spindle group.

The cells are maintained in the G2 phase until they are ready to enter the mitosis phase. In this state the cells can repair the DNA and recover or die if the DNA damage is irreversible<sup>101</sup>. The expression of all these genes has been enriched following consecutive light treatments with 21.6 J/cm<sup>2</sup>, showing the same tendency and in many cases were significant already after a single irradiation with long-lasting effects. Despite the presence of persistent DNA damage, cells can enter mitosis following a sustained checkpoint-imposed cell cycle arrest. This ability is called checkpoint adaptation. A checkpoint-regulated protein, Claspin, was increased in expression already after a single irradiation. Required for efficient DNA replication during a normal S phase, Claspin can mediate both activation of Chk1 and the inactivation after a prolonged G2/M arrest, permitting the entry into mitosis. Cells that enter in mitosis following adaptation will arrest in metaphase that can lead to “mitotic catastrophe”<sup>102</sup>. This adaptation represents an alternative elimination process of cells with unrepairable damage<sup>103</sup>.

The lower rate of DNA synthesis, cell count and the latter hypothesis of arrest in G2 / M phase suggested deleterious effects of high doses of blue light during 3T3-L1 cell differentiation.

### **4.2 Effects of multiple exposures of blue light at dose of 21.6 J/cm<sup>2</sup> and 43.3 J/cm<sup>2</sup> on mature adipocytes**

Since mature adipocytes constitute one-third of adipose tissue, blue light effects were tested after complete 3T3-L1 differentiation. Multiple blue light irradiations were applied on cells for 7 days using a dose of 21.6 J/cm<sup>2</sup> equal to an irradiation time of 30 minutes and 43.2 J/cm<sup>2</sup>

## Discussion

equal to an irradiation time of 60 minutes. Evaluation of lipid accumulation was performed as before using Oil Red O staining and related quantification. Both fluences showed a slight and insignificant increase in the lipid amount compared to dark controls (Figure 17). Thus, blue light irradiation did not affect the number of lipid droplets and lipid amount. Gene expression analysis was consistent with Oil Red O staining results. First we investigated whether adipogenic markers were affected by 453nm blue light in differentiated adipocytes. No differences were found between treated and untreated. Choi et al.<sup>104</sup> have tested the effects of several wavelengths in the visible light between 410nm and 690nm observing that only irradiation at 590nm enhance the breakdown of lipid droplets. Probably the wavelength of 453nm chosen for this study was not suitable to induce an activation of lipolysis or reduction of lipid droplets.

XTT and ATP assays were performed in order to evaluate metabolic activity and mitochondria status. While XTT showed a slight decrease directly after 30 min of irradiation that did not vanish after 24h, no significant changes were recorded after 60 min of treatment (Figure 19). Instead, a different trend was observed for the ATP levels where the magnitude of the increase was dependent on the dose of radiations. While after 24 hours the ATP levels were comparable to controls in samples exposed 30 minutes a day to blue light, the levels remained still high after 60 minutes exposures (Figure 21). Blue light stimulated mitochondria in adipocytes that led to an increase in ATP synthesis that was not enough to stimulate cytoplasmic lipase activity. All studies reported lipolysis or fat reduction after LLLT treatment used higher wavelengths from 635 nm upwards<sup>105</sup>.

Compared to irradiated preadipocytes, differentiated adipocytes appear less sensible to radiation. Despite a reduction in oxidative phosphorylation for both fluences, mitochondria and respiratory chain were not completely damaged since were still able to produce ATP. Also ROS levels did not increase following irradiation (Figure 26) and genes involved in detoxification systems were not significantly deregulated in treated cells.

Cell counting with Hoechst staining also has not shown differences between treated and controls. This data could be explained with the adipocyte's characteristic of being a terminally differentiated cell. Once completely differentiated, adipocytes can increase or decrease in size but not in number. The number of adipocytes increases only in severe obesity in which

## Discussion

paracrine/autocrine factors secreted from the various cells within adipose tissue stimulate preadipocytes to form new mature cells<sup>106</sup>. In line, also gene expression did not reflect a significant de-regulation in cell cycle or apoptosis pathways. Thus, blue light seems not to affect proliferation nor induce apoptosis in mature adipocytes.

Also genes involved in JAK-STAT or Cytochrome p450 up-regulated pathways did not show significant changes. This difference between NES of KEGG pathway and expression of a gene is due to a different system analysis. Therefore a gene can be up-regulated in relation to the other genes considered in the same pathway (KEGG analysis) but it can be down regulated or not significantly expressed if the absolute value of expression of that gene is considered.

### 4.3 Conclusions

In conclusion, this preliminary in vitro study showed the different effects at transcriptional and metabolic level during and after adipocyte differentiation. During differentiation cells were more responsive to irradiation, especially in the early stages. This is probably due to a series of processes that are triggered in the first 48 hours from induction in a phase known as mitotic clonal expansion (MCE). During this period the cells rearrange their morphology and trigger the transcription of genes essential for the adipocyte phenotype. A single irradiation at a dose of  $21.6 \text{ j/cm}^2$  at the first day of induction a partial reduction in differentiation was seen evidenced by a reduced lipid amount and a downregulation of adipogenic markers. Slight metabolic effects were observed with a reduction in proliferation and activation of apoptotic processes induced by damage to DNA and biological systems, albeit with moderate effects. Cells are able to partially recover by triggering mechanisms of repair that inevitably lead to a delay in the cell cycle. The cells that are repaired from the damage continue in proliferation and differentiation. Pronounced effects occur as a result of multiple irradiations. After two weeks of treatments the cells interrupted differentiation and are morphologically similar to fibroblasts. Continued exposure to blue light causes an increase in ROS levels which are not attenuated by the detoxification system. Chronic damage occurs and the proliferation/death ratio shifts in favour of the latter following a prolonged arrest in the G2/M phase, confirmed by overexpression of genes involved in mechanisms of damage repair.

Mature adipocytes, on the other hand, did not show significant metabolic or transcriptional changes although a more pronounced trend was obtained at higher doses.

## Discussion

To date, blue light seems to be able to treat conditions of adipocyte hyperplasia but not hypertrophy, although taking into account cellular damage.

In vitro results alone are not sufficient to promote or reject blue light as a therapeutic means in the treatment of diseases involving dysfunction of adipose tissue. Further studies are needed especially in vivo where the effects could be systemic due to a cross-talk between different cells lines present in higher layers, such as the skin. These cell lines can be detected in fibroblasts and keratinocytes that, being more accustomed to exposure to radiation, i.e. solar radiations, can activate modulatory mechanisms even in the layers of the hypodermis involving the adipocytes.



## 5 Summary

Phototherapy was applied to treat medical conditions since 3,500 years, when the ancient Egyptians and Indians used sunlight to treat various diseases. It was only with the invention of electric light in the late 19th century that an alternative emerged. From that time on, the use of phototherapy in the medical field grew, techniques were perfected and developed and eventually gained widespread acceptance. To date, over 2000 scientific articles have been published in PubMed focusing on the various physiological effects of red and NIR radiation. These wavelengths of light have been shown to penetrate through human tissues and to locally and systematically influence cell metabolism, cell signalling, inflammatory processes and growth. This treatment is now called "photobiomodulation" (PBM) therapy. Despite the numerous studies reported, variability in irradiation settings and parameters has led to inconsistent outcomes. The greatest lack of knowledge is related to the effects of low wavelengths of blue/green light. Compared to red/NIR light, blue light is used for a limited range of medical applications because of its inhibitory and cytotoxic effects. However blue light effects have rarely been reported in adipogenesis or lipogenesis studies on adipose tissue. Hence, the biomodulatory potential of blue light at 453 nm wavelength was tested on 3T3-L1 cells during and after the differentiation process with respect to adipogenesis/lipogenesis, metabolic processes, cell proliferation and transcriptome changes.

PBM using blue light revealed dose dependent effects during preadipocytes 3T3-L1 differentiation. A single irradiation performed at the first day of induction (Day0) led to a slight effect with a reduced lipid accumulation and changes in the expression of adipogenic markers that appeared down-regulated already after one exposure. Also metabolism, reflecting mitochondria activity, was negatively affected by blue light since oxidative phosphorylation and ATP contents were decreased with effects that were long lasting until 24h. Tests with repeated irradiations for all differentiation period showed an enhanced inhibition in lipid accumulation and metabolism. This chronic exposure was supposed to rise the ROS amount leading to DNA damages that have had as consequence a cell cycle delay, reduced proliferation rate and cell death processes. Gene expression analysis supported this hypothesis by an up-regulation of the p53 pathway and for all the other genes involved in repair systems such as ATM, Chk1 and Claspin. The blue light spectrum, being close to the

## Summary

harmful UVs wavelength, seems to induce cell death mediated by oxidative stress and damages accumulation in differentiating preadipocytes.

On the other hand mature adipocytes treated with  $21.6 \text{ j/cm}^2$  or  $43.2 \text{ j/cm}^2$  of blue light have proven to be less responsive. No significant differences were reported in metabolism, growth and lipid storage. Similarly apoptosis has not been deregulated and no changes in ROS levels or cellular damages have been observed.

In conclusion adipocytes seem to be more sensitive to blue light exposure during early rather than in late differentiation phases. Furthermore, the high doses of irradiation chosen led to inhibitory effects on metabolism and differentiation promoting cell death in preadipocytes subjected to chronic exposure while no effects were recorded in irradiated mature adipocytes. The results indicated that an optimal choice of irradiation parameters, particularly the dose or irradiation time, is important. Too high doses can lead to expected inhibitory but also deleterious effects on cells. Though inhibitory effects in adipogenesis or proliferation are requested relating to the treatment of hyperplastic obesity or dysregulation of lipid accumulation during childhood, the formation of aberrant cells has to be avoided. Therefore additional studies are needed to promote or reject blue light application in these fields. If tetraploid or aneuploid cells formation is not observed, blue light could be a possible alternative to pharmacological or surgical solutions in some obese subjects. However, there is currently no evidence of a possible application in hypertrophic obesity condition.

## 6 References

1. Grzybowski, A, Pietrzak, K: From patient to discoverer--Niels Ryberg Finsen (1860-1904) --the founder of phototherapy in dermatology. *Clin Dermatol*, 30: 451-455, 2012.
2. Mester, E, Spiry, T, Szende, B, Tota, JG: Effect of laser rays on wound healing. *Am J Surg*, 122: 532-535, 1971.
3. Mester, E, Mester, AF, Mester, A: The biomedical effects of laser application. *Lasers Surg Med*, 5: 31-39, 1985.
4. Anders, JJ, Lanzafame, RJ, Arany, PR: Low-level light/laser therapy versus photobiomodulation therapy. *Photomed Laser Surg*, 33: 183-184, 2015.
5. Ezzati, K, Fekrazad, R, Raoufi, Z: The Effects of Photobiomodulation Therapy on Post-Surgical Pain. *J Lasers Med Sci*, 10: 79-85, 2019.
6. Jenkins, PA, Carroll, JD: How to report low-level laser therapy (LLLT)/photomedicine dose and beam parameters in clinical and laboratory studies. *Photomed Laser Surg*, 29: 785-787, 2011.
7. Hadis, MA, Zainal, SA, Holder, MJ, Carroll, JD, Cooper, PR, Milward, MR, Palin, WM: The dark art of light measurement: accurate radiometry for low-level light therapy. *Lasers Med Sci*, 31: 789-809, 2016.
8. Schulz, H: Über die Theorie der Arzneimittelwirkung. *Virchows Archiv*, 1877.
9. Schulz, H: Über Hefegiste. *Pflügers Archiv Gesamte Physiologie*, 1888.
10. Huang, YY, Sharma, SK, Carroll, J, Hamblin, MR: Biphasic dose response in low level light therapy - an update. *Dose Response*, 9: 602-618, 2011.
11. Huang, YY, Chen, AC, Carroll, JD, Hamblin, MR: Biphasic dose response in low level light therapy. *Dose Response*, 7: 358-383, 2009.
12. Chung, H, Dai, T, Sharma, SK, Huang, YY, Carroll, JD, Hamblin, MR: The nuts and bolts of low-level laser (light) therapy. *Ann Biomed Eng*, 40: 516-533, 2012.
13. Abergel, RP, Lyons, RF, Castel, JC, Dwyer, RM, Uitto, J: Biostimulation of wound healing by lasers: experimental approaches in animal models and in fibroblast cultures. *J Dermatol Surg Oncol*, 13: 127-133, 1987.
14. Afonso, SG, Enriquez de Salamanca, R, Batlle, AM: The photodynamic and non-photodynamic actions of porphyrins. *Braz J Med Biol Res*, 32: 255-266, 1999.
15. Eichler, M, Lavi, R, Shainberg, A, Lubart, R: Flavins are source of visible-light-induced free radical formation in cells. *Lasers Surg Med*, 37: 314-319, 2005.
16. Karu, T: Primary and secondary mechanisms of action of visible to near-IR radiation on cells. *J Photochem Photobiol B*, 1999.
17. Avci, P, Gupta, A, Sadasivam, M, Vecchio, D, Pam, Z, Pam, N, Hamblin, MR: Low-level laser (light) therapy (LLLT) in skin: stimulating, healing, restoring. *Semin Cutan Med Surg*, 32: 41-52, 2013.
18. Hamblin, MR: Mechanisms and applications of the anti-inflammatory effects of photobiomodulation. *AIMS Biophys*, 4: 337-361, 2017.
19. Beaches, HSotP: *COLD LASER THERAPY*. Online: <https://www.healthsolutionsofthepalmbeaches.com/laser>, Stand:09.03.2020

20. Neira, R, Toledo, L, Arroyave, J, Solarte, E, Isaza, C, Gutierrez, O, Criollo, W, Ramirez, H, Gutierrez, MI, Ortiz-Neira, CL: Low-level laser-assisted liposuction: the Neira 4 L technique. *Clin Plast Surg*, 33: 117-127, vii, 2006.
21. Brown, SA, Rohrich, RJ, Kenkel, J, Young, VL, Hoopman, J, Coimbra, M: Effect of low-level laser therapy on abdominal adipocytes before lipoplasty procedures. *Plast Reconstr Surg*, 113: 1796-1804; discussion 1805-1796, 2004.
22. Neira, R, Arroyave, J, Ramirez, H, Ortiz, CL, Solarte, E, Sequeda, F, Gutierrez, MI: Fat liquefaction: effect of low-level laser energy on adipose tissue. *Plast Reconstr Surg*, 110: 912-922; discussion 923-915, 2002.
23. Neira, R, Ortiz-Neira, C: Low-level laser-assisted liposculpture: clinical report of 700 cases. *Aesthet Surg J*, 22: 451-455, 2002.
24. Sasaki, GH, Oberg, K, Tucker, B, Gaston, M: The effectiveness and safety of topical PhotoActiv phosphatidylcholine-based anti-cellulite gel and LED (red and near-infrared) light on Grade II-III thigh cellulite: a randomized, double-blinded study. *J Cosmet Laser Ther*, 9: 87-96, 2007.
25. Lach, E: Reduction of subcutaneous fat and improvement in cellulite appearance by dual-wavelength, low-level laser energy combined with vacuum and massage. *J Cosmet Laser Ther*, 10: 202-209, 2008.
26. Gold, MH, Khatri, KA, Hails, K, Weiss, RA, Fournier, N: Reduction in thigh circumference and improvement in the appearance of cellulite with dual-wavelength, low-level laser energy and massage. *J Cosmet Laser Ther*, 13: 13-20, 2011.
27. Jackson R.F., RGC, Wisler K.: Reduction in Cholesterol and Triglyceride Serum. *Am J Surg*, Vol. 27, No. 4,: 177-184, 2010.
28. Caruso-Davis, MK, Guillot, TS, Podichetty, VK, Mashtalir, N, Dhurandhar, NV, Dubuisson, O, Yu, Y, Greenway, FL: Efficacy of low-level laser therapy for body contouring and spot fat reduction. *Obes Surg*, 21: 722-729, 2011.
29. Nestor, MS, Zarraga, MB, Park, H: Effect of 635nm Low-level Laser Therapy on Upper Arm Circumference Reduction: A Double-blind, Randomized, Sham-controlled Trial. *J Clin Aesthet Dermatol*, 5: 42-48, 2012.
30. Honnor, RC, Dhillon, GS, Londos, C: cAMP-dependent protein kinase and lipolysis in rat adipocytes. II. Definition of steady-state relationship with lipolytic and antilipolytic modulators. *J Biol Chem*, 260: 15130-15138, 1985.
31. E., C: Photoprotective Effects of Blue Light Absorbing Filter against LED Light Exposure on Human Retinal Pigment Epithelial Cells In Vitro. *J Carcinog Mutagen*: 2-7, 2013.
32. de Sousa, NT, Santos, MF, Gomes, RC, Brandino, HE, Martinez, R, de Jesus Guirro, RR: Blue Laser Inhibits Bacterial Growth of Staphylococcus aureus, Escherichia coli, and Pseudomonas aeruginosa. *Photomed Laser Surg*, 33: 278-282, 2015.
33. Alba, MN, Gerenutti, M, Yoshida, VM, Grotto, D: Clinical comparison of salicylic acid peel and LED-Laser phototherapy for the treatment of Acne vulgaris in teenagers. *J Cosmet Laser Ther*, 19: 49-53, 2017.
34. Macula store, Tm: *The blue light threat*. Online: <https://maculastore.com/pages/damaging-effects-of-blue-light>, Stand:11.03.2020
35. Hockberger, PE, Skimina, TA, Centonze, VE, Lavin, C, Chu, S, Dadras, S, Reddy, JK, White, JG: Activation of flavin-containing oxidases underlies light-induced

- production of H<sub>2</sub>O<sub>2</sub> in mammalian cells. *Proc Natl Acad Sci U S A*, 96: 6255-6260, 1999.
36. Massey, V: The chemical and biological versatility of riboflavin. *Biochem Soc Trans*, 28: 283-296, 2000.
37. Garza, ZCF, Born, M, Hilbers, PAJ, van Riel, NAW, Liebmann, J: Visible Blue Light Therapy: Molecular Mechanisms and Therapeutic Opportunities. *Curr Med Chem*, 25: 5564-5577, 2018.
38. Lewis, JB, Wataha, JC, Messer, RL, Caughman, GB, Yamamoto, T, Hsu, SD: Blue light differentially alters cellular redox properties. *J Biomed Mater Res B Appl Biomater*, 72: 223-229, 2005.
39. Liebmann, J, Born, M, Kolb-Bachofen, V: Blue-light irradiation regulates proliferation and differentiation in human skin cells. *J Invest Dermatol*, 130: 259-269, 2010.
40. Regazzetti, C, Sormani, L, Debayle, D, Bernerd, F, Tulic, MK, De Donatis, GM, Chignon-Sicard, B, Rocchi, S, Passeron, T: Melanocytes Sense Blue Light and Regulate Pigmentation through Opsin-3. *J Invest Dermatol*, 138: 171-178, 2018.
41. Yuan, Y, Yan, G, Gong, R, Zhang, L, Liu, T, Feng, C, Du, W, Wang, Y, Yang, F, Li, Y, Guo, S, Ding, F, Ma, W, Idiatullina, E, Pavlov, V, Han, Z, Cai, B, Yang, L: Effects of Blue Light Emitting Diode Irradiation On the Proliferation, Apoptosis and Differentiation of Bone Marrow-Derived Mesenchymal Stem Cells. *Cell Physiol Biochem*, 43: 237-246, 2017.
42. Pagin, MT, de Oliveira, FA, Oliveira, RC, Sant'Ana, AC, de Rezende, ML, Gregghi, SL, Damante, CA: Laser and light-emitting diode effects on pre-osteoblast growth and differentiation. *Lasers Med Sci*, 29: 55-59, 2014.
43. Haslam, DW, James, WP: Obesity. *Lancet*, 366: 1197-1209, 2005.
44. Fonseca-Alaniz, MH, Takada, J, Alonso-Vale, MI, Lima, FB: Adipose tissue as an endocrine organ: from theory to practice. *J Pediatr (Rio J)*, 83: S192-203, 2007.
45. Pi-Sunyer, X: The medical risks of obesity. *Postgrad Med*, 121: 21-33, 2009.
46. Grundy, SM: Multifactorial causation of obesity: implications for prevention. *Am J Clin Nutr*, 67: 563s-572s, 1998.
47. Chalk, MB: Obesity: addressing a multifactorial disease. *Case Manager*, 15: 47-49; quiz 50, 2004.
48. Beunza, JJ, Toledo, E, Hu, FB, Bes-Rastrollo, M, Serrano-Martinez, M, Sanchez-Villegas, A, Martinez, JA, Martinez-Gonzalez, MA: Adherence to the Mediterranean diet, long-term weight change, and incident overweight or obesity: the Seguimiento Universidad de Navarra (SUN) cohort. *Am J Clin Nutr*, 92: 1484-1493, 2010.
49. van der Heijden, AA, Hu, FB, Rimm, EB, van Dam, RM: A prospective study of breakfast consumption and weight gain among U.S. men. *Obesity (Silver Spring)*, 15: 2463-2469, 2007.
50. Wyatt, HR: Update on treatment strategies for obesity. *J Clin Endocrinol Metab*, 98: 1299-1306, 2013.
51. Bray, GA, Tartaglia, LA: Medicinal strategies in the treatment of obesity. *Nature*, 404: 672-677, 2000.
52. Ottaviani, E, Malagoli, D, Franceschi, C: The evolution of the adipose tissue: a neglected enigma. *Gen Comp Endocrinol*, 174: 1-4, 2011.

53. Coelho, M, Oliveira, T, Fernandes, R: Biochemistry of adipose tissue: an endocrine organ. *Arch Med Sci*, 9: 191-200, 2013.
54. Saely, CH, Geiger, K, Drexel, H: Brown versus white adipose tissue: a mini-review. *Gerontology*, 58: 15-23, 2012.
55. B., B: *Medical gallery of Blausen Medical 2014*. 2014. Online: [https://en.wikiversity.org/wiki/WikiJournal\\_of\\_Medicine/Medical\\_gallery\\_of\\_Blausen\\_Medical\\_2014](https://en.wikiversity.org/wiki/WikiJournal_of_Medicine/Medical_gallery_of_Blausen_Medical_2014), Stand:12.02.2020
56. Jo, J, Gavrilova, O, Pack, S, Jou, W, Mullen, S, Sumner, AE, Cushman, SW, Periwé, V: Hypertrophy and/or Hyperplasia: Dynamics of Adipose Tissue Growth. *PLoS Comput Biol*, 5: e1000324, 2009.
57. Choe, SS, Huh, JY, Hwang, IJ, Kim, JI, Kim, JB: Adipose Tissue Remodeling: Its Role in Energy Metabolism and Metabolic Disorders. *Front Endocrinol (Lausanne)*, 7: 30, 2016.
58. Gregoire, FM, Smas, CM, Sul, HS: Understanding adipocyte differentiation. *Physiol Rev*, 78: 783-809, 1998.
59. Turchin V,: *Tissue Optics: Light Scattering Methods and Instruments for Medical Diagnosis*. SPIE PRESS, Washington, 2000.
60. Bashkatov, AN: Optical Properties of the Subcutaneous Adipose Tissue in the Spectral Range 400–2500 nm. *Opt Spectrosc*, 99: 836, 2005.
61. Tang, QQ, Otto, TC, Lane, MD: Mitotic clonal expansion: a synchronous process required for adipogenesis. *Proc Natl Acad Sci U S A*, 100: 44-49, 2003.
62. Qiu, Z, Wei, Y, Chen, N, Jiang, M, Wu, J, Liao, K: DNA synthesis and mitotic clonal expansion is not a required step for 3T3-L1 preadipocyte differentiation into adipocytes. *J Biol Chem*, 276: 11988-11995, 2001.
63. Caprio, M, Fève, B, Claes, A, Viengchareun, S, Lombes, M, Zennaro, MC: Pivotal role of the mineralocorticoid receptor in corticosteroid-induced adipogenesis. *Faseb j*, 21: 2185-2194, 2007.
64. Tang, QQ, Gronborg, M, Huang, H, Kim, JW, Otto, TC, Pandey, A, Lane, MD: Sequential phosphorylation of CCAAT enhancer-binding protein beta by MAPK and glycogen synthase kinase 3beta is required for adipogenesis. *Proc Natl Acad Sci U S A*, 102: 9766-9771, 2005.
65. Rosen, ED, MacDougald, OA: Adipocyte differentiation from the inside out. *Nat Rev Mol Cell Biol*, 7: 885-896, 2006.
66. Moseti, D, Regassa, A, Kim, WK: Molecular Regulation of Adipogenesis and Potential Anti-Adipogenic Bioactive Molecules. *Int J Mol Sci*, 17, 2016.
67. Ohsumi, J, Sakakibara, S, Yamaguchi, J, Miyadai, K, Yoshioka, S, Fujiwara, T, Horikoshi, H, Serizawa, N: Troglitazone prevents the inhibitory effects of inflammatory cytokines on insulin-induced adipocyte differentiation in 3T3-L1 cells. *Endocrinology*, 135: 2279-2282, 1994.
68. Keller, DC, Du, XX, Srour, EF, Hoffman, R, Williams, DA: Interleukin-11 inhibits adipogenesis and stimulates myelopoiesis in human long-term marrow cultures. *Blood*, 82: 1428-1435, 1993.
69. Lee, JE, Schmidt, H, Lai, B, Ge, K: Transcriptional and Epigenomic Regulation of Adipogenesis. *Mol Cell Biol*, 39, 2019.

## Appendix

70. Musri, MM, Parrizas, M: Epigenetic regulation of adipogenesis. *Curr Opin Clin Nutr Metab Care*, 15: 342-349, 2012.
71. Kiehn, JT, Tsang, AH, Heyde, I, Leinweber, B, Kolbe, I, Leliavski, A, Oster, H: Circadian Rhythms in Adipose Tissue Physiology. *Compr Physiol*, 7: 383-427, 2017.
72. Gomez-Santos, C, Gomez-Abellan, P, Madrid, JA, Hernandez-Morante, JJ, Lujan, JA, Ordovas, JM, Garaulet, M: Circadian rhythm of clock genes in human adipose explants. *Obesity (Silver Spring)*, 17: 1481-1485, 2009.
73. Mehra, A, Macdonald, I, Pillay, TS: Variability in 3T3-L1 adipocyte differentiation depending on cell culture dish. *Anal Biochem*, 362: 281-283, 2007.
74. Zebisch, K, Voigt, V, Wabitsch, M, Brandsch, M: Protocol for effective differentiation of 3T3-L1 cells to adipocytes. *Anal Biochem*, 425: 88-90, 2012.
75. Lee, J, Lee, J, Jung, E, Kim, YS, Roh, K, Jung, KH, Park, D: Ultraviolet A regulates adipogenic differentiation of human adipose tissue-derived mesenchymal stem cells via up-regulation of Kruppel-like factor 2. *J Biol Chem*, 285: 32647-32656, 2010.
76. Kim, EJ, Kim, YK, Kim, JE, Kim, S, Kim, MK, Park, CH, Chung, JH: UV modulation of subcutaneous fat metabolism. *J Invest Dermatol*, 131: 1720-1726, 2011.
77. Li, WH, Pappas, A, Zhang, L, Ruvoilo, E, Cavender, D: IL-11, IL-1alpha, IL-6, and TNF-alpha are induced by solar radiation in vitro and may be involved in facial subcutaneous fat loss in vivo. *J Dermatol Sci*, 71: 58-66, 2013.
78. Bijland, S, Mancini, SJ, Salt, IP: Role of AMP-activated protein kinase in adipose tissue metabolism and inflammation. *Clin Sci (Lond)*, 124: 491-507, 2013.
79. Wataha, JC, Lewis, JB, Messer, RL, Caughman, GB, Yamamoto, T, Hsu, SD: Blue light differentially alters cellular redox properties. *J Biomed Mater Res B Appl Biomater*, 72: 223-229, 2005.
80. Karu, T: Primary and secondary mechanisms of action of visible to near-IR radiation on cells. *J Photochem Photobiol B*, 49: 1-17, 1999.
81. Chen, AC, Arany, PR, Huang, YY, Tomkinson, EM, Sharma, SK, Kharkwal, GB, Saleem, T, Mooney, D, Yull, FE, Blackwell, TS, Hamblin, MR: Low-level laser therapy activates NF-kB via generation of reactive oxygen species in mouse embryonic fibroblasts. *PLoS One*, 6: e22453, 2011.
82. Wang, Y, Huang, Y-Y, Wang, Y, Lyu, P, Hamblin, MR: Red (660 nm) or near-infrared (810 nm) photobiomodulation stimulates, while blue (415 nm), green (540 nm) light inhibits proliferation in human adipose-derived stem cells. *Sci Rep*, 7, 2017.
83. Hamblin, MR: Photobiomodulation for Alzheimer's Disease: Has the Light Dawned? *Photonics*, 6, 2019.
84. Dey, R, Moraes, CT: Lack of oxidative phosphorylation and low mitochondrial membrane potential decrease susceptibility to apoptosis and do not modulate the protective effect of Bcl-x(L) in osteosarcoma cells. *J Biol Chem*, 275: 7087-7094, 2000.
85. Harman, D: The aging process. *Proc Natl Acad Sci U S A*, 78: 7124-7128, 1981.
86. Osborne, NN, Alvarez, CN, del Olmo Aguado, S: Targeting mitochondrial dysfunction as in aging and glaucoma. *Drug Discov Today*, 19: 1613-1622, 2014.
87. Muller, FL, Liu, Y, Van Remmen, H: Complex III releases superoxide to both sides of the inner mitochondrial membrane. *J Biol Chem*, 279: 49064-49073, 2004.

## Appendix

88. Poglio, S, Galvani, S, Bour, S, Andre, M, Prunet-Marcassus, B, Penicaud, L, Casteilla, L, Cousin, B: Adipose tissue sensitivity to radiation exposure. *Am J Pathol*, 174: 44-53, 2009.
89. Taoufik, K, Mavrogonatou, E, Eliades, T, Papagiannoulis, L, Eliades, G, Kletsas, D: Effect of blue light on the proliferation of human gingival fibroblasts. *Dent Mater*, 24: 895-900, 2008.
90. Mignon, C, Uzunbajakava, NE, Castellano-Pellicena, I, Botchkareva, NV, Tobin, DJ: Differential response of human dermal fibroblast subpopulations to visible and near-infrared light: Potential of photobiomodulation for addressing cutaneous conditions. *Lasers Surg Med*, 50: 859-882, 2018.
91. Chautan, M, Chazal, G, Cecconi, F, Gruss, P, Golstein, P: Interdigital cell death can occur through a necrotic and caspase-independent pathway. *Curr Biol*, 9: 967-970, 1999.
92. Yoshida, H, Kong, YY, Yoshida, R, Elia, AJ, Hakem, A, Hakem, R, Penninger, JM, Mak, TW: Apaf1 is required for mitochondrial pathways of apoptosis and brain development. *Cell*, 94: 739-750, 1998.
93. Ricci, JE, Munoz-Pinedo, C, Fitzgerald, P, Bailly-Maitre, B, Perkins, GA, Yadava, N, Scheffler, IE, Ellisman, MH, Green, DR: Disruption of mitochondrial function during apoptosis is mediated by caspase cleavage of the p75 subunit of complex I of the electron transport chain. *Cell*, 117: 773-786, 2004.
94. Colell, A, Ricci, JE, Tait, S, Milasta, S, Maurer, U, Bouchier-Hayes, L, Fitzgerald, P, Guio-Carrion, A, Waterhouse, NJ, Li, CW, Mari, B, Barbry, P, Newmeyer, DD, Beere, HM, Green, DR: GAPDH and autophagy preserve survival after apoptotic cytochrome c release in the absence of caspase activation. *Cell*, 129: 983-997, 2007.
95. Shreder, K, Rapp, F, Tsoukala, I, Rzeznik, V, Wabitsch, M, Fischer-Posovszky, P, Fournier, C: Impact of X-ray Exposure on the Proliferation and Differentiation of Human Pre-Adipocytes. *Int J Mol Sci*, 19: 2717, 2018.
96. Eilers, M, Schirm, S, Bishop, JM: The MYC protein activates transcription of the alpha-prothymosin gene. *Embo j*, 10: 133-141, 1991.
97. Freytag, SO: Enforced expression of the c-myc oncogene inhibits cell differentiation by precluding entry into a distinct predifferentiation state in G0/G1. *Mol Cell Biol*, 8: 1614-1624, 1988.
98. Reichert, M, Eick, D: Analysis of cell cycle arrest in adipocyte differentiation. *Oncogene*, 18: 459-466, 1999.
99. Zhang, Y, Hunter, T: Roles of Chk1 in cell biology and cancer therapy. *Int J Cancer*, 134: 1013-1023, 2014.
100. Patil, M, Pabla, N, Dong, Z: Checkpoint kinase 1 in DNA damage response and cell cycle regulation. *Cell Mol Life Sci*, 70: 4009-4021, 2013.
101. Meuth, M: Chk1 suppressed cell death. *Cell Div*, 5: 21, 2010.
102. Vakifahmetoglu, H, Olsson, M, Zhivotovsky, B: Death through a tragedy: mitotic catastrophe. *Cell Death Differ*, 15: 1153-1162, 2008.
103. Bartek, J, Lukas, J: DNA damage checkpoints: from initiation to recovery or adaptation. *Curr Opin Cell Biol*, 19: 238-245, 2007.



## Appendix

104. Choi, MS, Kim, HJ, Ham, M, Choi, DH, Lee, TR, Shin, DW: Amber Light (590 nm) Induces the Breakdown of Lipid Droplets through Autophagy-Related Lysosomal Degradation in Differentiated Adipocytes. *Sci Rep*, 6: 28476, 2016.
105. Avci, P, Nyame, TT, Gupta, GK, Sadasivam, M, Hamblin, MR: Low-level laser therapy for fat layer reduction: a comprehensive review. *Lasers Surg Med*, 45: 349-357, 2013.
106. Hausman, DB, DiGirolamo, M, Bartness, TJ, Hausman, GJ, Martin, RJ: The biology of white adipocyte proliferation. *Obes Rev*, 2: 239-254, 2001.

## 7 Appendix

**Table 15: complete gene expression analysis of the first set-up: irradiation during differentiation process.** Down-regulated (Up-regulated) pathways are indicated by the negative (positive) NES coloured in green (red). Significant p-value and adjusted p-value (<0.05) are written in green.

Name	NES D1 vs Ctrl	NES D14 vs Ctrl	pvalue D1 vs Ctrl	Adj. pvalue D1 vs Ctrl	pvalue D14 vs Ctrl	Adj. pvalue D14 vs Ctrl
<b>1. Metabolism</b>						
<b>1.0 Global and overview maps</b>						
Metabolic pathways	-2.51	-2.55	0.0001	0.001302	0.000694	0.00375
Carbon metabolism	-2.81	-2.93	0.00012	0.001302	0.000299	0.002066
2-Oxocarboxylic acid metabolism	-2.12	-2.11	0.00017	0.001302	0.000504	0.002951
Fatty acid metabolism	-2.41	-2.74	0.00014	0.001302	0.00027	0.002066
Biosynthesis of amino acids	-2.42	-2.13	0.00013	0.001302	0.000281	0.002066
<b>1.1. Carbohydrate metabolism</b>						
Glycolysis Gluconeogenesis	-2.36	-2.08	0.00014	0.001302	0.000268	0.002066
Citrate cycle (TCA cycle)	-2.51	-2.75	0.00015	0.001302	0.000264	0.002066
Pentose phosphate pathway	-2.13	-1.96	0.00016	0.001302	0.00104	0.005409
Pentose and glucuronate interconversions	-0.95	0.89	0.52677	0.740633	0.61425	0.70111
Fructose and mannose metabolism	-2.09	-1.61	0.00015	0.001302	0.020011	0.057377
Galactose metabolism	-1.63	-1.06	0.01801	0.058164	0.360516	0.494171
Starch and sucrose metabolism	-1.89	-1.73	0.0005	0.00341	0.01333	0.040714
Amino sugar and nucleotide sugar metabolism	-1.18	0.62	0.24115	0.448493	0.97321	0.984994
Inositol phosphate metabolism	-1.42	-0.68	0.05245	0.143099	0.957883	0.978782
Pyruvate metabolism	-2.44	-2.68	0.00015	0.001302	0.000264	0.002066
Glyoxylate and dicarboxylate metabolism	-2.32	-2.5	0.00016	0.001302	0.000258	0.002066
Propanoate metabolism	-2.48	-2.82	0.00016	0.001302	0.000258	0.002066
<b>1.2. Energy metabolism</b>						
Oxidative phosphorylation	-2.74	-2.97	0.00012	0.001302	0.000296	0.002066
<b>1.3. Lipid metabolism</b>						
Fatty acid elongation	-1.67	-1.79	0.012	0.040983	0.004135	0.015703
Fatty acid degradation	-2.22	-2.4	0.00015	0.001302	0.000265	0.002066
Steroid biosynthesis	-2.14	-2.2	0.00017	0.001302	0.000255	0.002066
Steroid hormone biosynthesis	-1.38	-1.23	0.11448	0.245567	0.212864	0.337936
Glycerolipid metabolism	-2.16	-2.22	0.00014	0.001302	0.000269	0.002066
Glycerophospholipid metabolism	-2.08	-2.09	0.00013	0.001302	0.000281	0.002066
Ether lipid metabolism	-1.46	-1.29	0.06287	0.162086	0.154626	0.264938
Arachidonic acid metabolism	-1.71	-1.43	0.00918	0.032653	0.070931	0.156942
Sphingolipid metabolism	1.4	1.45	0.06219	0.161803	0.04428	0.109147
Biosynthesis of unsaturated fatty acids	-1.94	-2.15	0.00016	0.001302	0.00026	0.002066
<b>1.4. Nucleotide metabolism</b>						
Purine metabolism	-1.29	1.27	0.10859	0.236533	0.097269	0.197818
Pyrimidine metabolism	0.95	1.79	0.55437	0.752552	0.000478	0.00286
<b>1.5. Amino acid metabolism</b>						
Alanine, aspartate and glutamate metabolism	-1.88	-1.62	0.00016	0.001302	0.02105	0.058565
Glycine, serine and threonine metabolism	-1.76	-1.3	0.00398	0.017223	0.138273	0.245916

## Appendix








































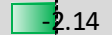

Cysteine and methionine metabolism	-1.8	-1.46	0.0029	0.013293	0.048128	0.11524
Valine, leucine and isoleucine degradation	-2.61	-2.96	0.00014	0.001302	0.000268	0.002066
Lysine degradation	-1.83	-1.57	0.00097	0.005277	0.017069	0.050487
Arginine and proline metabolism	-1.15	0.94	0.28816	0.496759	0.56254	0.672427
Tyrosine metabolism	-1.74	-1.66	0.00462	0.019665	0.021533	0.059321
Tryptophan metabolism	-1.91	-1.8	0.00016	0.001302	0.006753	0.024021
<b>1.6. Metabolism of other amino acids</b>						
beta-Alanine metabolism	-2.01	-1.96	0.00016	0.001302	0.001292	0.006481
Selenocompound metabolism	-1.41	-0.89	0.09268	0.217025	0.603175	0.69464
Glutathione metabolism	-1.76	0.93	0.00293	0.013293	0.578487	0.683004
<b>1.7. Glycan biosynthesis and metabolism</b>						
N-Glycan biosynthesis	1.37	1.34	0.0666	0.168593	0.084359	0.178231
Other glycan degradation	1.42	0.6	0.07585	0.186973	0.952113	0.978782
Other types of O-glycan biosynthesis	1.07	0.96	0.36701	0.592692	0.526471	0.651501
Mannose type O-glycan biosynthesis	0.92	1.35	0.56871	0.757381	0.112533	0.216587
Glycosaminoglycan biosynthesis	-0.38	-0.73	0.99746	0.999771	0.817998	0.867387
Glycosaminoglycan biosynthesis	-0.56	-0.59	0.95544	0.999771	0.943849	0.978677
Glycosylphosphatidylinositol (GPI)-anchor biosynthesis	-0.56	0.96	0.97045	0.999771	0.518362	0.644512
<b>1.8. Metabolism of cofactors and vitamins</b>						
One carbon pool by folate	0.78	1.47	0.77904	0.891746	0.049213	0.11524
Nicotinate and nicotinamide metabolism	-1.47	-1.38	0.05852	0.155311	0.101691	0.20266
Folate biosynthesis	-1.59	-1.5	0.02674	0.079921	0.067126	0.150899
Retinol metabolism	-1.59	-1.63	0.0254	0.076759	0.027429	0.072033
Porphyrin and chlorophyll metabolism	-1.75	-1.06	0.0053	0.021895	0.356681	0.491311
<b>1.9. Metabolism of terpenoids and polyketides</b>						
Terpenoid backbone biosynthesis	-2	-2.24	0.00016	0.001302	0.00026	0.002066
<b>1.11. Xenobiotics biodegradation and metabolism</b>						
Metabolism of xenobiotics by cytochrome P450	-1.86	-1.5	0.00147	0.007397	0.039159	0.098247
Drug metabolism	-1.7	-1.31	0.00835	0.030891	0.125924	0.230529
Drug metabolism (other enzymes)	-1.36	1.41	0.08562	0.207397	0.049016	0.11524
<b>2. Genetic Information Processing</b>						
<b>2.1. Transcription</b>						
RNA polymerase	-0.49	1.55	0.99082	0.999771	0.024178	0.065327
Basal transcription factors	-0.47	1.22	0.99757	0.999771	0.175764	0.292247
Spliceosome	2.1	2.26	0.00067	0.004206	0.000147	0.002066
<b>2.2. Translation</b>						
Aminoacyl-tRNA biosynthesis	-1.27	1.41	0.14918	0.297299	0.050647	0.117618
Ribosome biogenesis in eukaryotes	0.72	1.96	0.97009	0.999771	0.000155	0.002066
Ribosome	1.77	1.78	0.00065	0.004206	0.000294	0.002066
RNA transport	1.08	2.07	0.2594	0.458429	0.000145	0.002066
mRNA surveillance pathway	0.68	1.54	0.98514	0.999771	0.009035	0.030225
<b>2.3. Folding, sorting and degradation</b>						
RNA degradation	-1	1.31	0.47084	0.700604	0.077006	0.167742
Proteasome	-0.82	1.45	0.7337	0.858182	0.037946	0.096063

## Appendix

Protein export	-1.68	-1.7	0.01211	0.040983	0.010957	0.035718
Ubiquitin mediated proteolysis	0.84	1.58	0.86925	0.961646	0.002353	0.010012
SNARE interactions in vesicular transport	0.7	0.92	0.92204	0.992698	0.596172	0.689401
Protein processing in endoplasmic reticulum	-0.53	1.04	0.99977	0.999771	0.377092	0.506999
<b>2.4. Replication and repair</b>						
DNA replication	2.04	2.39	0.00032	0.002237	0.000161	0.002066
Base excision repair	0.87	1.58	0.67478	0.83736	0.015814	0.047274
Nucleotide excision repair	1.61	1.84	0.00862	0.031046	0.000478	0.00286
Mismatch repair	1.35	1.87	0.10491	0.235236	0.000816	0.004327
Homologous recombination	0.8	1.49	0.81171	0.918799	0.026665	0.070686
Fanconi anemia pathway	1.13	1.52	0.2426	0.448493	0.018084	0.052933
<b>3. Environmental Information Processing</b>						
<b>3.1. Membrane transport</b>						
ABC transporters	-1.71	-1.69	0.00857	0.031046	0.011058	0.035718
<b>3.2. Signal transduction</b>						
MAPK signaling pathway	0.93	1.1	0.72116	0.852378	0.242267	0.37405
ErbB signaling pathway	-0.6	1.17	0.9863	0.999771	0.193829	0.314831
Ras signaling pathway	0.88	1.07	0.81313	0.918799	0.327807	0.456009
Rap1 signaling pathway	1.27	1.21	0.04303	0.123394	0.117519	0.223127
Calcium signaling pathway	-1.14	1.1	0.25609	0.455448	0.257034	0.392231
cGMP-PKG signaling pathway	-1.5	-1.43	0.01558	0.051508	0.022442	0.061224
cAMP signaling pathway	-1.12	1.2	0.27561	0.481026	0.130036	0.232739
NF-kappa B signaling pathway	1.35	1.56	0.05097	0.140425	0.012795	0.039508
HIF-1 signaling pathway	-2.14	-1.75	0.00013	0.001302	0.001734	0.007735
FoxO signaling pathway	-1.3	1.1	0.08533	0.207397	0.258288	0.392231
Phosphatidylinositol signaling system	-0.95	0.95	0.55136	0.752552	0.553637	0.667692
Sphingolipid signaling pathway	-0.61	0.9	0.98704	0.999771	0.656983	0.732588
Phospholipase D signaling pathway	-0.69	0.89	0.94296	0.999771	0.691879	0.765425
mTOR signaling pathway	-0.92	0.66	0.62627	0.79922	0.99042	0.993957
PI3K-Akt signaling pathway	-1.03	-1.29	0.40317	0.629387	0.027768	0.072247
AMPK signaling pathway	-2.13	-2.34	0.00012	0.001302	0.000297	0.002066
Wnt signaling pathway	1.22	1.14	0.0896	0.213822	0.215472	0.33922
Notch signaling pathway	-0.53	0.46	0.98905	0.999771	0.998884	0.998884
Hedgehog signaling pathway	1.43	0.92	0.04893	0.136139	0.594212	0.689401
TGF-beta signaling pathway	-0.7	-0.67	0.90857	0.991884	0.973928	0.984994
VEGF signaling pathway	-0.68	1.11	0.91712	0.991884	0.294776	0.424044
Apelin signaling pathway	-1.22	-1.25	0.16137	0.317098	0.098743	0.198192
Hippo signaling pathway	1.47	1.1	0.00969	0.034044	0.277199	0.405693
Hippo signaling pathway	1.79	1.24	0.0033	0.014704	0.185083	0.304142
JAK-STAT signaling pathway	-0.9	0.92	0.63392	0.802395	0.618774	0.70111
TNF signaling pathway	1.55	1.65	0.00695	0.026383	0.002423	0.010012
<b>3.3. Signaling molecules and interaction</b>						
Cytokine-cytokine receptor interaction	1.21	1.49	0.10444	0.235236	0.011712	0.037398
Neuroactive ligand-receptor interaction	-0.96	-1.14	0.53614	0.749528	0.236025	0.368461
ECM-receptor interaction	-1	-1.37	0.47181	0.700604	0.065408	0.148222
Cell adhesion molecules (CAMs)	1.02	1.31	0.40238	0.629387	0.091746	0.190968

## Appendix

<b>4. Cellular Processes</b>							
<b>4.1. Transport and catabolism</b>							
Autophagy (other)	-1.36	-0.57	0.10715	0.235236	0.983879	0.990932	
Mitophagy	-1.27	-0.73	0.13351	0.279977	0.925853	0.963573	
Autophagy	-1.23	-0.76	0.13531	0.280274	0.949375	0.978782	
Lysosome	1.53	0.89	0.00689	0.026383	0.699985	0.770413	
Endocytosis	1.22	1.41	0.0443	0.125731	0.007299	0.025322	
Phagosome	1.28	1.34	0.05568	0.150438	0.048884	0.11524	
Peroxisome	-2.51	-2.87	0.00013	0.001302	0.000281	0.002066	
<b>4.2. Cell growth and death</b>							
Cell cycle	1.66	2.08	0.00185	0.008966	0.000149	0.002066	
Oocyte meiosis	1.3	1.65	0.04748	0.133408	0.002422	0.010012	
p53 signaling pathway	1.37	1.63	0.04203	0.121768	0.005562	0.020841	
Apoptosis	0.93	1.47	0.65275	0.818856	0.012261	0.038498	
Apoptosis (multiple species)	-0.91	0.72	0.57907	0.76345	0.884908	0.927833	
Ferroptosis	-1.72	-1.27	0.00481	0.020172	0.139375	0.246316	
Necroptosis	-0.86	1.32	0.71012	0.849127	0.057437	0.132292	
Cellular senescence	1.02	1.67	0.40154	0.629387	0.000577	0.003188	
Focal adhesion	1.23	1.24	0.06486	0.1657	0.091591	0.190968	
Adherens junction	0.93	1.14	0.60576	0.784414	0.248993	0.382334	
Tight junction	0.97	1.22	0.52671	0.740633	0.125692	0.230529	
Gap junction	1.46	1.46	0.02247	0.068637	0.030284	0.078072	
Signaling pathways regulating pluripotency of stem cells	-0.63	0.76	0.97794	0.999771	0.918972	0.959967	
Regulation of actin cytoskeleton	1.41	1.54	0.00618	0.024449	0.002306	0.009971	
<b>5. Organismal Systems</b>							
<b>5.1. Immune system</b>							
Chemokine signaling pathway	1.26	1.58	0.05859	0.155311	0.003591	0.013824	
Complement and coagulation cascades	-0.92	-1.26	0.56433	0.757381	0.158923	0.26902	
Platelet activation	1.1	1.03	0.25023	0.450727	0.412145	0.541182	
Antigen processing and presentation	1.69	1.9	0.00256	0.011978	0.000159	0.002066	
Toll-like receptor signaling pathway	1.69	1.69	0.0021	0.009981	0.002483	0.01011	
NOD-like receptor signaling pathway	1.77	1.97	0.00126	0.006418	0.000148	0.002066	
RIG-I-like receptor signaling pathway	1.81	1.49	0.00071	0.004342	0.025183	0.067395	
Cytosolic DNA-sensing pathway	1.8	2.1	0.0017	0.008367	0.000159	0.002066	
C-type lectin receptor signaling pathway	1.23	1.52	0.10608	0.235236	0.01233	0.038498	
Hematopoietic cell lineage	-0.88	-0.99	0.63912	0.805348	0.466084	0.592622	
Natural killer cell mediated cytotoxicity	1.04	1.54	0.37673	0.604921	0.015382	0.046477	
IL-17 signaling pathway	1.32	1.69	0.06176	0.161803	0.0028	0.011083	
Th1 and Th2 cell differentiation	0.81	1.12	0.83567	0.935547	0.273973	0.40307	
Th17 cell differentiation	-0.45	1.03	0.99947	0.999771	0.405481	0.534931	
T cell receptor signaling pathway	1.11	1.47	0.24225	0.448493	0.020481	0.057552	
B cell receptor signaling pathway	0.72	1.3	0.93696	0.999771	0.103787	0.205381	
Fc epsilon RI signaling pathway	0.95	1.31	0.54716	0.752552	0.106977	0.208755	
Fc gamma R-mediated phagocytosis	1.2	1.48	0.14015	0.285075	0.019931	0.057377	
Leukocyte transendothelial migration	1.62	1.76	0.00629	0.024565	0.0014	0.006713	




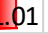







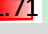





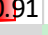








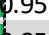

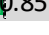
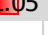


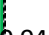

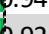

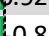
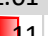
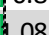









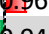


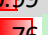



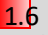






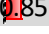
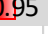











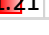
<b>5.2. Endocrine system</b>							
PPAR signaling pathway		-2.48	-2.98	0.00014	0.001302	0.00027	0.002066
Insulin signaling pathway		-2.08	-2.11	0.00012	0.001302	0.000301	0.002066
Insulin secretion		-0.89	0.83	0.62065	0.79922	0.753792	0.811554
GnRH signaling pathway		0.94	1.03	0.5913	0.772812	0.400777	0.533736
Ovarian steroidogenesis		-1.3	0.81	0.16361	0.319261	0.743435	0.805747
Progesterone-mediated oocyte maturation		1.25	1.6	0.09103	0.214947	0.005881	0.02146
Estrogen signaling pathway		0.9	1.11	0.7	0.847845	0.267227	0.399419
Melanogenesis		1.23	0.96	0.12665	0.26758	0.52862	0.651501
Prolactin signaling pathway		-0.83	0.88	0.72947	0.857656	0.670241	0.744418
Thyroid hormone synthesis		-0.92	-0.94	0.58115	0.76345	0.541321	0.660145
Thyroid hormone signaling pathway		-0.76	1.03	0.85589	0.95061	0.404249	0.534931
Adipocytokine signaling pathway		-1.81	-1.94	0.00096	0.005277	0.000548	0.003141
Oxytocin signaling pathway		0.97	1.11	0.51681	0.73718	0.269693	0.400973
Glucagon signaling pathway		-1.97	-2.04	0.00013	0.001302	0.000285	0.002066
Regulation of lipolysis in adipocytes		-1.93	-2.11	0.00057	0.003847	0.000269	0.002066
Renin secretion		-1.35	-1.1	0.09785	0.225385	0.294008	0.424044
Aldosterone synthesis and secretion		-1.48	-1.27	0.02803	0.082906	0.116756	0.223127
Relaxin signaling pathway		-0.77	-0.95	0.85248	0.950582	0.570881	0.676868
Cortisol synthesis and secretion		-1.3	-0.97	0.13928	0.285075	0.4899	0.614538
Parathyroid hormone synthesis, secretion and action		0.74	0.66	0.9479	0.999771	0.974478	0.984994
<b>5.3. Circulatory system</b>							
Cardiac muscle contraction		-1.99	-2.06	0.00028	0.002024	0.000267	0.002066
Adrenergic signaling in cardiomyocytes		1.09	0.9	0.2623	0.460656	0.653011	0.73106
Vascular smooth muscle contraction		-0.82	0.69	0.76312	0.885148	0.955187	0.978782
<b>5.4. Digestive system</b>							
Salivary secretion		-1.1	-1.04	0.33115	0.538459	0.379781	0.508183
Gastric acid secretion		0.98	0.95	0.47384	0.700604	0.535292	0.656843
Pancreatic secretion		-1.34	-1.36	0.09999	0.228423	0.079625	0.172112
Carbohydrate digestion and absorption		-1.2	-0.93	0.2476	0.450727	0.542681	0.660145
Protein digestion and absorption		-0.99	-1.84	0.47621	0.700604	0.001616	0.007324
Fat digestion and absorption		-2.02	-2.07	0.00017	0.001302	0.001531	0.007054
Bile secretion		-1.13	1.13	0.31747	0.53419	0.12766	0.230529
Mineral absorption		-1.02	1.06	0.44591	0.68098	0.3704	0.502814
Cholesterol metabolism		-1.85	-2.14	0.00106	0.005638	0.000264	0.002066
<b>5.5. Excretory system</b>							
Aldosterone-regulated sodium reabsorption		-0.88	-0.92	0.6248	0.79922	0.56341	0.672427
Endocrine and other factor-regulated calcium reabsorption		0.87	0.89	0.67033	0.837171	0.639265	0.718534
Vasopressin-regulated water reabsorption		1.04	1.1	0.38563	0.615685	0.315418	0.443162
Collecting duct acid secretion		-0.98	-0.83	0.49055	0.713526	0.701871	0.770413
<b>5.6. Nervous system</b>							
Long-term potentiation		1.07	1.31	0.32518	0.537503	0.097793	0.197818
Synaptic vesicle cycle		0.99	1.14	0.47138	0.700604	0.259626	0.392231
Neurotrophin signaling pathway		1.05	1.2	0.32712	0.537544	0.146628	0.254719
Retrograde endocannabinoid signaling		-2.14	-1.88	0.00013	0.001302	0.000579	0.003188
Glutamatergic synapse		-0.86	0.77	0.68844	0.844765	0.859885	0.908374



## Appendix

Cholinergic synapse	1.13	1.07	0.21797	0.41108	0.335043	0.463778
Serotonergic synapse	1.12	1.51	0.24991	0.450727	0.020463	0.057552
GABAergic synapse	0.97	1.12	0.50185	0.721086	0.2856	0.415822
Dopaminergic synapse	0.99	1.16	0.4722	0.700604	0.204904	0.330909
Long-term depression	-0.63	1.13	0.94326	0.999771	0.120534	0.227316
<b>5.7. Sensory system</b>						
Olfactory transduction	-0.98	0.94	0.49261	0.713526	0.551511	0.667692
Taste transduction	0.8	1.13	0.73602	0.858182	0.3095	0.438949
Inflammatory mediator regulation of TRP channels	0.85	1.27	0.77179	0.888826	0.125255	0.230529
<b>5.8. Development</b>						
Axon guidance	1.11	-0.83	0.21438	0.407036	0.874684	0.920548
Osteoclast differentiation	0.78	1.1	0.91776	0.991884	0.295775	0.424044
<b>5.9. Aging</b>						
Longevity regulating pathway	-1.64	-1.69	0.00594	0.02383	0.002561	0.010281
Longevity regulating pathway	-1.48	-1.17	0.03528	0.103271	0.206228	0.331027
<b>5.10. Environmental adaptation</b>						
Circadian rhythm	-1.63	-0.82	0.01867	0.059621	0.735362	0.800918
Circadian entrainment	1.02	1.13	0.41067	0.637557	0.106282	0.208755
Thermogenesis	-2.55	-2.69	0.00011	0.001302	0.000338	0.00211
<b>6. Human Diseases</b>						
<b>6.1. Cancers: Overview</b>						
Pathways in cancer	-0.91	0.95	0.71811	0.852378	0.616682	0.70111
Transcriptional misregulation in cancer	1.02	1.34	0.38879	0.617224	0.041242	0.102557
Viral carcinogenesis	1.11	1.55	0.19294	0.370221	0.001433	0.006713
Chemical carcinogenesis	-1.65	-1.37	0.01033	0.035832	0.082629	0.1759
Proteoglycans in cancer	1.4	1.13	0.00558	0.022715	0.047133	0.114176
MicroRNAs in cancer	1.54	1.57	0.00345	0.01514	0.002196	0.00964
Central carbon metabolism in cancer	-1.98	-1.42	0.00027	0.002024	0.046836	0.114176
Choline metabolism in cancer	-0.96	0.85	0.52714	0.740633	0.760031	0.815147
<b>6.2. Cancers: Specific types</b>						
Colorectal cancer	-0.58	1	0.99223	0.999771	0.458346	0.585433
Renal cell carcinoma	-1.15	-0.85	0.25462	0.455448	0.745531	0.805747
Pancreatic cancer	0.9	1.16	0.69746	0.847845	0.216087	0.33922
Endometrial cancer	0.95	1.34	0.55195	0.752552	0.076208	0.167301
Glioma	1.29	1.43	0.06823	0.17118	0.030614	0.078204
Prostate cancer	1.24	1.16	0.09763	0.225385	0.207334	0.331027
Thyroid cancer	0.87	1.27	0.67644	0.83736	0.144907	0.254492
Basal cell carcinoma	1.9	1.62	0.00067	0.004206	0.010206	0.033739
Melanoma	1.17	1.36	0.18331	0.355251	0.069848	0.155772
Bladder cancer	0.92	0.93	0.59974	0.780223	0.581429	0.683605
Chronic myeloid leukemia	0.72	1.22	0.9629	0.999771	0.147755	0.254719
Acute myeloid leukemia	-1.25	0.8	0.15848	0.313611	0.811683	0.863951
Small cell lung cancer	0.98	1.21	0.50296	0.721086	0.15842	0.26902
Non-small cell lung cancer	0.77	1.13	0.91542	0.991884	0.097853	0.197818
Breast cancer	1.17	1.19	0.14514	0.291325	0.162394	0.273251
Hepatocellular carcinoma	-0.83	1.23	0.78067	0.891746	0.097107	0.197818
Gastric cancer	1.18	1.24	0.13565	0.280274	0.108732	0.210715

## Appendix

<b>6.3. Immune diseases</b>							
Autoimmune thyroid disease	 1.34	 1.31	0.11162	0.241266	0.126979	0.230529	
Inflammatory bowel disease (IBD)	 -0.65	 1.01	0.91336	0.991884	0.437632	0.564104	
Systemic lupus erythematosus	 -0.98	 1.16	0.4915	0.713526	0.238338	0.370016	
Rheumatoid arthritis	 1.18	 1.28	0.19367	0.370221	0.121454	0.227523	
Allograft rejection	 1.62	 1.67	0.01638	0.053509	0.007829	0.026829	
Graft-versus-host disease	 1.63	 1.71	0.01505	0.050338	0.005852	0.02146	
<b>6.4. Neurodegenerative diseases</b>							
Alzheimer disease	 -2.52	 -2.59	0.00012	0.001302	0.000321	0.002084	
Parkinson disease	 -2.7	 -2.83	0.00012	0.001302	0.000296	0.002066	
Amyotrophic lateral sclerosis (ALS)	 -1.14	 0.91	0.29223	0.500714	0.610629	0.700355	
Huntington disease	 -2.56	 -2.42	0.00011	0.001302	0.000326	0.002084	
Prion diseases	 1.17	 1.42	0.24792	0.450727	0.065122	0.148222	
<b>6.5. Substance dependence</b>							
Cocaine addiction	 1.37	 1.11	0.08979	0.213822	0.310857	0.438949	
Amphetamine addiction	 1.56	 0.197	0.0197	0.062213	0.183018	0.302518	
Morphine addiction	 -0.95	 0.98	0.54464	0.752552	0.490368	0.614538	
Alcoholism	 -0.85	 1.05	0.72194	0.852378	0.367678	0.501542	
<b>6.6. Cardiovascular diseases</b>							
Hypertrophic cardiomyopathy (HCM)	 -1.1	 -1.19	0.32333	0.537503	0.18821	0.307482	
Arrhythmogenic right ventricular cardiomyopathy (ARVC)	 -0.94	 0.92	0.56006	0.756622	0.593112	0.689401	
Dilated cardiomyopathy (DCM)	 -0.92	 -1.01	0.58142	0.76345	0.418334	0.544476	
Viral myocarditis	 -0.8	 1.11	0.76545	0.885148	0.304729	0.434664	
Fluid shear stress and atherosclerosis	 -1.08	 1.22	0.33151	0.538459	0.127981	0.230529	
<b>6.7. Endocrine and metabolic diseases</b>							
Type II diabetes mellitus	 -1.42	 -1.09	0.07276	0.180942	0.323654	0.452471	
Insulin resistance	 -1.92	 -2.06	0.00013	0.001302	0.000289	0.002066	
Non-alcoholic fatty liver disease (NAFLD)	 -2.67	 -2.84	0.00012	0.001302	0.000311	0.00208	
AGE-RAGE signaling pathway in diabetic complications	 0.96	 1.02	0.54643	0.752552	0.424349	0.549503	
Cushing syndrome	 -0.94	 0.99	0.56702	0.757381	0.479293	0.606672	
Type I diabetes mellitus	 1.59	 1.76	0.02143	0.06617	0.002925	0.011415	
<b>6.8. Infectious diseases: Bacterial</b>							
Bacterial invasion of epithelial cells	 1.01	 1.23	0.4159	0.642133	0.146968	0.254719	
Salmonella infection	 1.1	 1.6	0.2804	0.486371	0.008894	0.03011	
Pertussis	 0.98	 0.91	0.47554	0.700604	0.62629	0.706777	
Legionellosis	 -1.34	 -0.92	0.10643	0.235236	0.584252	0.684061	
Staphylococcus aureus infection	 -0.83	 -1.16	0.68805	0.844765	0.272913	0.40307	
Tuberculosis	 0.85	 0.95	0.83304	0.935547	0.564743	0.672427	
<b>6.9. Infectious diseases: Viral</b>							
Hepatitis C	 1.47	 1.78	0.00725	0.027166	0.000298	0.002066	
Hepatitis B	 1.18	 1.51	0.11637	0.247718	0.006973	0.024494	
Measles	 1.93	 1.99	0.00098	0.005277	0.000153	0.002066	
Human cytomegalovirus infection	 1.29	 1.53	0.02106	0.065761	0.001423	0.006713	
Influenza A	 1.84	 2.11	0.00121	0.006288	0.000149	0.002066	
Human papillomavirus infection	 1.04	 1.21	0.31345	0.530605	0.082311	0.1759	



## Appendix

Human T-cell leukemia virus 1 infection	0.89	1.53	0.81417	0.918799	0.001424	0.006713
Kaposi sarcoma-associated herpesvirus infe	1.15	1.6	0.14102	0.285075	0.001158	0.005917
Herpes simplex infection	1.83	1.95	0.00077	0.004592	0.000145	0.002066
Epstein-Barr virus infection	1.91	2.05	0.00081	0.00474	0.000144	0.002066
Human immunodeficiency virus 1 infection	1.62	1.99	0.00086	0.004952	0.000143	0.002066
<b>6.10. Infectious diseases: Parasitic</b>						
Leishmaniasis	-0.63	0.79	0.94678	0.999771	0.807107	0.862347
Chagas disease (American trypanosomiasis)	-0.71	1.05	0.9044	0.991884	0.376631	0.506999
Malaria	1.03	-0.97	0.41968	0.644426	0.492068	0.614538
Toxoplasmosis	-0.9	1.02	0.62857	0.79922	0.41853	0.544476
Amoebiasis	-1.11	-1.21	0.3123	0.530605	0.165878	0.277451
<b>6.12. Drug resistance: Antineoplastic</b>						
EGFR tyrosine kinase inhibitor resistance	0.89	0.86	0.70855	0.849127	0.725694	0.793463
Endocrine resistance	0.89	1.01	0.70506	0.849127	0.446979	0.573521
Antifolate resistance	0.85	1.7	0.69815	0.847845	0.006365	0.022931
Platinum drug resistance	-1.1	1.12	0.32342	0.537503	0.264957	0.398144

**Table 16: complete gene expression analysis of the second set-up: irradiation on mature adipocytes.**  
Down-regulated (Up-regulated) pathways are indicated by the negative (positive) NES coloured in green (red). Significant p-value and adjusted p-value (<0.05) are written in green.

Name	NES 60min vs Ctrl	NES BL30min vs Ctrl	pvalue 60min vs Ctrl	Adj. pvalue 60min vs	pvalue 30min vs Ctrl	Adj. pvalue 30min vs Ctrl
<b>1. Metabolism</b>						
<b>1.0 Global and overview maps</b>						
Metabolic pathways	-1.41	-1.27	0.00017	0.004806	0.253861	0.596324
Carbon metabolism	-1.56	-1.52	0.00151	0.017163	0.000212	0.004753
2-Oxocarboxylic acid metabolism	-1.79	-1.76	0.00177	0.019425	0.600303	0.849276
Fatty acid metabolism	-0.96	-1.03	0.51343	0.694245	0.166525	0.477788
Biosynthesis of amino acids	-1.68	-1.59	0.00134	0.015953	0.493848	0.782842
<b>1.1. Carbohydrate metabolism</b>						
Glycolysis Gluconeogenesis	-1.4	-1.11	0.03794	0.168809	0.339763	0.677
Citrate cycle (TCA cycle)	-2.02	-2.05	0.00019	0.004806	0.052701	0.242521
Pentose phosphate pathway	0.9	0.91	0.62005	0.73213	0.739402	0.915308
Pentose and glucuronate interconversions	-1.44	-1.22	0.04504	0.189414	0.257556	0.596324
Fructose and mannose metabolism	-1.25	-0.97	0.14769	0.360978	0.293118	0.633713
Galactose metabolism	-1.47	-1.06	0.03176	0.152326	0.792069	0.938861
Ascorbate and aldarate metabolism	-1.29	-1.44	0.13115	0.335519	0.038104	0.191303
Starch and sucrose metabolism	-1.42	-1.17	0.05534	0.218055	0.000676	0.009464
Amino sugar and nucleotide sugar metabolism	-1.67	-1.33	0.0025	0.026506	0.785472	0.938861
Inositol phosphate metabolism	-1.11	-1.77	0.249	0.477763	0.279482	0.608518
Pyruvate metabolism	-1.57	-1.21	0.01232	0.085971	0.184811	0.502097
Glyoxylate and dicarboxylate metabolism	-1.21	-1.01	0.18166	0.412083	0.31194	0.652147
Propanoate metabolism	-1.88	-1.85	0.0002	0.004806	0.619231	0.864108
Butanoate metabolism	-1.12	-1.01	0.28949	0.503922	0.244754	0.594416
<b>1.2. Energy metabolism</b>						
Oxidative phosphorylation	-1.91	-1.74	0.00019	0.004806	0.016205	0.097055
Nitrogen metabolism	0.98	0.94	0.48128	0.671603	0.396679	0.715306
<b>1.3. Lipid metabolism</b>						
Fatty acid elongation	-1.13	0.83	0.27119	0.492629	0.449576	0.746053
Fatty acid degradation	-1.38	-1.12	0.05073	0.209485	0.052928	0.242521
Steroid biosynthesis	-1.29	-1.12	0.14933	0.360978	0.054693	0.246657
Primary bile acid biosynthesis	-0.76	-0.77	0.80245	0.832273	0.818644	0.949712
Steroid hormone biosynthesis	-1.46	-1.37	0.01481	0.098852	0.000739	0.009869
Glycerolipid metabolism	-1.07	-1	0.32603	0.535436	0.210959	0.539703
Glycerophospholipid metabolism	-1.13	-1.16	0.21237	0.444703	0.278559	0.608518
Ether lipid metabolism	-0.94	0.93	0.56408	0.724575	0.011544	0.081643
Arachidonic acid metabolism	-0.93	-1.29	0.60681	0.73213	0.630993	0.864798
Linoleic acid metabolism	-1.45	-0.97	0.03024	0.148898	0.855608	0.959394
alpha-Linolenic acid metabolism	-1.57	-1.14	0.02006	0.123159	0.322923	0.665352
Sphingolipid metabolism	-0.88	0.75	0.66576	0.760286	0.065857	0.27152
Biosynthesis of unsaturated fatty acids	0.83	0.84	0.73896	0.801629	0.022336	0.124674
<b>1.4. Nucleotide metabolism</b>						
Purine metabolism	-1.06	-1.07	0.30753	0.519442	0.678656	0.909813
Pyrimidine metabolism	1	1.18	0.43424	0.637852	0.898616	0.959394

## Appendix

<b>1.5. Amino acid metabolism</b>						
Arginine biosynthesis	-1.16	-0.79	0.26161	0.48188	0.441643	0.736872
Alanine, aspartate and glutamate metabolism	-0.93	-1.08	0.56062	0.724575	0.000659	0.009464
Glycine, serine and threonine metabolism	-0.67	-0.9	0.97655	0.982954	0.374366	0.702703
Cysteine and methionine metabolism	-1.07	-1.13	0.32962	0.538255	0.158846	0.467489
Valine, leucine and isoleucine degradation	-1.35	-1.14	0.06379	0.238819	0.568819	0.829109
Lysine degradation	0.92	0.98	0.58507	0.729892	0.071442	0.281187
Arginine and proline metabolism	-1.25	1.06	0.125	0.32975	0.486786	0.782426
Histidine metabolism	1.35	1.59	0.10121	0.296259	0.26426	0.596324
Tyrosine metabolism	1.05	1.03	0.36636	0.570925	0.921672	0.960308
Phenylalanine metabolism	0.96	1	0.50206	0.691171	0.700488	0.910063
Tryptophan metabolism	1.31	1.39	0.09643	0.290244	0.091437	0.342332
<b>1.6. Metabolism of other amino acids</b>						
beta-Alanine metabolism	1.08	1.42	0.32614	0.535436	0.156569	0.467489
Selenocompound metabolism	-0.79	0.76	0.76625	0.815426	0.171908	0.488665
Glutathione metabolism	1.8	1.75	0.00063	0.009505	0.425922	0.734209
<b>1.7. Glycan biosynthesis and metabolism</b>						
N-Glycan biosynthesis	-1.29	-1.1	0.10343	0.296752	0.000843	0.010783
Other glycan degradation	1.22	1.63	0.20106	0.434682	0.423469	0.734209
Mucin type O-glycan biosynthesis	0.98	0.89	0.47248	0.66538	0.055438	0.246657
Other types of O-glycan biosynthesis	-0.74	0.74	0.86493	0.88511	0.326581	0.668402
Mannose type O-glycan biosynthesis	-1.08	-1.1	0.34218	0.549992	0.123494	0.416156
Glycosaminoglycan degradation	1.46	1.56	0.05118	0.209485	0.580967	0.837355
Glycosaminoglycan biosynthesis	0.84	-0.85	0.68744	0.768086	0.723556	0.914122
Glycosaminoglycan biosynthesis	-0.92	-0.72	0.56383	0.724575	0.099032	0.361937
Glycosylphosphatidylinositol (GPI)-anchor biosynthesis	0.95	1.05	0.51695	0.694245	0.021608	0.122848
Glycosphingolipid biosynthesis	-0.76	0.85	0.83873	0.864066	0.469874	0.768568
Glycosphingolipid biosynthesis	1.35	1.37	0.11527	0.315958	0.550847	0.822319
Glycosphingolipid biosynthesis	0.89	1.29	0.60913	0.73213	0.001496	0.017661
<b>1.8. Metabolism of cofactors and vitamins</b>						
One carbon pool by folate	-1.24	-1.46	0.18524	0.412083	0.000185	0.004753
Thiamine metabolism	0.88	1.11	0.62961	0.740496	0.000184	0.004753
Nicotinate and nicotinamide metabolism	1.16	1.28	0.22968	0.458216	0.000182	0.004753
Pantothenate and CoA biosynthesis	-1.23	-0.91	0.19929	0.434682	0.733535	0.915308
Folate biosynthesis	-0.79	0.83	0.78973	0.827465	0.00033	0.006341
Retinol metabolism	1.04	1.25	0.35658	0.563159	0.003157	0.026926
Porphyrin and chlorophyll metabolism	1.58	1.53	0.01466	0.098852	0.002336	0.022223
<b>1.9. Metabolism of terpenoids and polyketides</b>						
Terpenoid backbone biosynthesis	-0.94	-0.99	0.53678	0.704243	0.390679	0.715306
<b>1.11. Xenobiotics biodegradation and metabolism</b>						
Metabolism of xenobiotics by cytochrome P450	1.9	1.87	0.00042	0.007585	0.213916	0.542747
Drug metabolism	1.91	1.89	0.00042	0.007585	0.470654	0.768568
Drug metabolism (other enzymes)	1.72	1.79	0.00063	0.009505	0.336911	0.677

## Appendix

<b>2. Genetic Information Processing</b>							
<b>2.1. Transcription</b>							
RNA polymerase	0.6	-0.73	0.98912	0.989117	0.00198	0.020963	
Basal transcription factors	-0.75	-0.76	0.90137	0.916294	0.522041	0.809907	
Spliceosome	1.1	1.14	0.23275	0.458216	0.398428	0.715306	
<b>2.2. Translation</b>							
Aminoacyl-tRNA biosynthesis	-1.81	-1.78	0.00135	0.015953	0.912519	0.959394	
Ribosome biogenesis in eukaryotes	-1.24	-1.19	0.11424	0.315958	0.018508	0.107209	
Ribosome	-1.33	1.26	0.03915	0.1717	0.174231	0.489467	
RNA transport	-1.36	-1.38	0.01948	0.122044	0.132171	0.429894	
mRNA surveillance pathway	0.79	-0.7	0.92434	0.936542	0.068101	0.27152	
RNA degradation	-1	-1.18	0.43247	0.637852	0.009928	0.074342	
<b>2.3. Folding, sorting and degradation</b>							
Proteasome	1.09	1.32	0.28998	0.503922	0.996904	0.996904	
Protein export	-2.06	-2.01	0.00019	0.004806	0.147765	0.45822	
Ubiquitin mediated proteolysis	-0.88	-1.08	0.7834	0.824068	0.907951	0.959394	
SNARE interactions in vesicular transport	-1.4	-1.31	0.06096	0.23658	0.907265	0.959394	
Protein processing in endoplasmic reticulum	-2.21	-2.07	0.00019	0.004806	0.523828	0.809907	
<b>2.4. Replication and repair</b>							
DNA replication	1.07	0.95	0.33937	0.548357	0.175379	0.489467	
Base excision repair	-0.87	-0.75	0.67113	0.760286	0.079488	0.305034	
Nucleotide excision repair	0.66	-0.71	0.98235	0.985564	0.000213	0.004753	
Mismatch repair	-0.86	-0.92	0.67069	0.760286	0.033913	0.176749	
Homologous recombination	-0.96	-0.77	0.51786	0.694245	0.894068	0.959394	
Fanconi anemia pathway	1.02	0.86	0.40871	0.612988	0.96301	0.982207	
<b>3. Environmental Information Processing</b>							
<b>3.1. Membrane transport</b>							
ABC transporters	1.42	1.2	0.04102	0.177388	0.560996	0.828009	
MAPK signaling pathway	1.25	0.96	0.0304	0.148898	0.884624	0.959394	
ErbB signaling pathway	1.16	0.87	0.18207	0.412083	0.712858	0.914122	
Ras signaling pathway	-0.96	-0.86	0.57167	0.726472	0.571404	0.829109	
Rap1 signaling pathway	1.15	0.91	0.13248	0.336128	0.753626	0.925453	
Calcium signaling pathway	0.99	-1.05	0.45647	0.657924	0.92694	0.961387	
cGMP-PKG signaling pathway	-1.03	-1.18	0.35771	0.563159	0.702557	0.910063	
cAMP signaling pathway	1.18	1.11	0.10133	0.296259	0.298926	0.638973	
NF-kappa B signaling pathway	1.16	0.86	0.17174	0.397876	0.105093	0.370844	
HIF-1 signaling pathway	-0.99	-0.87	0.46555	0.65863	0.194644	0.519614	
FoxO signaling pathway	1.38	0.98	0.02091	0.125895	0.000678	0.009464	
Phosphatidylinositol signaling system	-1.1	-1.74	0.2581	0.48188	0.333683	0.677	
Sphingolipid signaling pathway	-1.17	-1.09	0.14792	0.360978	0.788634	0.938861	
Phospholipase D signaling pathway	-1.18	-1.55	0.13025	0.335519	0.779204	0.938861	
mTOR signaling pathway	-0.93	-0.93	0.63725	0.743859	0.479374	0.774568	
PI3K-Akt signaling pathway	-0.97	0.96	0.53178	0.700678	0.000441	0.007398	
AMPK signaling pathway	-0.94	-0.88	0.59297	0.731087	0.247857	0.594416	
Wnt signaling pathway	0.94	-0.82	0.60869	0.73213	0.001857	0.020361	
Notch signaling pathway	0.88	1.06	0.6684	0.760286	0.00237	0.022223	
Hedgehog signaling pathway	0.89	0.72	0.64883	0.751861	0.068093	0.27152	

## Appendix

TGF-beta signaling pathway	-0.86	-0.95	0.74934	0.807723	0.546007	0.822319
VEGF signaling pathway	-1.05	-0.98	0.3552	0.563159	0.865907	0.959394
Apelin signaling pathway	-1.03	-1.02	0.36892	0.572017	0.255958	0.596324
Hippo signaling pathway	0.94	0.83	0.60656	0.73213	0.100636	0.363472
Hippo signaling pathway	0.81	-0.94	0.75205	0.807723	0.059135	0.255697
JAK-STAT signaling pathway	-1.57	-1.54	0.00086	0.011737	0.014658	0.097055
TNF signaling pathway	-1.28	-1.03	0.06277	0.237891	0.263987	0.596324
<b>3.3. Signaling molecules and interaction</b>						
Cytokine-cytokine receptor interaction	-1.6	-1.54	0.00022	0.004806	0.000231	0.004753
Neuroactive ligand-receptor interaction	-1.47	-1.41	0.00088	0.011737	0.067694	0.27152
ECM-receptor interaction	-0.97	0.88	0.50559	0.692924	0.006773	0.051984
Cell adhesion molecules (CAMs)	-1.17	-1.32	0.12567	0.32975	0.034725	0.177675
<b>4.1. Transport and catabolism</b>						
Autophagy (other)	-1.32	-1.4	0.10306	0.296752	0.263227	0.596324
Mitophagy	-1.5	-1.48	0.01582	0.103312	0.644378	0.879217
Autophagy	-0.9	-1.08	0.71657	0.787263	0.572544	0.829109
Lysosome	-1.1	-1.27	0.23582	0.458216	0.791237	0.938861
Endocytosis	-1.4	-1.35	0.00403	0.038663	0.833794	0.958707
Phagosome	-1.1	-1.3	0.20802	0.444703	0.898717	0.959394
Peroxisome	-1.27	-1.09	0.08894	0.281794	0.695029	0.910063
<b>4.2. Cell growth and death</b>						
Cell cycle	-1.38	-1.27	0.02134	0.125989	0.88891	0.959394
Oocyte meiosis	-1.02	-0.95	0.40026	0.608322	0.90605	0.959394
p53 signaling pathway	-0.99	0.8	0.44928	0.65681	0.524988	0.809907
Apoptosis	-0.91	-0.87	0.68092	0.765722	0.243281	0.594416
Apoptosis (multiple species)	-1.02	0.74	0.40932	0.612988	0.312266	0.652147
Ferroptosis	-1.11	0.74	0.27868	0.497375	0.810256	0.945813
Necroptosis	-1.2	-0.97	0.09828	0.292925	0.267767	0.596324
Cellular senescence	-1.13	-1.09	0.17237	0.397876	0.956843	0.979169
<b>4.3. Cellular community - eukaryotes</b>						
Focal adhesion	-1.06	-0.96	0.28028	0.497375	0.341808	0.677
Adherens junction	-1.07	-1.03	0.31778	0.527346	0.943442	0.968685
Tight junction	0.85	-1.09	0.86395	0.88511	0.551785	0.822319
Gap junction	-1.22	-0.79	0.12061	0.321975	0.177427	0.489643
Signaling pathways regulating pluripotency	0.87	-0.96	0.79587	0.830552	0.491093	0.782842
<b>4.5. Cell motility</b>						
Regulation of actin cytoskeleton	0.99	-0.93	0.45563	0.657924	0.40143	0.716505
<b>5. Organismal Systems</b>						
<b>5.1. Immune system</b>						
Chemokine signaling pathway	-1.05	-1.04	0.30794	0.519442	0.966684	0.982689
Complement and coagulation cascades	-1.57	-1.73	0.00594	0.055223	0.898451	0.959394
Platelet activation	-1	-1.05	0.43022	0.637852	0.543897	0.822319
Antigen processing and presentation	-1.09	-1.42	0.27825	0.497375	0.564161	0.828696
Toll-like receptor signaling pathway	-1.37	-1.28	0.03017	0.148898	0.71808	0.914122
NOD-like receptor signaling pathway	-1.33	-1.36	0.0229	0.130195	0.03174	0.170953
RIG-I-like receptor signaling pathway	-1.28	-1.21	0.08911	0.281794	0.375385	0.702703
Cytosolic DNA-sensing pathway	-1.67	-1.52	0.00313	0.030948	0.22037	0.55003
C-type lectin receptor signaling pathway	-1.16	-1.01	0.1567	0.374736	0.938897	0.967253



## Appendix

Hematopoietic cell lineage	1.36	1.6	0.03354	0.156005	0.537511	0.820975
Natural killer cell mediated cytotoxicity	1.23	1.2	0.09525	0.289517	0.000182	0.004753
IL-17 signaling pathway	1.15	0.84	0.18394	0.412083	0.320118	0.664028
Th1 and Th2 cell differentiation	1.39	1.26	0.02919	0.148898	0.024248	0.132931
Th17 cell differentiation	1.39	1.17	0.02382	0.130611	0.5944	0.847777
T cell receptor signaling pathway	0.99	0.86	0.46147	0.65808	0.072975	0.283588
B cell receptor signaling pathway	1.14	1.11	0.21746	0.44563	0.016439	0.097055
Fc epsilon RI signaling pathway	1.22	0.92	0.13727	0.344102	0.147384	0.45822
Fc gamma R-mediated phagocytosis	1.24	1.04	0.10825	0.304874	0.015738	0.097055
Leukocyte transendothelial migration	1.29	1.21	0.0554	0.218055	0.408511	0.724931
Intestinal immune network for IgA production	1.16	1.01	0.21795	0.44563	0.00176	0.020015
<b>5.2. Endocrine system</b>						
PPAR signaling pathway	-1.29	-1.36	0.0791	0.261106	0.088552	0.335623
Renin-angiotensin system	-0.91	-0.91	0.60455	0.73213	0.163374	0.473167
Insulin signaling pathway	-1.06	-1.08	0.30648	0.519442	0.787269	0.938861
Insulin secretion	0.86	0.87	0.76554	0.815426	0.247009	0.594416
GnRH signaling pathway	0.86	0.8	0.77792	0.823522	0.609066	0.857721
Ovarian steroidogenesis	1.33	1.2	0.07641	0.257776	0.3525	0.693701
Progesterone-mediated oocyte maturation	1.27	1.2	0.07737	0.258166	0.364598	0.702703
Estrogen signaling pathway	0.97	0.84	0.51624	0.694245	0.114589	0.399759
Melanogenesis	-0.96	-0.98	0.52963	0.700678	0.432064	0.734209
Prolactin signaling pathway	0.91	0.79	0.61106	0.73213	0.432873	0.734209
Thyroid hormone synthesis	-1.14	-1.09	0.21919	0.44563	0.819784	0.949712
Thyroid hormone signaling pathway	1.18	0.83	0.13786	0.344102	0.003772	0.031242
Adipocytokine signaling pathway	-0.91	-0.82	0.61566	0.73213	0.44007	0.736872
Oxytocin signaling pathway	1.23	0.82	0.07411	0.255623	0.723291	0.914122
Glucagon signaling pathway	-1.29	-1.41	0.07031	0.245279	0.995702	0.996904
Regulation of lipolysis in adipocytes	1.35	1.25	0.06856	0.241945	0.146308	0.45822
Renin secretion	1.14	1.03	0.21796	0.44563	0.992262	0.996904
Aldosterone synthesis and secretion	1.04	0.81	0.36118	0.565729	0.198511	0.521128
Relaxin signaling pathway	-0.88	0.83	0.76762	0.815426	0.126067	0.416156
Cortisol synthesis and secretion	1.28	1.1	0.08995	0.281794	0.531022	0.815119
Parathyroid hormone synthesis, secretion and action	1.14	-0.77	0.19273	0.425676	0.15989	0.467489
<b>5.3. Circulatory system</b>						
Cardiac muscle contraction	1.15	-1.06	0.2005	0.434682	0.750927	0.925453
Adrenergic signaling in cardiomyocytes	0.99	-0.88	0.46301	0.65808	0.096793	0.358018
Vascular smooth muscle contraction	-0.95	-1.08	0.57146	0.726472	0.853039	0.959394
<b>5.4. Digestive system</b>						
Salivary secretion	1.1	0.8	0.26188	0.48188	0.36756	0.702703
Gastric acid secretion	0.93	-1.01	0.57786	0.726472	0.737905	0.915308
Pancreatic secretion	0.86	-1.13	0.79809	0.830552	0.691545	0.910063
Carbohydrate digestion and absorption	1.38	1.11	0.06165	0.23658	0.249771	0.594416
Protein digestion and absorption	0.95	-0.85	0.55882	0.724575	0.768333	0.936027
Fat digestion and absorption	0.97	1.25	0.48864	0.678791	0.921716	0.960308
Bile secretion	1.53	1.19	0.01091	0.07788	0.15881	0.467489
Vitamin digestion and absorption	1.26	1.23	0.15746	0.374736	0.133029	0.429894

## Appendix

Mineral absorption	1.48	1.09	0.02945	0.148898	0.912027	0.959394
Cholesterol metabolism	-1.26	-1.13	0.11691	0.317624	0.494695	0.782842
<b>5.5. Excretory system</b>						
Aldosterone-regulated sodium reabsorption	1.38	0.73	0.06668	0.240834	0.930207	0.961527
Endocrine and other factor-regulated calcium reabsorption	0.85	-0.98	0.73638	0.801629	0.262418	0.596324
Vasopressin-regulated water reabsorption	-1.09	-0.9	0.3055	0.519442	0.866115	0.959394
Proximal tubule bicarbonate reclamation	1.15	1.03	0.26213	0.48188	0.875603	0.959394
Collecting duct acid secretion	0.89	0.89	0.61998	0.73213	0.912003	0.959394
<b>5.6. Nervous system</b>						
Long-term potentiation	1.2	-1	0.16187	0.382254	0.016097	0.097055
Synaptic vesicle cycle	0.9	0.87	0.66471	0.760286	0.122015	0.416156
Neurotrophin signaling pathway	0.89	0.73	0.71803	0.787263	0.382439	0.711569
Retrograde endocannabinoid signaling	-1.04	-1.15	0.33421	0.542867	0.900876	0.959394
Glutamatergic synapse	0.99	0.73	0.45892	0.65808	0.880999	0.959394
Cholinergic synapse	-1.1	-1.12	0.24166	0.466599	0.268055	0.596324
Serotonergic synapse	0.96	1.19	0.52671	0.700003	0.974635	0.987502
GABAergic synapse	-1.03	-0.96	0.37719	0.578984	0.611991	0.857906
Dopaminergic synapse	-1.22	-1.14	0.09496	0.289517	0.661563	0.894713
Long-term depression	1.31	0.85	0.08389	0.271092	0.001166	0.014312
<b>5.7. Sensory system</b>						
Olfactory transduction	1.03	1.1	0.26687	0.487678	0.36747	0.702703
Taste transduction	1.56	-0.84	0.00635	0.057305	0.698993	0.910063
Phototransduction	-1.16	-1.05	0.25199	0.480505	0.00314	0.026926
Inflammatory mediator regulation of TRP channels	1.16	0.88	0.14905	0.360978	0.585315	0.839681
<b>5.8. Development</b>						
Axon guidance	-1.18	-1.12	0.1125	0.313977	0.922772	0.960308
Osteoclast differentiation	1.01	0.78	0.40357	0.610318	0.475853	0.772947
<b>5.9. Aging</b>						
Longevity regulating pathway	-0.85	-0.82	0.7838	0.824068	0.630532	0.864798
Longevity regulating pathway	-0.75	-0.89	0.93967	0.94894	0.411122	0.72537
<b>5.10. Environmental adaptation</b>						
Circadian rhythm	0.96	1.01	0.49815	0.688887	0.002926	0.026416
Circadian entrainment	-0.92	-0.86	0.61511	0.73213	0.119489	0.41217
Thermogenesis	-1.59	-1.42	0.00037	0.007572	0.859189	0.959394
<b>6. Human Diseases</b>						
<b>6.1. Cancers: Overview</b>						
Pathways in cancer	1.21	1.19	0.02223	0.128751	0.62684	0.864798
Transcriptional misregulation in cancer	1.22	1.17	0.07604	0.257776	0.875275	0.959394
Viral carcinogenesis	1.27	1.22	0.03742	0.168809	0.422154	0.734209
Chemical carcinogenesis	1.89	1.97	0.00021	0.004806	0.194248	0.519614
Proteoglycans in cancer	0.92	0.88	0.69493	0.770197	0.278285	0.608518
MicroRNAs in cancer	1.5	1.02	0.0011	0.01406	0.826847	0.954293
Central carbon metabolism in cancer	0.93	-0.92	0.57497	0.726472	0.135851	0.434441
Choline metabolism in cancer	1.13	0.86	0.21033	0.444703	0.159625	0.467489
<b>6.2. Cancers: Specific types</b>						
Colorectal cancer	1.13	0.94	0.20988	0.444703	0.809846	0.945813

## Appendix

Renal cell carcinoma	1.01	1.05	0.4153	0.618919	0.010522	0.076913
Pancreatic cancer	1.13	1	0.23309	0.458216	0.441525	0.736872
Endometrial cancer	1.18	1.03	0.18282	0.412083	0.299714	0.638973
Glioma	0.9	-0.71	0.65424	0.755082	0.849817	0.959394
Prostate cancer	1.09	1.03	0.26157	0.48188	0.207623	0.539703
Thyroid cancer	0.89	0.95	0.63195	0.740496	0.657866	0.893651
Basal cell carcinoma	-0.89	0.8	0.67677	0.763852	0.149491	0.458938
Melanoma	1.29	1.02	0.08068	0.263494	0.550942	0.822319
Bladder cancer	1.66	1.55	0.00804	0.063299	0.722454	0.914122
Chronic myeloid leukemia	1.12	0.93	0.23415	0.458216	0.102805	0.366992
Acute myeloid leukemia	1.58	1.65	0.00755	0.060973	0.791764	0.938861
Small cell lung cancer	1.1	0.82	0.2546	0.48188	0.732198	0.915308
Non-small cell lung cancer	1.13	0.87	0.23481	0.458216	0.000182	0.004753
Breast cancer	0.99	0.91	0.47565	0.666784	0.69281	0.910063
Hepatocellular carcinoma	1.43	1.38	0.00858	0.06588	0.005292	0.041657
Gastric cancer	0.9	0.91	0.72348	0.790422	0.052715	0.242521
<b>6.3. Immune diseases</b>						
Asthma	0.91	1.21	0.57976	0.726472	0.040078	0.193875
Autoimmune thyroid disease	1.57	1.92	0.00734	0.060894	0.033968	0.176749
Inflammatory bowel disease (IBD)	1.29	1.55	0.09339	0.289517	0.003867	0.031242
Systemic lupus erythematosus	-1.11	0.86	0.22106	0.446484	0.038634	0.191303
Rheumatoid arthritis	1.13	1.32	0.06606	0.240834	0.210002	0.539703
Allograft rejection	1.57	1.78	0.00996	0.072807	0.217127	0.546377
Graft-versus-host disease	1.57	1.85	0.00958	0.071698	0.000174	0.004753
Primary immunodeficiency	0.83	1.05	0.75247	0.807723	0.000173	0.004753
<b>6.4. Neurodegenerative diseases</b>						
Alzheimer disease	-2.11	-1.98	0.00019	0.004806	0.013434	0.091652
Parkinson disease	-1.96	-1.76	0.00019	0.004806	0.040417	0.193875
Amyotrophic lateral sclerosis (ALS)	0.92	-0.88	0.58724	0.729892	0.125351	0.416156
Huntington disease	-1.83	-1.73	0.00019	0.004806	0.066183	0.27152
Prion diseases	-1.39	-1.03	0.0654	0.240834	0.000183	0.004753
<b>6.5. Substance dependence</b>						
Cocaine addiction	0.96	0.96	0.50895	0.694245	0.806311	0.945813
Amphetamine addiction	-0.92	-0.98	0.58971	0.730003	0.366695	0.702703
Morphine addiction	0.83	0.84	0.83836	0.864066	0.554463	0.822319
Nicotine addiction	1.28	1.6	0.11875	0.319799	0.340273	0.677
Alcoholism	-1.29	-1	0.03056	0.148898	0.431211	0.734209
<b>6.6. Cardiovascular diseases</b>						
Hypertrophic cardiomyopathy (HCM)	1.09	0.87	0.27871	0.497375	0.385177	0.712345
Arrhythmogenic right ventricular cardiomyopathy (ARVC)	0.99	-1	0.45641	0.657924	0.989859	0.996904
Dilated cardiomyopathy (DCM)	1.04	0.82	0.34789	0.556263	0.371042	0.702703
Viral myocarditis	1.41	1.3	0.02752	0.148248	0.521403	0.809907
Fluid shear stress and atherosclerosis	1.39	1.56	0.01615	0.103312	0.860431	0.959394
<b>6.7. Endocrine and metabolic diseases</b>						
Type II diabetes mellitus	0.86	-0.91	0.71783	0.787263	0.396703	0.715306
Insulin resistance	-0.97	-0.91	0.52546	0.700003	0.016403	0.097055
Non-alcoholic fatty liver disease (NAFLD)	-1.71	-1.6	0.00019	0.004806	0.596482	0.847777



## Appendix

AGE-RAGE signaling pathway in diabetic complications	1.16	1.03	0.17219	0.397876	0.002389	0.022223
Cushing syndrome	0.96	0.9	0.53922	0.70443	0.860282	0.959394
Type I diabetes mellitus	1.39	1.63	0.04368	0.186243	0.712673	0.914122
Maturity onset diabetes of the young	1.34	0.91	0.10505	0.298604	0.68245	0.910063
<b>6.8. Infectious diseases: Bacterial</b>						
Bacterial invasion of epithelial cells	-1.07	-1.07	0.31623	0.527346	0.016197	0.097055
Salmonella infection	0.89	0.82	0.6887	0.768086	0.672423	0.905412
Pertussis	1.14	1.14	0.21294	0.444703	0.62809	0.864798
Legionellosis	-0.88	-0.9	0.69053	0.768086	0.768335	0.936027
Staphylococcus aureus infection	1.78	2.13	0.00021	0.004806	0.198606	0.521128
Tuberculosis	0.94	-0.92	0.61822	0.73213	0.000183	0.004753
<b>6.9. Infectious diseases: Viral</b>						
Hepatitis C	1.62	1.46	0.00065	0.009505	0.011701	0.081643
Hepatitis B	1.35	1.29	0.0238	0.130611	0.80912	0.945813
Measles	1.45	1.32	0.00688	0.060363	0.057682	0.252976
Human cytomegalovirus infection	1.26	1.27	0.03742	0.168809	0.000374	0.00676
Influenza A	1.44	1.48	0.0073	0.060894	0.000185	0.004753
Human papillomavirus infection	1.18	1.23	0.06809	0.241945	0.369516	0.702703
Human T-cell leukemia virus 1 infection	1.14	1.1	0.12908	0.335519	0.733982	0.915308
Kaposi sarcoma-associated herpesvirus infection	1.24	1.1	0.05538	0.218055	0.429987	0.734209
Herpes simplex infection	1.56	1.64	0.00065	0.009505	0.84918	0.959394
Epstein-Barr virus infection	1.62	1.69	0.00022	0.004806	0.06757	0.27152
Human immunodeficiency virus 1 infection	1.27	1.35	0.03349	0.156005	0.002109	0.021578
<b>6.10. Infectious diseases: Parasitic</b>						
Leishmaniasis	0.93	1.2	0.57536	0.726472	0.178632	0.489643
Chagas disease (American trypanosomiasis)	0.81	0.95	0.90023	0.916294	0.307779	0.651642
African trypanosomiasis	1.05	0.84	0.37188	0.573708	0.241901	0.594416
Malaria	1.07	1.29	0.31332	0.525617	0.000231	0.004753
Toxoplasmosis	-0.91	0.86	0.649	0.751861	0.000458	0.007398
Amoebiasis	1.02	0.88	0.38865	0.593614	0.694843	0.910063
<b>6.12. Drug resistance: Antineoplastic</b>						
EGFR tyrosine kinase inhibitor resistance	1.08	0.96	0.29053	0.503922	0.000232	0.004753
Endocrine resistance	1.08	1.02	0.28465	0.502232	0.395364	0.715306
Antifolate resistance	1.11	-0.72	0.29269	0.504813	0.523068	0.809907
Platinum drug resistance	1.66	1.46	0.00294	0.030098	0.470421	0.768568

## 8 Curriculum vitae

### Personal informations

Name: Stefania

Surname: Palumbo

Date of birth: 16.05.1988

Place of birth: Naples (NA), Italy

Nationality: Italian

Civil status: Unmarried

Email address: [Stefaniapalumbo4@gmail.com](mailto:Stefaniapalumbo4@gmail.com)

LinkedIn: Stefania Palumbo

### Academic qualifications

July 2016-to date Mannheim, Germany	<b>Doctoal studies,</b> Medical Research Center, University of Heidelberg, Germany. <b>Thesis:</b> Effects of photobiomodulation with blue light during and after adipocyte differentiation
April 2012-June 2014, Naples, Italy	<b>Master of Medical Biotechnology,</b> University of Naples, Federico II <b>Thesis:</b> “Acil Peptide Idrolase in fish: identification of a new cluster with surprising antioxidant functions in Antarctic Nototenioids fishes ” Final mark: magna (110/110) cum laude

## Curriculum vitae

September 2007-March 2012  
Naples, Italy

### **Bachelor of Biotechnology,**

University of Naples, Federico II

**Thesis:** "Effects of the treatment with the Citarabine on the expression of the Zinc-finger protein ZNF224 "

Final mark: 102/110

September 2002-July 2007  
Naples, Italy

### **High School "Adolfo Pansini"**

Specializing in classical studies

## **Publication**

Daniele C., **Palumbo S.**, Huang J., Kraenzlin B., Sticht C., Gretz N.,  
"Cisplatin-induced rat model of kidney injury: physiological, functional, histological and gene expression profile evaluations".

Submitted to Scientific Reports on 27 November 2019.

## 9 Acknowledgments

I would like to express my sincere gratitude to Prof. Norbert Gretz for his supervision, support and all his valuable advice during the period of research and writing this thesis. I also thank him for allowing me to participate in the doctoral program "Cooperative Research Training Group Tissue Analytics for Stem Cell Diagnostics and Therapy (TASCDT)".

It has been a highly formative experience for me and I will treasure what I have learned over the years.

I would like to thank Dr. Carsten Sticht and Dr. Carolina De La Torre for helping me with gene expression analysis.

Thanks to all my colleagues at ZMF, but a special thanks goes to Sina and Edda for their support for all the documents and paperwork but especially for all the encouraging and funny conversations. Without you I would have gone crazy in a short time.

A big thanks also to the "blue light team" who shared with me the time in lab and the wake-up call at dawn for the Tuesday meetings at which I was often late. The "typical Italian style" would say Prof. Gretz.

Anna and Natalia, my adorable colleagues, thank you for the support and the brain storming. Eating gummy bears and chocolate with you was a pleasure.

A special thought to Cinzia and even more to Daniela who have shared with me the last 3 and a half years of life. Thank you for always being there.

My biggest and deepest thanks go to my family, my boyfriend and my friends in Italy. You made me feel your love despite the distance; thank you for always believing in me and being by my side during this long journey of ups and (many) downs.

Each one of you has helped to build the person I am today.

A little thanks goes to myself and the strength I didn't know I had.